UNIVERSITY OF URBINO CARLO BO

DEPARTMENT OF BIOMOLECULAR SCIENCES

PhD Course in Sciences of Life, Healthcare and Biotechnologies

Curriculum in Biochemical and Pharmacological Sciences and Biotechnologies

XXX Cycle

Evaluation of the host cell response following *Leishmania infantum* infection

Academic Discipline: BIO-13

Tutor

Luca Galluzzi

PhD Student

Aurora Diotallevi

Co-tutor

Mauro De Santi

ACADEMIC YEAR 2016-2017

Summary

1. INTRODUCTION

Leishmaniases are a complex of parasitic diseases caused by protozoa of *Leishmania* genus, and transmitted by the bite of phlebotomine sand-fly, with different clinical manifestations depending on host characteristics and *Leishmania* species. Cutaneous leishmaniasis shows ulcerative lesions of the skin nearby the sand-fly bite site, which, in most cases, are self-healing. The variant of the cutaneous form is the mucocutaneous leishmaniasis, which is characterized by the destruction of the mucosal tissue of mouth, nose and pharynx. Visceral leishmaniasis is the most severe form of the disease and consists in a chronic infection affecting internal organs such as the liver, the spleen and the bone marrow. If not treated, the visceral leishmaniasis is fatal in developing countries in 100% of the cases. (Podinovskaia and Descoteaux, 2015).

The development of the three main forms of leishmaniases generally depend on both particular species of *Leishmania* and the host immune response to infection. At least 20 species of *Leishmania* cause the disease in humans: visceral leishmaniasis (VL) is triggered by species of the *Leishmania donovani* complex, including *L. donovani* and *L. infantum*; cutaneous leishmaniasis (CL) is caused by species of the Old World, such as *L. major* and the New World, such as *L. Mexicana*. These species can also circulate to other areas of the skin, resulting in diffuse CL (DCL). Although the form caused by species of the *Viannia* subgenus, including *Leishmania braziliensis,* are normally responsible for the CL, the parasite can also migrate to the oro-naso-pharyngeal tissues in a small number of cases, resulting in the mucocutaneous leishmaniasis (MCL) (Rogers *et al.*, 2011).

Transmission of *Leishmania* parasites is mediated by female sand-flies of either the genus *Phlebotomus* or the genus *Lutzomyia*. In the midgut of the sand-fly, pathogens replicate as promastigotes and, during a blood meal, parasites are injected into a new vertebrate host. There are several vertebrate hosts of *Leishmania* parasites that range from canids and humans to wild rodents (Podinovskaia and Descoteaux, 2015).

1.1 CLASSIFICATION

The classification of the Protozoa kingdom is quite complex and over the years has been subjected to considerable changes. In this kingdom, more than 50,000 species have been defined, some of which are classified as commensals (generally not harmful), while others are considered to be pathogenic and therefore life-threatening (Yaeger, 1996). The Protozoa include the phylum Euglenozoa, enclosing a large variety of eukaryotes. A recent revisited taxonomy places Kinetoplastea, with Euglenida, Symbiontida and Diplonemea into Euglenozoa (Lukes *et al.*, 2014) (Figure. 1). Kinetoplastid protists are grouped in the class Kinetoplastea (Cavalier-Smith, 1981) the name of which derives from the presence of the kinetoplast, a concentrated extranuclear DNA within the single mitochondrion (Vickerman, 1976).

This kinetoplast DNA (kDNA) can have different location: it can be placed close to the flagellar base (eukinetoplast) or scattered through the mitochondrial lumen as multiple bodies (polykinetoplast) or diffuse masses irregularly disseminated (pankinetoplast) (Moreira *et al.*, 2004). *Leishmania* genus belongs to the phylum Euglenozoa.

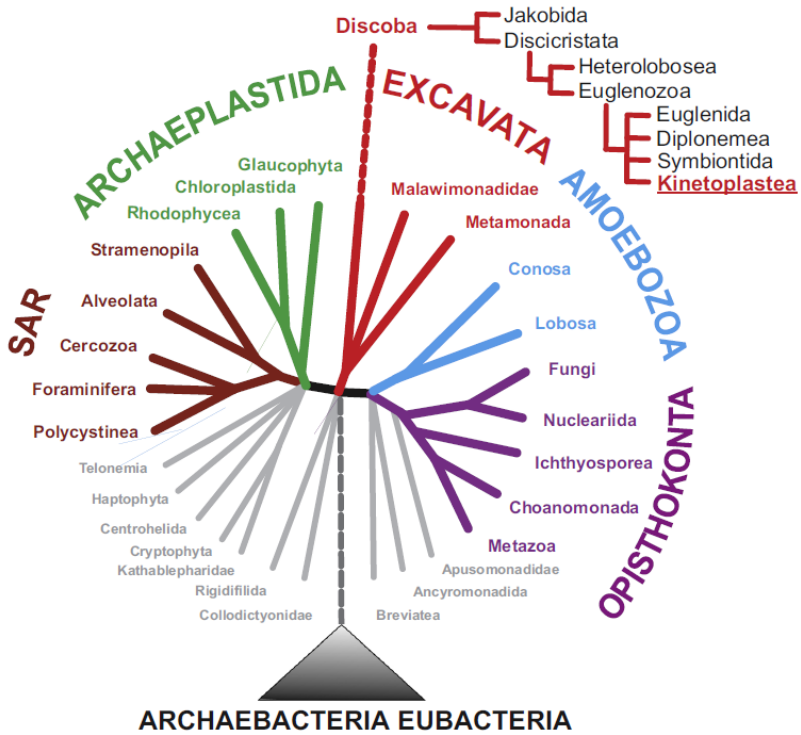

Fig. 1. A view based on the recent classification of general eukaryote phylogeny (Adl, *et al*., 2012) focusing on the taxonomic disposition of Kinetoplastea. (Lukes *et al*., 2014)

Currently, the new classification divides *Leishmania* species into two major phylogenetic lineages: *Euleishmania* and *Paraleishmania* (Cupolillo *et al.*, 2000). *Euleishmania* encompasses four subgenera: *Leishmania (Leishmania), Leishmania (Viannia), Leishmania (Sauroleishmania), Leishmania (enriettii)*. Section *Paraleishmania* comprises *L. hertigi*, *L. deanei*, *L. herreri*, *L. equatorensis*, and *L. colombiensis* (the only found to be pathogenic to humans) (Figure 2). The subgenus *Viannia* is limited to the Tropical America, while the subgenus *Leishmania* occurs in both the New and Old World (Akhoundi *et al.*, 2016).

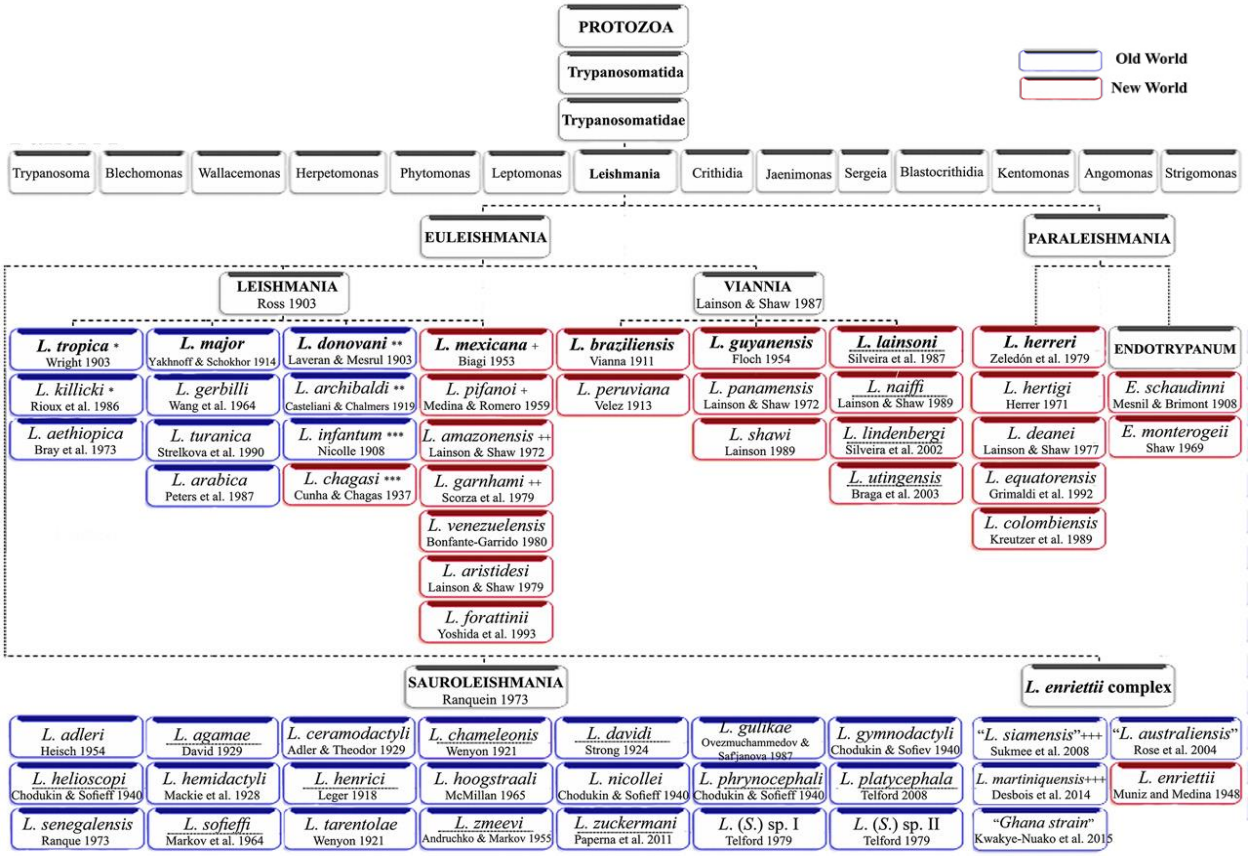

Fig. 2. Classification of *Leishmania* species. (Akhoundi *et al.*, 2016)

About 20 *Leishmania* species cause infection in humans. These include the species of subgenus *Leishmania*: the *L. donovani* complex (*L. donovani, L. infantum,* also called *L. chagasi* in South America), the *L. mexicana* complex (L. *mexicana, L. amazonensis*), *L. tropica*, *L. major*, *L. aethiopica*; and the species belonging to subgenus Viannia: *L. braziliensis, L. guyanensis, L. panamensis* and *L. peruviana* (Figure 3). All these species are morphologically indistinguishable,

but they can be characterized by molecular methods, isoenzyme analysis or monoclonal antibodies. (CDC https://www.cdc.gov/parasites/leishmaniasis/biology.html)

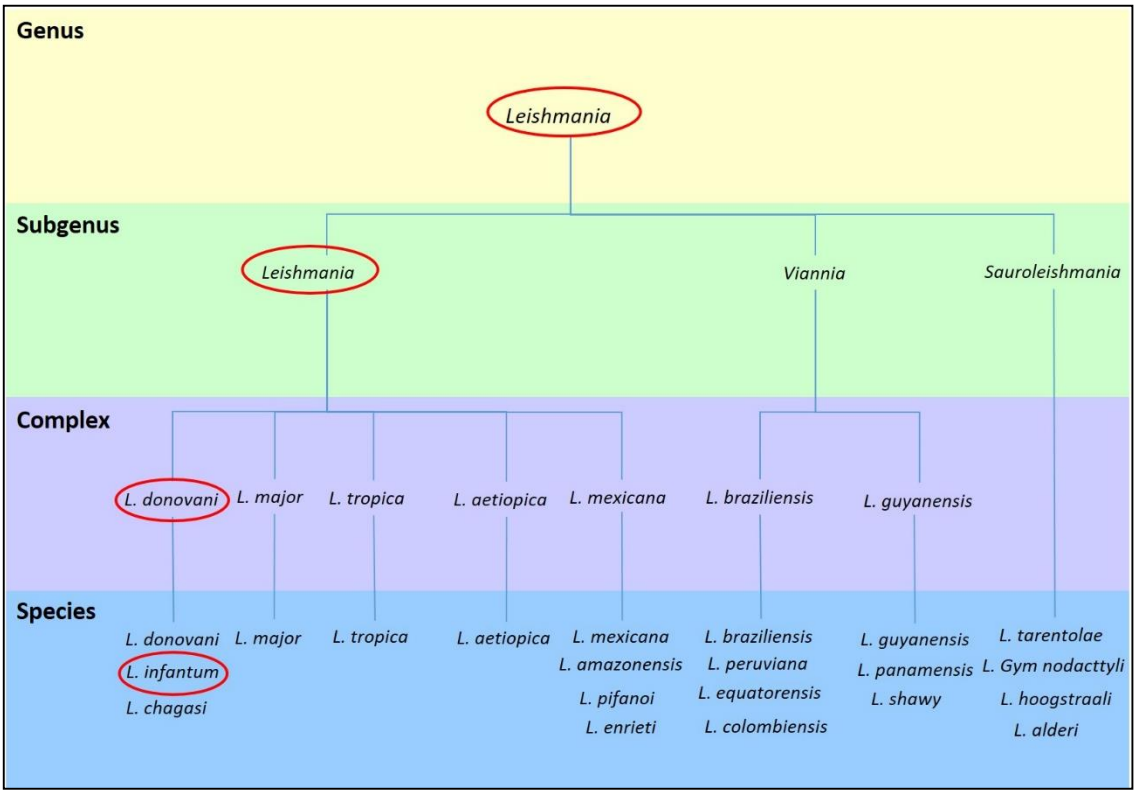

Fig. 3. *Leishmania* genus classification focusing on pathogenic species. The classification of *L. infantum* species is evidenced (Adapted from Bates, 2007 and from NCBI classification).

Throughout the years there have been several criteria for the classification of *Leishmania* genus. Since morphology cannot be used for the identification of the different species, other criteria have been used for the classification of *Leishmania* species, such as the clinical manifestations following the infection and the geographical spread. In the last decade, classification of *Leishmania* genus has been revised following the introduction of new molecular biology and biochemical techniques (Lainson and Shaw, 1987; Bates, 2007).

The classification of *Leishmania* subgenera also depends on which parts of the sand-fly gut the parasites are going to colonize. *Leishmania (Leishmania)* subgenus comprises species able to colonize only the midgut and foregut of female sand-flies (*Phlebotomus* species in the Old World, *Lutzomyia* species in the New World), whereas *Leishmania (Viannia),* which includes parasites from the New World and then vectors of *Lutzomyia* species, comprises parasites that develop a

protracted phase in the hindgut with later migration to the midgut and foregut. Regarding vectors of the subgenus *Leishmania (Sauroleishmania)*, they are members of the genus *Sergentomyia*, which are known to feed on reptiles as well as other vertebrates (Bates, 2007). Fifty-three named species in all subgenera and complexes have been characterized: 29 of these species are in the Old World, 20 in the New World, 3 species (*L*. *siamensis*, *L*. *martiniquensis*, and *L*. *infantum*) are present in both Old and New World, and one species (*L*. *australiensis*) in Australia. (Maroli *et al.*, 2012). Table 1 summarizes the *Leishmania* species classification related to clinical diseases, possible reservoir and geographic location.

Emerging approaches, such as whole-genome sequencing and SNP analysis as well as further analysis by multilocus sequence typing (MLST) and multilocus microsatellite typing (MLMT) and an adequate sampling and inclusion of representatives of all species (with sufficient numbers of isolates from different areas of distribution) will contribute to further improvement of the classification of the *Leishmania* genus (Akhoundi *et al.*, 2016).

Table 1. Geographical distribution of *Leishmania* species, associated with clinical manifestation and the possible reservoir of infection.

Clinical Disease	Leishmaniasis Species (Possible reservoir)	Geographic Location
Cutaneous leishmaniasis	*L. tropica* complex • *L. tropica* (dog) • *L. aethiopica* (rock hyrax) *L. major* (gerbils & rodents)	Old World
	L. mexicana complex • *L. mexicana* (woodrats, cat, and others) • *L. pifanoi* • *L. amazonensis* (small forest mammals, rodents, marsupials, and foxes) • *L. garnhami* *L. ve*nezuelensis	New World
	L. braziliensis complex • *L. peruviana* (domestic dog and probably a wild rodent) • *L. guyanensis* (arboreal sloths and anteaters) • *L. panamensis* (sloths, rodents, monkeys, procyonids) • *L. lainsoni* (agouti) *L. colombiensis* (sloth)	New World
	L. infantum	Old World
	L. chagasi	New World
Mucocutaneous leishmaniasis	*L. braziliensis* complex • *L. braziliensis* • *L. guyanensis* *L. panamensis*	New World
	L. mexicana	New World
	L. tropica	Old World
	L. major	Old World
Visceral leishmaniasis	*L. donovani* complex • *L. donovani* (no reservoir in Indian or Kenyan area, various rodents in Sudan , dogs in China) • *L. infantum* (human is accidental host, natural infection in dogs, other Canidae, and porcupines)	Old World
	• *L. chagasi* (domestic dogs and cats, foxes)	New World
	L. tropica	Old World
	L. amazonensis	New World

1.2 EPIDEMIOLOGY

Mammalian leishmaniasis shows a worldwide distribution. *Leishmania* is endemic in tropics, subtropics and Mediterranean areas, in at least 98 countries and 3 territories, with the highest number of cases in developing nations (WHO, 2012). *Leishmania* species are present in North, Central, and South America, in the Southeast Europe, Middle East, Central and Southeast Asia, the Indian subcontinent, Africa. Recently, the parasite presence has been reported also in Australia (Akhoundi *et al.*, 2016). A total of 350 million people are at risk and there are 12 million cases of infection. Moreover, incidences of 700,000 to 1.2 million cases of cutaneous leishmaniasis (CL) and 200,000 to 400,000 cases of visceral leishmaniasis (VL) per year have been estimated (Alvar *et al.*, 2012). The distribution of sand-flies and therefore the distribution of leishmaniasis has increased over the last decade, possibly due climate changes that have generated an increasingly favorable environment to vector species (González *et al.*, 2010).

1.2.1 Cutaneous Leishmaniasis

A large number of *Leishmania* spp., with location-specific reservoir species causes CL (Figure 4). In the Old World, the predominant cause of CL is *L. major* and its reservoirs include many rodent species. Vector and reservoir population distribution are tightly related to the course of the infection. Rise in rodent populations have been related with an increase in the number of zoonotic cutaneous leishmaniasis (ZCL) cases (Gramiccia and Gradoni, 2005). *L. aethiopica*, the etiological cause of ZCL, was isolated only in the highlands of Ethiopia, even though some reports have recognized this species even at lower altitudes, suggesting a more extensive distribution of the pathogen or that the endemicity area is growing (Gebre-Michael et al., 2004). *L. tropica* causes an anthroponotic CL, and therefore human represents one of the main reservoir of the parasite, even though different animal species, including dogs, can be infected and then become potential reservoirs.

In the New World have been identified numerous species of *Leishmania* (*Viannia*) subgenus causing CL. *L. mexicana* is found in Central America and Mexico, and moreover, cases have been described in Texas (Trainor *et al.*, 2010; Barnes *et al.*, 1993; Sellon *et al.*, 1993; Craig *et al.*, 1986). It is likely that rates of CL caused by *L. mexicana* will increase in the south of the United States due to the presence of vectors (González *et al.*, 2010).

South American species of *Leishmania* causing CL, including *L. amazonensis*, *L. braziliensis*, *L. guyanensis*, and *L. panamensis*, have sylvatic reservoirs, while two CL-causing species in South America have domestic animal reservoirs. *L. venezuelensis* has been identified in several urban and periurban areas, with a suspected domestic cat reservoir host (Bonfante-Garrido *et al.*, 1991). *L. peruviana*, a species once limited to altitudes of 1,200 to 3,000 m in the Peruvian Andes, uses the dog as a reservoir, although limited evidence of transmission to sand-flies exists (Llanos-Cuentas *et al*., 1999).

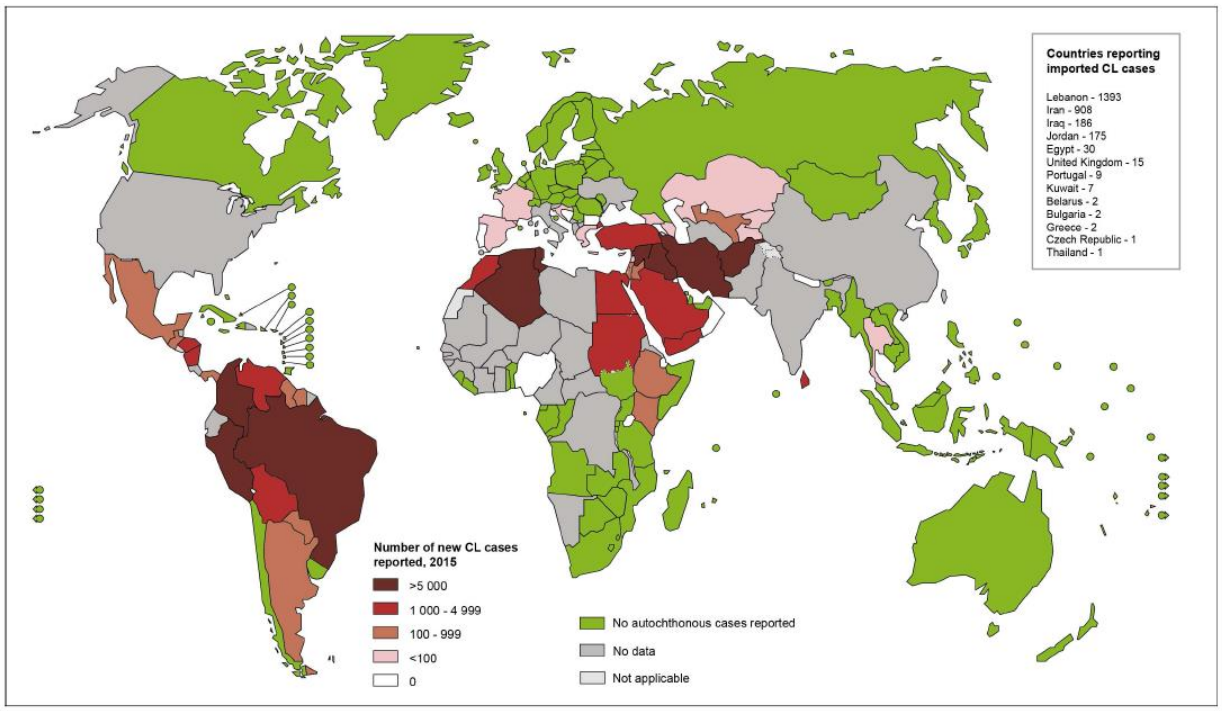

Fig. 4. Endemicity of cutaneous leishmaniasis worldwide, 2015 (WHO http://www.who.int/leishmaniasis/burden/en/)

1.2.2 Visceral Leishmaniasis

L. donovani is responsible for visceral leishmaniasis in Asia, India, Sudan, South Sudan, Kenya, and Ethiopia, while *L. infantum* (also kown as *L. chagasi* in the New World) is found in the Mediterranean basin, Middle East, central and southwestern Asia, northwestern China, northern and sub-Saharan Africa and Mexico, Central and South America (Figure 5). The majority of zoonosis-based human cases of VL is caused by *L. infantum*. Vectors for *Leishmania* in the New World are *Lutzomyia* spp., predominantly *Lutzomyia longipalpis*, and those in the Old World are species of the genus *Phlebotomus*. Canids are considered the primary reservoirs: foxes, jackals,

and wolves represent the sylvatic reservoirs, while dogs are the domestic reservoirs (Petersen, 2009; Gramiccia and Gradoni, 2005). Humans are rather resistant to *L. infantum* infection and very often show asymptomatic infection. The WHO estimated 200,000 to 400,000 clinical VL cases, 90% of which occur in India, Bangladesh, Sudan, South Sudan, Ethiopia, and Brazil (WHO, 2012), could be an underestimation of the impact of *L. infantum* infection on human health (Michel *et al.*, 2011). An asymptomatic, immunocompetent patient with low or absent levels of parasitemia and *L. infantum* compartmentalization within the bone marrow and the secondary lymphoid organs may have reduced transmission to vectors. When zoonotic visceral leishmaniasis (ZVL) occurs in immunologically compromised subjects, the parasite burden increases, and transmission is likely to occur, as well as the clinical disease.

The presence of infected animals was significantly related to human risk, but the incidence of human disease varied considerably in different countries where *L. infantum* is considered endemic (Lima *et al.*, 2012; Dujardin *et al.*, 2008). The expected incidence of human ZVL in Europe goes from 0.02 to 0.47 cases per 100,000 people, with the exception of Turkey, where was reported a higher incidence, with 1.6-8.53 cases/100,000 people (Dujardin *et al.*, 2008; Alvar *et al.*, 2012). In some endemic areas of Brazil the incidence of VL was twice the number of cases for the entire Mediterranean basin between 2004 and 2008 (Alvar *et al.*, 2012).

Risk factors for ZVL account for differences in human incidences in Brazil versus Europe. Numerous reports showed the association between the risk for ZVL based and the presence of domestic dogs, houses types (mud-walled, concrete or brick houses), education level, family income and disease knowledge (Lima *et al.*, 2012; Coura-Vital *et al.*, 2011; de Almeida *et al.*, 2011; Harhay *et al.*, 2011). Poor nutrition is also related with clinical ZVL (Harhay *et al.*, 2011).

Other risk factors for humans are associated to their immunological status and their ability to eliminate the infection or maintain it as asymptomatic condition. These factors comprise concurrent infection with HIV, helminth parasites, drug abuse, and other condition which lead to immune system suppressions. These comorbidities, particularly co-infection with HIV, increase the risk for the ZVL development (Nascimento *et al.*, 2011). Genetic susceptibility could also represent a risk factor for clinical disease development. Studies performed on a large-scale in different countries showed a role of genetic susceptibility, comprising polymorphisms of a number of gene involved in different patways, such as metabolic genes, genes implicated in the iron metabolism, chemokines, cytokines, and HLA alleles (Blackwell *et al.,*2009). All these aspects

propose a complex evolutionary interaction between the *Leishmania* and the host organism, which are likely related with susceptibility to the disease. (Esch and Petersen, 2013).

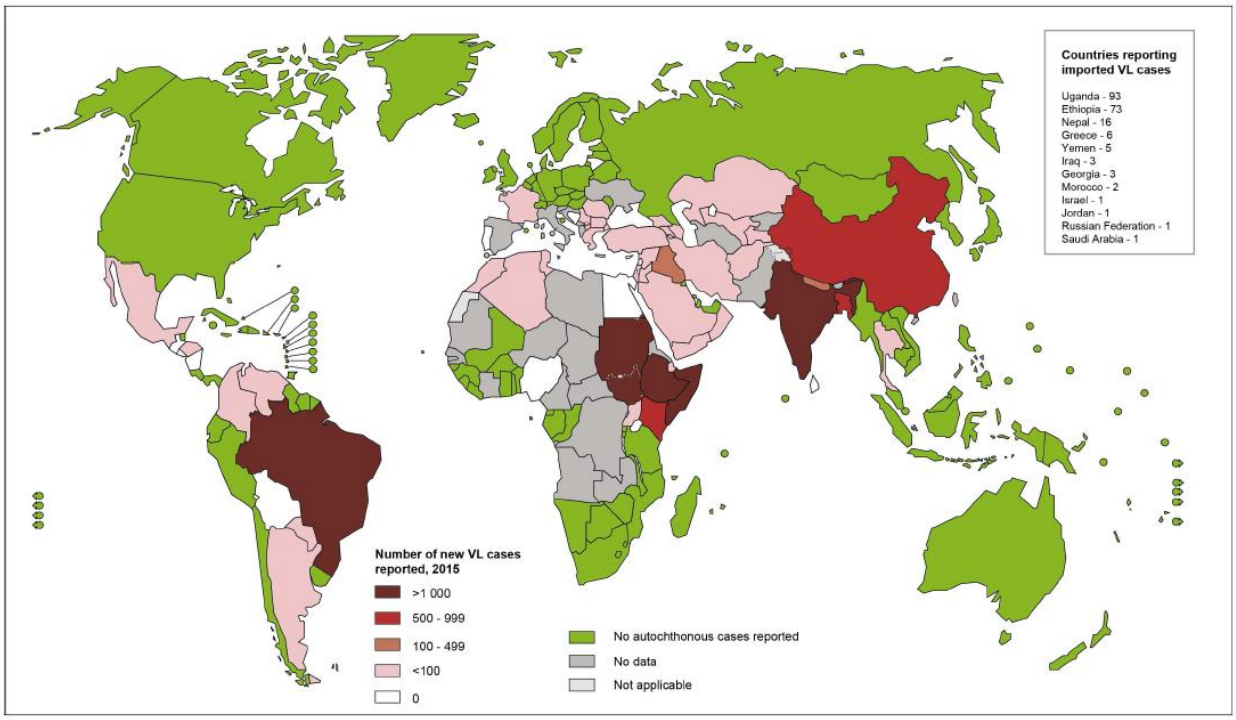

Fig. 5. Endemicity of visceral leishmaniasis worldwide, 2015. (WHO http://www.who.int/leishmaniasis/burden/en/)

1.2.3 Leishmaniasis in Italy

The first outbreak of Leishmaniasis documented in Italy, was observed between 1971 and 1972 near Bologna, with 60 new cases, 13 of which resulted fatal. Subsequently, between 1989 and 2009, Italy recorded an increase in human VL, with a number of cases exceeding 10-30 units reported per year since 1950. The epidemic peak has been reached between 2000 and 2004 with more than 200 cases/year (Figure 6), followed by a decrease in new infections in recent years. However, the reasons of this decrease are, still today, unclear (Gramiccia *et al.*, 2013).

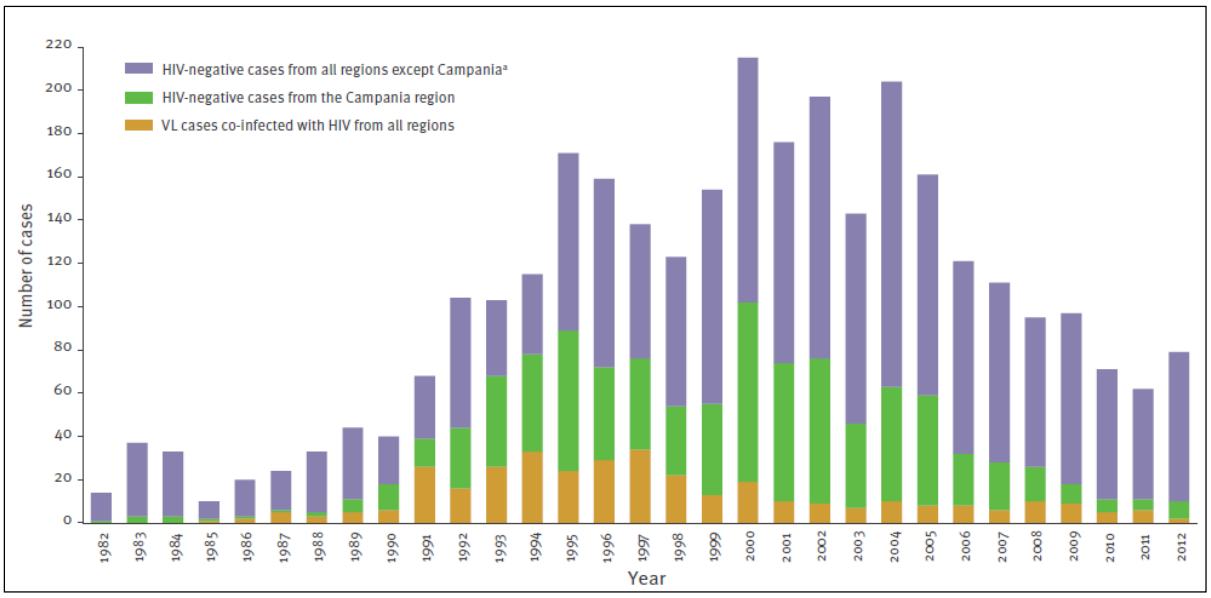

Fig. 6. VL in Italy from 1982 to 2012 (Gramiccia *et al*., 2013).

Overall, most of the cases of human leishmaniasis are reported in Sicily, Latium and, in particular, in Campania regions. Unfortunately, in many Italian regions, the available information are underestimated, while, in regions where active surveillance programs have been carried out (even for limited periods) such as Campania, Sicily and Liguria, there is a fair amount of reliable data (Gradoni *et al*., 2004).

From 1987 to 2005, 1296 Italian patients were screened: 58% were adults and 42% in pediatric age. 81% of the total of patients was immunocompetent and without any particular pathology, 14% was HIV-positive, and 5% immunodepress for other causes than coinfection with HIV-virus. Although immunocompetent pediatric patients are not taken into consideration, most of the observed cases (73%) were registered in healthy adults for whom VL susceptibility remains unclear (Gramiccia *et al*., 2013).

Although cases of human VL in Italy are rather limited, canine leishmaniasis (CanL) behavior is more problematic. As described above, the main reservoir for *L. (L.) infantum* is the dog, and hence the increase in the number of infected dogs could also be a risk to human health. Knowledge concerning the course of infection in the canine population is therefore important for the definition of prevention programs, even though the direct association between CanL prevalence with the Human VL in some cases is not always defined.

CanL is widespread in southern Europe, with the highest values of predicted seroprevalence most focused in Italy (Gramiccia *et al*., 2013). Here, CanL is endemic in all coastal and hilltop areas of the Tyrrhenian, Ionian and Central Adriatic (Liguria, Tuscany, Latium, Campania, Basilicata, Calabria, Apulia, Molise and Abruzzo) and in the islands (Figure 7). In some cases, serological tests (seroprevalence: antibody titer developed following the presence of a determined pathogen in the host serum) performed in the canine population of southern Italy, can reach 48.8% (Paradies *et al.*, 2006). Overall, a study conduct between 1971 and 2006 on 424,000 dogs showed that seroprevalence is approximately 18% with fluctuations of 11% -21% for the decades examined (Franco *et al*., 2011).

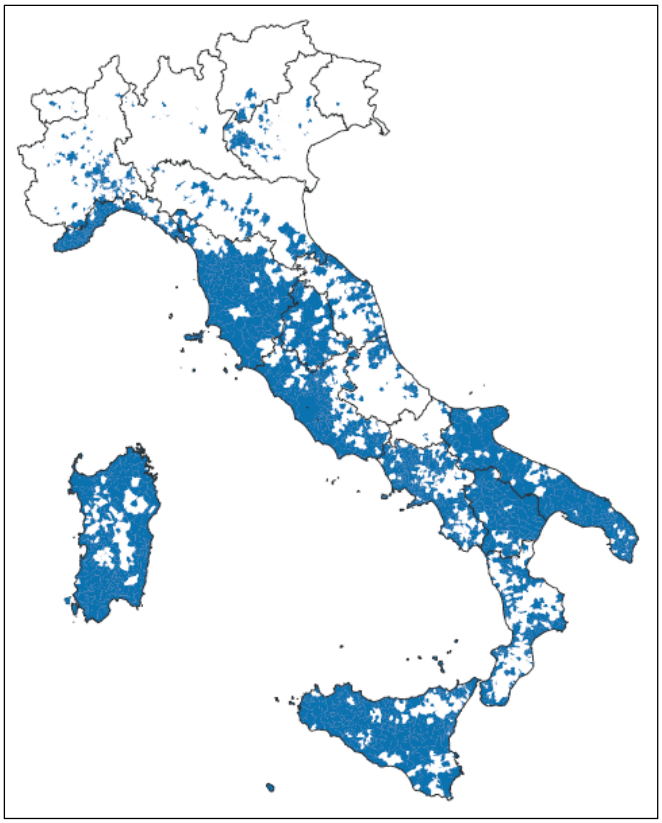

Fig. 7. Distribution Map of autochthonous CanL registered in Italy from 2005 to 2012 (Gramiccia *et al*., 2013).

As already mentioned, Campania is the Italian region most affected by human VL, with a peak of 83 cases in 2000. However, two studies conducted between 1999 and 2009 showed that seroprevalence rates limited to 15% in 1999 (data from Istituto Zooprofilattico Sperimentale del Mezzogiorno, Portici, Naples, Italy) and 14% between 2005 and 2009 in the canine population that did not justify the epidemic trend of the VL in humans (Gramiccia *et al.*, 2013).

The coastal and hilltop areas of Adriatic, Marche and east Emilia-Romagna region, and the Umbria region, are considered "endemic-sporadic areas" in which the real distribution of infection is not known. Until 1989 northern Italy was considered free of CanL, but for more than ten years there has been an increase of infection in the canine population and new cases of autochthonous infection have been found in Emilia Romagna, Piedmont, Valle d'Aosta, Lombardy, Veneto, Trentino and Friuli (Gradoni *et al.*, 2004). Notably, at present, the actual distribution of CanL on a national scale is not precisely known and it is likely to be largely underestimated. To address all these issues, the Istituto Superiore di Sanità has established Guidelines for the Control of CanL (Gradoni *et al.*, 2004). Afterwards, a series of regional control plans were established.

1.3 *LEISHMANIA* MORPHOLOGY

During its life cycle, *Leishmania* undergoes various morphological developments (Figure 8a) depending on the environmental conditions within their two hosts: the mammalian host and the sand-fly insect vector. In the vector, *Leishmania* grows and duplicates in the insect's gut as extracellular and motile flagellated cells known as promastigotes (Figure 8b, left). Can be distinguished two main forms of promastigote: procyclic promastigotes, that are the replicative, but not infective for mammals stage, residing in the midgut; metacyclic promastigotes, the non-dividing, infective for mammals stage of the parasite, in the salivary glands of the proboscis of the sand-fly. During the blood meal, metacyclic promastigotes, are inoculated into a mammalian host, phagocytosed by resident macrophages and differentiate into the intracellular aflagellate amastigote form (Figure 8b, right), that resides within the parasitophorous vacuole with lysosomal characteristics. During passage through the extra- and intracellular environments, *Leishmania* is exposed to many variation such as changes in the availability and type of nutrients, accessibility of oxygen temperature, pH. To survive to these changes, the parasites develop into forms highly specialized and adapted, distinguished by nutritional needs, growth rate and division ability, expression of surface molecules, and morphology.

Metacyclic promastigotes are different from the procyclic forms since they are pre-adapted for the mammalian host: for example, metacyclic promastigotes express stage-specific molecules and becoming complement-resistant after following host infection (Esch and Petersen, 2013). In the parasitophorous vacuole, amastigotes adapt morphologically to this compartment by reducing size and flagellum, which does not emerge from the flagellar pocket. Here, the amastigotes also adapt to the low pH of the parasitophorous vacuole becoming acidophilic (Besteiro *et al*., 2007).

The amastigote form is a rounded cell and represents the non-motile phase of the parasite. It is situated within the parasitophorous vacuole and has a reduced size: 2-5 µm length and 2-3 µm width; the cytoplasm is granular but generally homogeneous and the large nucleus is located centrally or peripherally. The kinetoplast appears as a rodshaped body and is located in an antinuclear position and adjacent to the reduced flagellum (not emerging from the flagellar pocket). Conversely, the promastigote represents the extracellular and motile form of the parasite *Leishmania* in the sand-fly vector where develops, differs and multiplies. The promastigote stage has a different cell morphology respect to the amastigote stage. The cellular

body becomes larger and more highly elongated, reaching 15-30 µm in length and 5 µm in width. The flagellum, long as the entire body, emerges from the flagellum pocket and ensures the mobility of the parasite inside the vector. The nucleus is in the center, and in front of this is located the kinetoplast body.

The two *Leishmania* differentiation events mostly investigate are the metacyclogenesis, that is the procyclic to metacyclic differentiation of promastigotes stage and the transformation starting from metacyclic promastigote to amastigote, occurring within the host macrophage (Besteiro *et al.*, 2007).

These events can be reproduced *in vitro* and have been well described. Under conditions of low pH, oxygen privation or nutritional depletion of tetrahydrobiopterin, metacyclogenesis can be induced. Moreover, environment simulating a phagolysosome-like condition (low pH, 37°C of temperature and elevated level of CO_2) can trigger the promastigote to amastigote differentiation (Barak *et al.*, 2005). Despite environmental factors inducing *Leishmania in vitro* differentiation were known for a long time, molecular mechanisms mediating the cellular remodeling are relatively unclear.

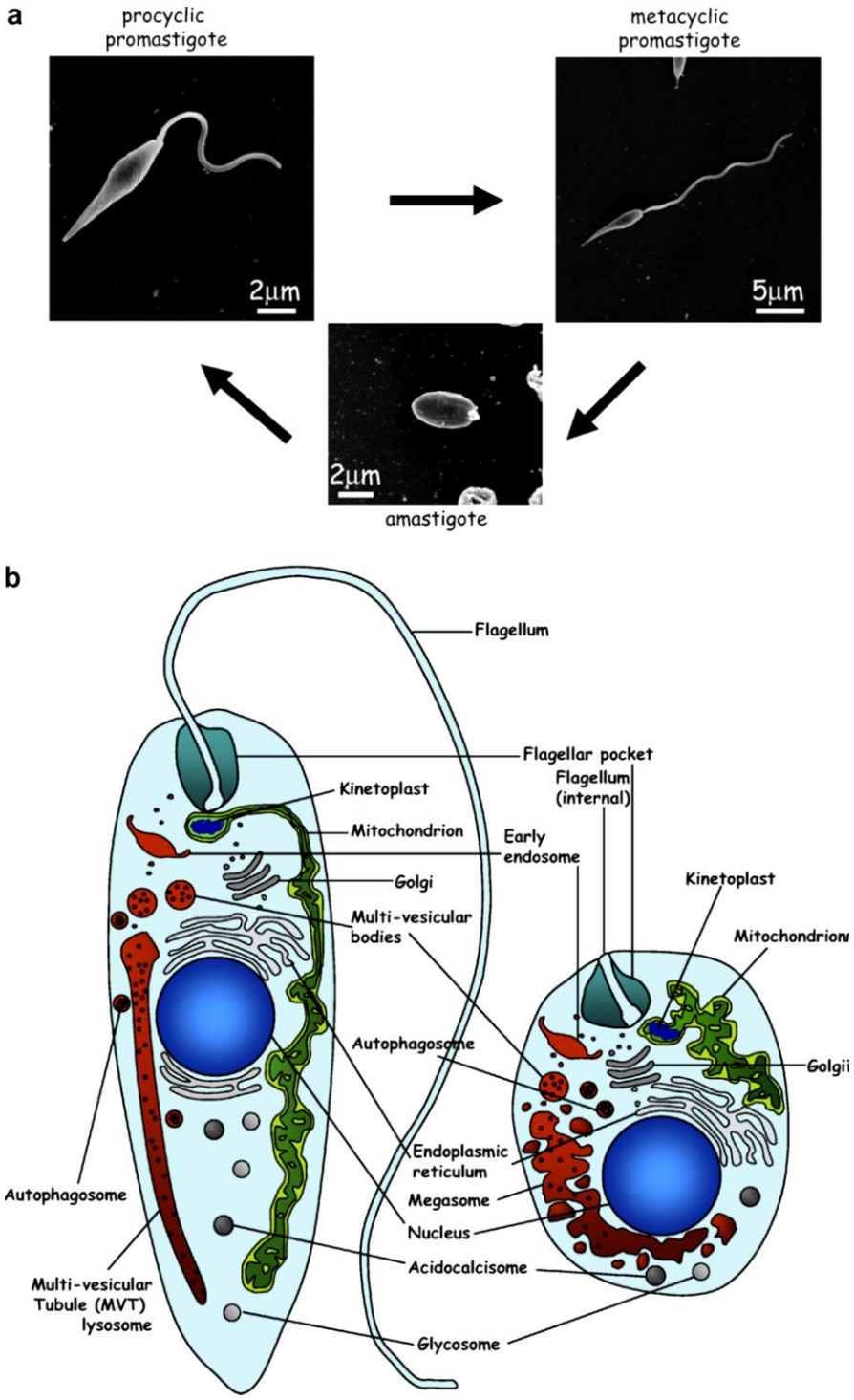

Fig. 8. Changes in cell shape during the *Leishmania* life-cycle. **(a)** Scanning electron microscope images of the main *Leishmania major* life-cycle stages, the procyclic and metacyclic promastigotes were grown in culture, the amastigote was isolated from an infected macrophage isolated from a mouse. **(b)** Schematic representation of the main intracellular organelles from *Leishmania* promastigote (left) or amastigote (right) forms. The flagellar pocket marks the anterior end of the cell. (Besteiro *et al.*, 2007)

1.4 LIFE CYCLE OF *LEISHMANIA* SPP

The life cycle of *Leishmania* spp. involves a vector stage and a mammalian host (Figure 9). Phlebotomine sand-flies of the genus *Phlebotomus* in the Old World and *Lutzomyia* in the New World represent the vectors for *Leishmania*. The female phlebotomine sand-fly injects infective promastigotes into a mammal during the blood meal. Promastigotes are internalized by resident phagocytes, mainly macrophages and other mononuclear phagocytic cells and transformed into tissue-stage amastigotes, which multiply through simple binary fission in the parasitophorous vacuole. When the host cell can no longer hold amastigotes, breaks and internalized parasites can infect new cells leading to a progressive infection of the surrounding tissue. Depending of both parasite and host characteristics, the subsequent localization of the amastigotes may vary: parasites could infect either a higher number of cells at the site of the inoculum and develop the cutaneous form of Leishmaniasis or migrate into in secondary lymphoid organs, developing visceral Leishmaniasis.

Through feeding, sand-flies become infected by ingesting amastigotes from the blood meal. In the vector, amastigotes transform into promastigotes within the gut (in the hindgut for parasites of the *Viannia* subgenus; in the midgut for the *Leishmania* subgenus). [CDC https://www.cdc.gov/parasites/leishmaniasis/biology.html]. From the gut, promastigotes migrate to the proboscis and wait for the initiation of feeding in the salivary glands, where they transform into infectious metacyclic promastigotes (Esch and Petersen, 2013).

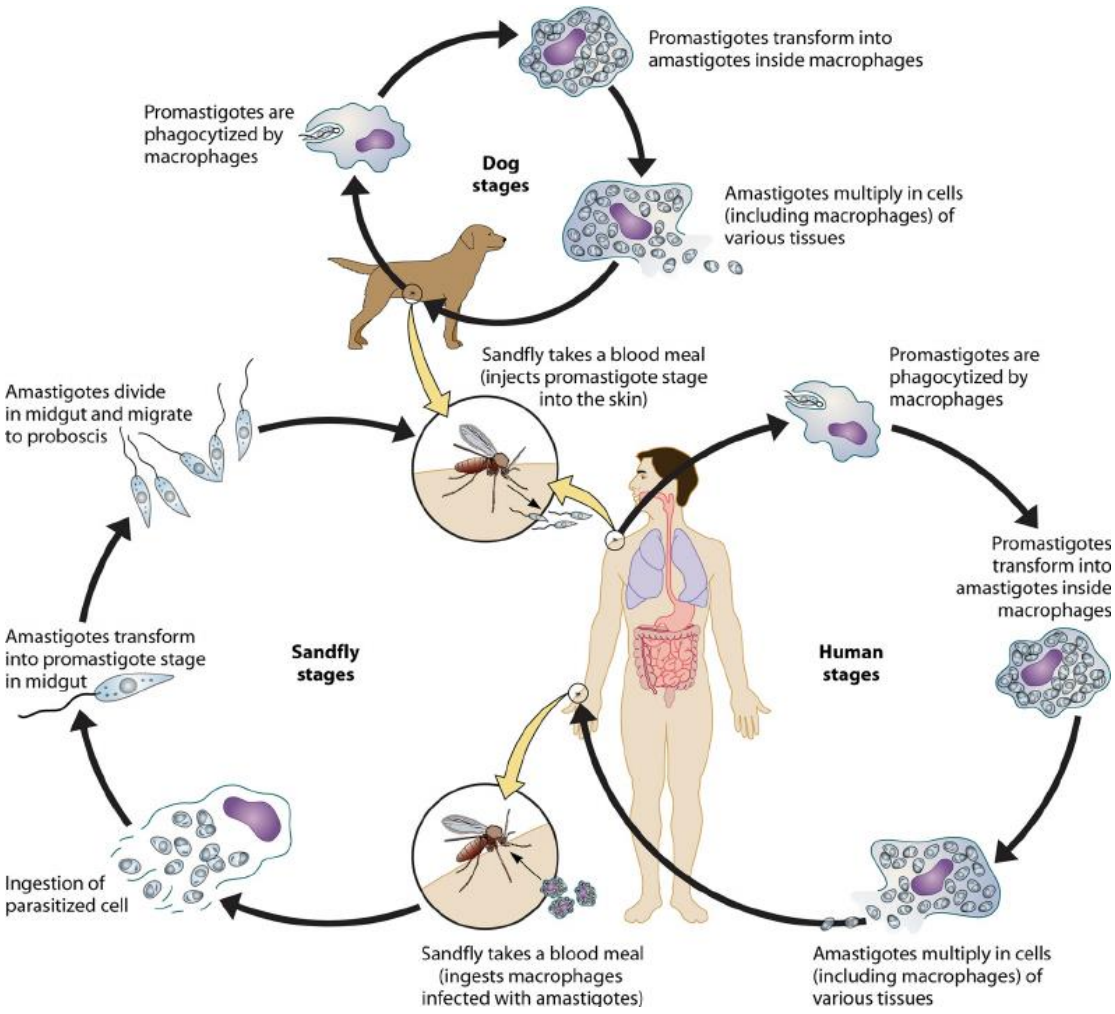

Fig. 9. The life cycle of *Leishmania* spp. Infected female phlebotomine sand-fly injects promastigotes into a mammal during the blood meal. Promastigotes are internalized by resident phagocytes, and transformed into amastigotes, which multiply through simple binary fission in the parasitophorous vacuole. When the host cell can no longer hold amastigotes, breaks and amastigotes can infect new cells leading to a progressive infection of the surrounding tissue. Through feeding, a new sand-flies become infected by ingesting amastigotes from the blood meal and within the gut (in the hindgut for parasites of the *Viannia* subgenus; in the midgut for the *Leishmania* subgenus) amastigotes transform into promastigotes and migrate to the salivary glands, where they develop into the infective stage metacyclic promastigotes (Esch and Petersen, 2013).

1.5 PATHOGENESIS

Once internalized by the host, *Leishmania* develop various strategies to infect cells and counteract the hostile environment of the macrophage, and therefore to survive and replicate (Podinovskaia and Descoteaux, 2015).

1.5.1 Recognition of the parasite and uptake by the target cells

During the infection, macrophages and neutrophils are rapidly recruited to the site of the sand-fly bite, through secretion of proteophosphoglycans release by the parasite (Rogers *et al.*, 2009) (Rogers *et al.*, 2010). Initial interaction between the promastigote and the macrophage takes place through the parasite flagellum, leading to the release of intracellular survival factors by the parasite and subsequent modulation of macrophage phagocytic activity (Rotureau *et al.*, 2009). Different species of *Leishmania* may interact with several macrophage receptors, including complement receptors (CRs), mannose receptors, fibronectin receptors and Fcγ receptors (FcγRs) (Ueno and Wilson, 2012), influencing the infection development. CR-mediated uptake inhibits inflammation, superoxide burst, and accumulation of the lysosomal markers LAMP1 and Cathepsin D, making more favorable conditions for the parasite within the macrophage phagosome. Mannose receptor signaling may trigger inflammatory pathways and more efficient delivery of hydrolytic enzymes into the phagolysosome. FcγR-mediated phagocytosis leads to enhanced activation of NADPH oxidase on the newly formed phagosome (Ueno and Wilson, 2012).

Interestingly, uptake or viability of the *L. donovani* or *L. major* parasites by murine bone marrow-derived macrophages were not affected by the receptor choice (Polando *et al.*, 2013), pointing to the complexity of *Leishmania*–macrophage interactions. Following recognition at host cell surface, promastigotes can be internalized via caveolae that are composed of cholesterol-rich membrane lipid microdomains, as shown for *L. chagasi* infection of murine bone marrow-derived macrophages Cholesterol depletion and subsequent lipid microdomain disruption by methyl-β-cyclodextrin compromised *Leishmania* promastigote uptake via nonopsonic pathways (Rodriguez *et al.*, 2011).

In addition to receptor- and lipid microdomain-regulated uptake, *Leishmania* infection also depends on actin-mediated uptake, and the integrity of the actin cytoskeleton of the host macrophage has recently been shown to be essential for *L. donovani* infectivity (Roy *et al.*, 2014).

Actin cytoskeleton destabilization induced by cytochalasin D treatment led to a reduction in promastigote attachment to macrophages and the concomitant reduction in intracellular amastigote load. Cellular F-actin levels strongly correlated with the reduction in *Leishmania* attachment and load in macrophages. In contrast, uptake of *E. coli* was unaffected following actin disruption (Roy *et al.*, 2014).

1.5.2 Phagosome maturation and parasite differentiation

Following phagocytosis, *L. donovani* promastigote-containing phagosomes of murine bone marrow-derived macrophages failed to acidify and were characterized by a reduced fusogenicity towards late endosomes and lysosomes. LAMP1 was recruited to the parasitophorous vacuole (PV) with delayed kinetics (Morandin and Descoteaux, 2012). The authors proposed that, at this stage, some lysosomes may fuse with the PV and promote promastigote-to-amastigote differentiation (Forestier *et al.*, 2011).

Promastigote-to-amastigote differentiation is believed to be triggered by the increase in temperature and a decrease in pH. Additionally, iron uptake and subsequent generation of hydrogen peroxide by *L. amazonensis* has been shown to be a major trigger in parasite differentiation (Mittra and Andrews, 2013; Mittra *et al.*, 2013). Iron mediates generation of reactive oxygen species (ROS), which are normally deleterious for pathogens, but in this case it was proposed to act as a signaling molecule regulating parasite differentiation. The *Leishmania* iron transporter LIT1 mediates iron acquisition by the parasite, which lead to parasite growth arrest and differentiation.

Promastigote-to-amastigote differentiation is associated with a reduction in growth rate and the induction of a distinct metabolic state characterized by a decrease in uptake and utilization of glucose and amino acids, reduced organic acid secretion and increased fatty acid beta-oxidation. Catabolism of hexose and fatty acids provide substrates for glutamate synthesis, which is essential for amastigote growth and survival. Notably, *in vitro* differentiated amastigotes displayed a metabolic profile similar to that of lesion-derived amastigotes, suggesting its coupling to differentiation signals rather than nutrient availability (Saunders *et al.*, 2014). Such changes likely facilitate amastigote survival in the nutrient-poor intracellular niche.

Both promastigotes and amastigotes are able to divert the classical phagosome maturation pathway, which occurs via a set of highly regulated fusion and fission events with vesicles including endosomes and lysosomes, and form PVs of very specific phenotypes. Fusion is strictly

species and stage-dependent. These observations denote the unique nature of host–parasite interactions for different parasite species and their vulnerability to perturbations.

1.5.3 Intracellular parasite growth

1.5.3.1 Membrane contribution from the endoplasmic reticulum

Once *Leishmania* establish infection within macrophages, their subsequent multiplication requires a source of nutrients and additional membrane for phagosome expansion. For this, the amastigote PV remains a highly dynamic organelle and interacts with the secretory pathway, which contains endoplasmic reticulum (ER) proteins destined for other organelles (Canton and Kima, 2012a). Importantly, recent studies by Canton *et al*. demonstrated that disruption of *Leishmania* PV fusion with ER vesicles resulted in control of *L. amazonensis* infection in RAW 264.7 macrophages (Canton *et al.*, 2012). Further characterization of *Leishmania* PVs in RAW 264.7 macrophages revealed that phagosomes containing *L. donovani* and *L. pifanoi* promastigotes recruit the ER proteins calnexin and Sec22b very early during PV maturation, whereas zymosan-containing phagosomes do not (Ndjamen *et al.*, 2010). Loss of the ER SNAREs Sec22b or its cognate partners D12, or Syntaxin 18, or knock-down of Syntaxin 5 had very little effect on the ER or secretion but led to a significant reduction in PV size, as well as a reduction in parasite replication (Canton and Kima, 2012b). These findings highlight the role of the ER SNAREs Sec22b and Syntaxin 5 in the delivery of ER content to *Leishmania* PVs that supports the infection. Interestingly, Sec22b was also required for cross-presentation and its presence in the phagosome may play a role in parasite control (Cebrian *et al.*, 2011).

1.5.3.2 Nutrient acquisition

Intracellular *Leishmania* parasites have complex nutritional requirements, with amino acids and polyamines being important carbon sources and growth-limiting nutrients. Long-term survival of the parasite within macrophages requires nutrient availability within the intracellular niche. The parasite may achieve some of its nutrient requirements through parasite-driven PV fusion with endosomes and ER-derived Sec22b- and calnexin-positive vacuoles (Ndjamen *et al.*, 2010). Actively scavenged metabolites include hexoses, amino acids, polyamines, purines, vitamins, sphingolipids, heme and cations Fe2+, Mg2+, among others. Amastigotes also produce amino acid permeases and cysteine proteases to generate alternative sources of amino acids (Besteiro *et al.*, 2007). Interestingly, classically activated macrophages may have depleted sources of

arginine, as it is used in nitric oxide (NO) production, as well as other amino acids that are essential for *Leishmania*, such as tryptophan (Naderer and Mcconville, 2008). Such nutrient limitations may contribute to the infection control by the classically activated macrophage. Conversely, alternatively activated macrophages have increased availability of ornithine and urea for polyamine biosynthesis and hence may promote amastigote growth (Naderer and Mcconville, 2008).

Additionally, lipid bodies (LBs) in the macrophage may fulfill some of the parasite's nutrient requirements. LBs are organelles with a core of neutral lipids mainly triacylglycerol and sterol esters, which may act as nutrient sources for parasites. Thus, LB interaction with parasite PVs may play a role in phagosome maturation (Melo and Dvorak, 2012) and fusion with other organelles, potentially providing additional nutrient sources. Indeed, LBs induced by *L. amazonensis* amastigote infection of dendritic leukocytes were observed to be in close apposition to the PV membrane (Lecoeur et al., 2013).

1.5.3.3 Iron acquisition

Iron is an essential element for most organisms, including parasites such as *Leishmania*. This nutrient is required for *Leishmania* growth and survival. Iron acquisition by *Leishmania* is facilitated via the parasite ferric iron reductase LFR1, ferrous iron transporter LIT1 and heme transporter LHR1. The three mediators of iron uptake are upregulated in response to low iron. LHR1 is essential for *Leishmania* viability whereas LFR1 and LIT1 are required for intracellular survival (Flannery *et al.*, 2013). The host has a complex set of iron homeostatic pathways to maximize iron availability to metabolizing cells and at the same time minimize the undesired oxidative properties of excess iron. During infection, macrophages play a central role in withdrawing iron from the circulation and limiting iron to infectious agents. The systemic iron regulator, hepcidin, facilitates iron sequestration within macrophages by mediating cell surface degradation of the iron exporter ferroportin. Such host defense tactics may actually benefit *Leishmania* as an intracellular parasite of macrophages. Hepcidin deficiency or overexpression of mutant ferroportin that is resistant to hepcidin-induced degradation inhibited parasite replication. Exogenous hepcidin or expression of dominant-negative ferroportin enhanced parasite growth and restored growth of parasites defective in iron acquisition (Ben-Othman *et al.*, 2014), highlighting the role of the hepcidin-ferroportin axis in macrophage–*Leishmania* interactions and the infection outcome.

1.5.4 Macrophage defenses

1.5.4.1 Oxidative damage

One of the major tactics used by macrophages to incapacitate pathogens is the generation of ROS and reactive nitrogen intermediates (RNI). Multiple approaches are used by the macrophage to tightly control production and elimination of these deleterious species, from global macrophage activation to responses localized to pathogen-containing phagosomes. NADPH oxidase assembly at *Leishmania*-containing phagosome stimulates ROS production and superoxide burst localized to the phagosomal lumen. These findings indicate a concerted effort by multiple macrophage defense mechanisms to induce oxidative damage to the parasite and compromise its ability to survive (Podinovskaia and Descoteaux, 2015).

1.5.4.2 Macrophage activation

The macrophage is an extremely plastic cell, which encapsulates and digests dead cells and cellular debris, foreign matter, tumor cells, and above all, plays a central anti-inflammatory role by decreasing immune reactions through release of cytokines. Classical activation by IFN-γ leads to inflammatory responses and inhibits *Leishmania* growth, whereas alternative activation by IL-4 inhibits inflammation through IL-10 production and stimulates *Leishmania* growth (Liu and Uzonna, 2012).

Peritoneal resident and inflammatory macrophages infected with *L. major* promastigotes showed increased expression of FasL, TNF, IL-6, and other proinflammatory markers following induction of a cellular stress response in macrophages, via the SAPK/JNK activation (Filardy *et al.*, 2014). Interestingly, the cellular stress response also promoted parasite survival and replication in macrophages (Filardy *et al.*, 2014). Inflammation-induced IFN-γ led to the activation of members of the PKC family of protein kinases, which were critical for macrophage activation and parasite killing (Liu and Uzonna, 2012) (Hardy *et al.*, 2009).

In the absence of the protein tyrosine phosphatase (PTP) SHP-1, phagosome acidification was impaired, and pro-Cathepsin D was not processed to the active enzyme (Gomez *et al.*, 2012). This is consistent with the phagosomal profile of activated macrophages, in which phagosomal degradative capacity is decreased to promote more efficient antigen presentation (Yates et al., 2007).

Recently, IGF-1, which is negatively regulated by IFN-γ and macrophage activation, has been implicated in the control of *L. major* promastigote infection in RAW 264.7 macrophages. IGF-1

was expressed in macrophages and colocalized with parasites. IGF-1 production was inhibited by IFN-γ stimulation, which led to a reduced parasite load. Addition of extrinsic IGF-1 reversed the reduction in parasite load completely (Reis *et al.*, 2013). IGF-1-mediated mechanisms of parasite growth control remain to be explored.

1.5.5 Leishmania evasion of host defenses

1.5.5.1 Curbing inflammation

Leishmania employs a number of intervention mechanisms to counteract host defenses. *Leishmania* targets multiple signaling pathways in the macrophage to reduce infection-induced inflammation. Even as early as during inoculation of the parasites by the sand-fly vector, the parasite-produced proteophosphoglycan-rich secretory gel enhances alternative activation and arginase activity of host macrophages to promote *L. mexicana* survival (Rogers *et al.*, 2009). Infection of murine peritoneal macrophages with *L. amazonensis* stationary phase promastigotes led to suppressed LPS-induced inflammatory responses, such as the production of IL-12, IL-17 and IL-6. Interestingly, *Leishmania* also augmented LPS-induced proinflammatory cytokines IL-1α, TNF, MIP-1α and MCP-1 and the anti-inflammatory cytokine IL-10 (Lapara and Kelly, 2013). Hence, *Leishmania* may possess selectivity over manipulation of certain cytokines in order to stimulate a unique activation state in the macrophage suitable for the parasite survival.

Recently, *L. donovani* promastigote infection of murine peritoneal macrophages was shown to induce expression of host PPARγ, which is known to curb inflammation and protect the host from excessive injury. Inhibition of PPARγ facilitated removal of the parasite (Chan *et al.*, 2012). *Leishmania* also induced host PTP activation, including PTP1B, TC-PTP, PTP-PEST and SHP-1. Activation of PTPs leads to a number of events favorable for the parasite, such as the reduction of proinflammatory processes, a reduction in IL-12, NO, TNF, phagolysosomal maturation and MHC class II antigen presentation (Liu and Uzonna, 2012) (Gomez and Olivier, 2010). TRAF3 is another recently identified target of *L. donovani* promastigotes. The parasite inhibited TRAF3 degradation in order to impair TLR4-mediated inflammatory host response in RAW 264.7 cells and in bone marrow-derived macrophages. TRAF3 degradative ubiquitination is required for TLR4 activation. Reduction in TRAF3 by shRNA decreased parasite burden (Gupta *et al.*, 2014). The above studies reveal the multitude of host targets that *Leishmania* exploits in order to evade macrophage activation and the accompanying proinflammatory response.

As *Leishmania* establishes infection inside the macrophage and proliferates, the macrophage may eventually undergo apoptosis. The parasite delays macrophage apoptosis but ultimately exploits the apoptotic host cell to spread to neighboring uninfected macrophages, with minimal exposure to extracellular immune recognition systems. Cell-to-cell transfer of *L. amazonensis* amastigotes, which were isolated from BALB/c mice and used to infect bone marrow derived macrophages, was mediated by parasitophorous extrusions, enriched in lysosomal enzymes. The

PV components such as LAMP1/2 and Rab7 were shown to be internalized by recipient macrophages together with the rescued parasite and stimulate production of the anti-inflammatory cytokine IL-10 by the recipient macrophage (Real *et al.*, 2014). Thus, even at the most vulnerable stages of its life cycle, *Leishmania* successfully manipulates its host to avoid immune recognition and subsequent inflammation.

1.5.5.2 Host cell signaling interferences

Macrophages infected with *Leishmania* are defective in the expression of activation-associated functions and are unresponsive to IFN-γ (Shio *et al.*, 2012). Studies with *L. donovani* revealed that this parasite targets distinct steps along the JAK-STAT pathway. Upon contact with macrophages, *L. donovani* promastigotes activated the PTP SHP-1, which dephosphorylated JAK2. In addition, proteasome-mediated degradation of STAT1 was rapidly induced, preventing its nuclear translocation. *L. donovani* promastigotes were also reported to downregulate the IFN-γ receptor and to induce the expression of the suppressor of cytokine signaling SOCS3 (Bhattacharya *et al.*, 2011). *L. donovani* promastigotes can thus efficiently shut off the predominant signaling cascade of one of the most important macrophage activators. Similar to promastigotes, *L. donovani* amastigotes inhibited IFN-γ-induced expression of MHC class II and iNOS. However, infection with *L. donovani* amastigotes downregulated IFN-γ-induced gene expression without affecting STAT1 activation. Rather, amastigotes inhibited IFN-γ-induced STAT1 nuclear translocation by blocking the interaction of STAT1 with the karyopherin importin-α5 (Matte and Descoteaux, 2010). The underlying mechanisms remain to be elucidated.

1.5.5.3 Limiting oxidative damage

Leishmania responses to oxidative stress vary greatly depending on *Leishmania* species and host cell type (Olivier *et al.*, 2012). For example, *L. major*-infected peritoneal macrophages produced ROS, whereas in *L. amazonensis*-infected cells ROS production was inhibited (Almeida *et al.*, 2012). Various approaches are used by different *Leishmania* species to counteract oxidative stress. For example, *L. donovani* axenic amastigotes were able to impair cellular and mitochondrial ROS via the induction of mitochondrial uncoupling protein 2 (UCP2). *L. donovani* degraded the transcription factor USF-1, hence facilitating recruitment of the transcription factors SREBP2 and Sp1 to the UCP2 promoter, leading to UPC2 upregulation and inhibition of ROS (Ball *et al.*, 2014).

Leishmania is also able to avoid oxidative damage by preventing NADPH oxidase assembly at the phagosomal membrane and generation of ROS within the PV. A recent study by Matheoud and colleagues has demonstrated that *L. donovani* and *L. major* stationary phase promastigotes achieve this by cleaving the host SNARE VAMP8, which was necessary for NADPH oxidase recruitment to the phagosome of bone marrow-derived macrophages (Matheoud *et al.*, 2013). Disruption of lipid microdomains by insertion of the surface glycolipid lipophosphoglycan (LPG) in the phagosomal membrane by the parasite may also inhibit recruitment of the cytosolic components of the NADPH oxidase to the PV (Moradin and Descoteaux, 2012). As well as harming the parasite directly, oxidative damage by ROS induces apoptosis in macrophages, which destroys the replicative niche of the parasite. Apoptosis was suppressed by *L. donovani* stationary phase promastigote infection of RAW 264.7 macrophages via the induction of the suppressors of cytokine signaling SOCS1 and SOCS3, which enhanced parasite survival (Srivastav *et al.*, 2014).

1.5.5.4 Counteracting antigen presentation

Antigen cross-presentation is a critical process for immunity against pathogens. It involves presentation of foreign proteins derived from phagocytosed cargo on MHC class I for detection by cytotoxic CD8+ T cells and for orchestration of a systemic immune response. As a professional antigen presenting cell (APC), the macrophage participates in cross-presentation of *Leishmania*-derived proteins. *Leishmania* evades host immunity by inhibiting antigen cross-presentation through cleavage of the SNARE VAMP8 in murine bone marrow derived macrophages infected with *L. major* or *L. donovani* stationary phase promastigotes but not *L. donovani* amastigotes isolated from spleens of infected hamsters. Disruption of VAMP8 prevented NADPH oxidase assembly which led to more efficient phagosomal acidification and proteolysis, thereby inhibiting MHC class I presentation and T cell activation (Matheoud *et al.*, 2013) (Rybicka *et al.*, 2012) (Savina *et al.*, 2006). Both VAMP8 and VAMP3 were excluded from *Leishmania* PVs. The consequences of VAMP3 exclusion from *Leishmania* PVs are unknown. Interestingly, MHC class II-dependent antigen presentation was also compromised in *Leishmania* infection but in VAMP8-independent manner (Matheoud *et al.*, 2013) (Meier *et al.*, 2003).

Inhibition of antigen cross-presentation was also achieved via disruption of membrane lipid microdomains by the parasite (Chakraborty *et al.*, 2005). Indeed, membrane cholesterol levels were found to be reduced in infected cells and the antigen presentation defect could be corrected with liposomal delivery of exogenous cholesterol. Liposomal cholesterol was also

found to promote ROS, proinflammatory cytokine expression and intracellular parasite killing, and was implicated in cellular stress and ROS-induced apoptosis of peritoneal exudate cells infected with *L. donovani* promastigotes (Ghosh *et al.*, 2013a). Hence, lower cholesterol levels, whether through dysregulated macrophage lipid metabolism or *Leishmania*-driven cholesterol displacement or depletion, may favor *Leishmania* survival.

1.5.5.5 Autophagy induction

Induction of autophagy in by *L. amazonensis* amastigotes and stationary phase promastigotes improves intracellular parasite survival. Autophagy inhibitors, such as 3-methyladenine (3MA) or wortmannin, reduced parasite load, whereas autophagy inductors such as rapamycin or starvation did not alter or increased parasite load (Pinheiro *et al.*, 2009) (Cyrino *et al.*, 2012). Induction of autophagy was associated with NO decrease and highlights the role of this pathway in the outcome of infection (Pinheiro *et al.*, 2009).

1.5.6 *Leishmania* intracellular survival factors

A number of survival factors are secreted by the parasite and directly interact with macrophage proteins within specific signaling pathways to modulate phagosome biogenesis, macrophage defense mechanisms and systemic inflammation.

1.5.6.1 Exosomes release

Before internalization, promastigotes can release microvesicles or exosomes, into the extracellular environment to carry molecules able to modulate macrophages activity. Exposure of macrophages to exosomes could induced IL-8 secretion but not TNF, influencing parasite uptake, as well as further downstream events (Podinovskaia and Descoteaux, 2015).

Exosome composition is governed by external factors, such as temperature and pH. In fact, exosome release is upregulated at 37°C and low pH, the conditions the parasite encounters following inoculation by the sand-fly into a mammalian host, as observed with *L. donovani* stationary phase promastigotes (Silverman *et al.*, 2010a). Within 4 h of temperature shift from 26°C to 37°C, a rapid increase in protein release was induced in *L. mexicana* promastigotes via the exosomes budding from the parasite surface. *Leishmania*-secreted molecules disrupted macrophage intracellular signaling pathways, including cleavage of PTPs, altered translocation of NF-κB and AP-1 in macrophages and inhibition of NO production (Lambertz *et al.*, 2012; Hassani *et al.*, 2011). Thus, exosomes provide a means for the parasite to efficiently deliver effector molecules to macrophages and modify their behavior to benefit parasite survival.

1.5.6.2 Lipophosphoglycan

One of the best studied *Leishmania* molecules is LPG, the most abundant surface glycolipid of promastigotes. LPG shows wide variation in sugar composition between and within species. *L. braziliensis* LPG results in higher levels of TNF, IL-1β, IL-6 and NO production and a stronger but more transient MAPK activation than *L. infantum* LPG, as observed in thioglycolate-elicited peritoneal macrophages infected with late-log phase promastigotes (Ibraim *et al.*, 2013).

LPG may protect the parasite by scavenging ROS and inhibiting NADPH oxidase assembly at the phagosome (Lodge *et al.*, 2006). LPG accumulated in lipid microdomains during phagocytosis and interfered with vesicle attachment and fusion and recruitment of host mediators of phagosome maturation. As well as causing local modifications in macrophage behavior that are restricted to individual phagosomes, LPG has a more global effect on macrophages by targeting intracellular

signaling pathways. Thus, *L. mexicana* LPG activated ERK and p38 MAPK through their phosphorylation and led to the production of TNF, IL-1β, IL-12p40, IL-12p70 and IL-10 in ERK/p38 MAPK-dependent manner, as observed in human periferal blood monocyte-derived macrophages infected with *L. mexicana* stationary phase promastigotes (Rojas-Bernabe *et al.*, 2014). Production of these cytokines was also TLR2/4-dependent, and LPG has been shown to interact with TLR2 (Rojas-Bernabe *et al.*, 2014). The changes in cytokine levels affect the activation status of the macrophage as well as the more systemic inflammatory pathways. TLR9 activation has been shown to protect the host, however recent findings revealed that LPG interacts with TLR2 to decrease TLR9 to favor survival of *L. braziliensis* and *L. major* promastigotes in bone marrow-derived macrophages and thioglycolate-elicited peritoneal macrophages, respectively (Weinkopff *et al.*, 2013) (Srivastava et al., 2013). *L. chagasi* LPG upregulated heme oxygenase-1 (HO-1), a key enzyme triggered by cellular stress, which was associated with diminished production of TNF and ROS and enhanced parasite survival (Luz *et al.*, 2012).

Differentiation of promastigotes into amastigotes is accompanied by a 1000-fold downregulation in LPG levels, underlying major differences between the two life cycle stages in the two intracellular niches (Forestier *et al.*, 2011).

1.5.6.3 GP63

GP63 is metalloprotease expressed by promastigotes and is thought to be released from the parasite via exosomes (Olivier *et al.*, 2012) (Silverman *et al.*, 2010a). Indeed, parasite phagocytosis seems not to be involved in the GP63 uptake and successive intracellular changes, suggesting that *Leishmania* could modulate cell behavior prior to parasite uptake (Contreras *et al.*, 2010).

Within macrophages, GP63 induces modifications to host proteins, including cleavage of phosphorylated adaptor protein p130Cas, PTP-PEST, cortactin, TC-PTP and caspase-3, inactivation of p38 MAPK, through cleaving TAB1 (Hallé *et al.*, 2009). Additionally, studies in B10R macrophage cell line infected with *L. major* promastigotes showed that GP63 cleaves the transcription factor AP-1, which regulates proinflammatory cytokine and NO production (Contreras *et al.*, 2010). Furthermore, GP63 expressed by *L. major* stationary phase promastigotes was able to repress induction of type I IFN responses in B10R cells at translational level by targeting mTOR, the negative regulator of translation initiation by the eukaryotic initiation factor 4F (Jaramillo *et al.*, 2011). Manipulation of the macrophage by the parasite via

GP63 leads to a reduction of TNF, IL-12 and NO production among other changes geared to protect the parasite and promote its survival (Isnard *et al.*, 2012).

GP63 also targets pre-miRNA processor Dicer1 to downregulate miRNA-122, which plays a role in regulation of lipid metabolic genes. Restoration of miRNA-122 or Dicer1 increased serum cholesterol and reduced parasite burden in *L. donovani*-infected mouse liver (Ghosh *et al.*, 2013b). GP63 is also responsible for the cleavage of VAMP8 in murine bone marrow-derived macrophages infected with *L. major* promastigotes (Matheoud *et al.*, 2013). As mentioned above, this SNARE is responsible for recruiting NOX2 to phagosomes and its disruption leads to reduced ROS and compromised MHC class I presentation. GP63 also plays a role in MHC class II presentation, although the mechanisms of such effects are yet to be determined.

1.5.6.4 Inhibitors of serine peptidase

Inhibitors of serine peptidase (ISP), produced by *Leishmania,* could inhibit several of host enzymes, such as neutrophil elastase, trypsin and chymotrypsin, and it is also implicated in preventing activation of the macrophage protein kinase, PKR. PKR is generally activated in presence of dsRNA, such as during viral infections, but also in response to LPS via the TLR2/4 signaling pathway. Moreover, the production of NF-κB, TNF and IL-6 is regulated by PKR activity. Disruption of PKR activity by *L. major* purified metacyclic promastigotes inhibited activation of bone marrow-derived macrophages and killing of the parasite (Faria *et al.*, 2014).

1.6 Endoplasmic Reticulum Stress and Unfolded Protein Response

The endoplasmic reticulum (ER) is an organelle implicated in several intracellular functions: proteins synthesis, modification, folding and transportation, calcium storage lipid and sterols formation and carbohydrates metabolism. The physiological status of ER can be altered in many conditions (*e.g.*, imbalance in the ER folding capacity, nutrient privation, oxidative stress, hypoxia, ER calcium ion imbalance or N-linked glycosylation by drugs such as thapsigargin and tunicamycin). In order to restore the ER homeostasis, and therefore to ensure cell survival, a process named ER stress response or unfolded protein response (UPR) is triggered. In mammals, the UPR is sensed by three ER-transmembrane proteins, which activate three signaling pathways, operating in parallel: PERK ((PKR)-like endoplasmic reticulum kinase), IRE1 (inositol-requiring enzyme 1) and ATF6 (activating transcription factor 6). The activation of PERK and IRE1 occurs by dimerization and autophosphorylation, while ATF6 translocates to the Golgi apparatus where is activated via proteolytic cleavage. IRE1 activation triggers the C-terminal endoribonuclease domain, which removes 26 nucleotides from cytoplasmic XBP1 mRNA and lead to the translation of the spliced XBP1 (sXBP1) transcription factor (Yoshida *et al.*, 2001). sXBP1 induces the expression of ER chaperones, proteins involved in the ERAD system (ER-associated degradation), lipid production (Lee *et al.*, 2008), autophagic response (Margariti *et al.*, 2013) and proinflammatory cytokines (Martinon *et al.*, 2010). IRE1 can also contribute to the mRNAs degradation localized to the ER membrane through a process known as regulated IRE1 dependent decay (RIDD), in a condition of persistent ER stress (Figure 10) (Kimmig *et al.*, 2012). RIDD helps to maintain ER homeostasis under low ER stress but, after prolonged and unmitigated ER stress RIDD becomes cytotoxic triggering cell apoptosis (Maruel *et al.*, 2014). Moreover, activated IRE1 recruits TRAF2, that phosphorylates IκB activating NF-κB and therefore, triggering inflammatory pathways (Hu *et al.*, 2006).

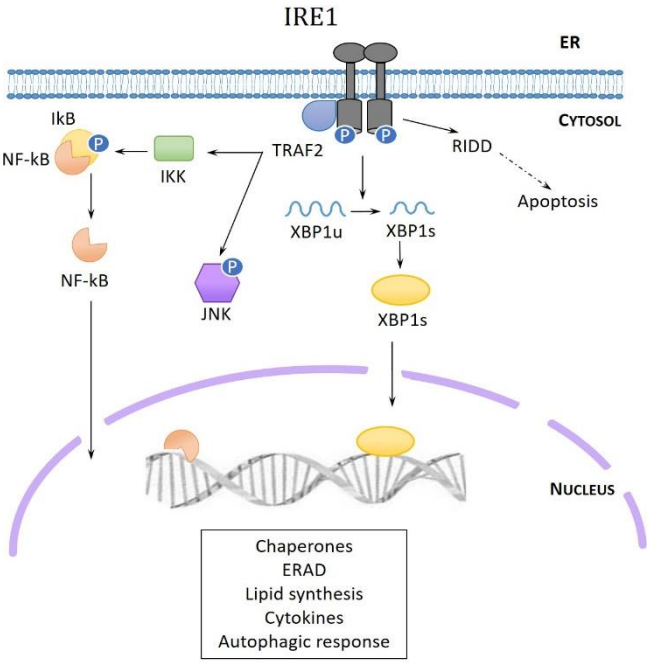

Fig. 10. IRE1 signaling in the UPR. IRE1 dimerization and autophosphorylation activates its endoribonuclease domain, which cleaves XBP1 mRNA, generating an sXBP1 mRNA that allows the translation of the active sXBP1 transcription factor. IRE1 can also contribute to the degradation of mRNAs associated with ribosomes at the ER through a process known as RIDD. Moreover, phosphorylated IRE1α interacts with IKK and JNK via the recruitment of TRAF2, therefore controlling the activation of the two major inflammatory transcription factors NF-κB and AP-1 (Galluzzi *et al.*, 2017 modified).

Once activated, PERK phosphorylates the α subunit of eIF2α, inducing a general translation reduction, therefore reducing folding requirements in the ER. At the same time, the ATF4 transcription factor eludes translation inhibition through an alternative translation initiation site and induces the expression of the transcription factor DDIT3/CHOP and GADD34, a phosphatase that regulate the eIF2α phosphorylation (Figure 11) (Novoa *et al.*, 2003). Moreover, PERK induces the expression of genes related to the antioxidant response via phosphorylation of the transcription factor NFE2L2/NRF2 (Cullinan and Diehl, 2004).

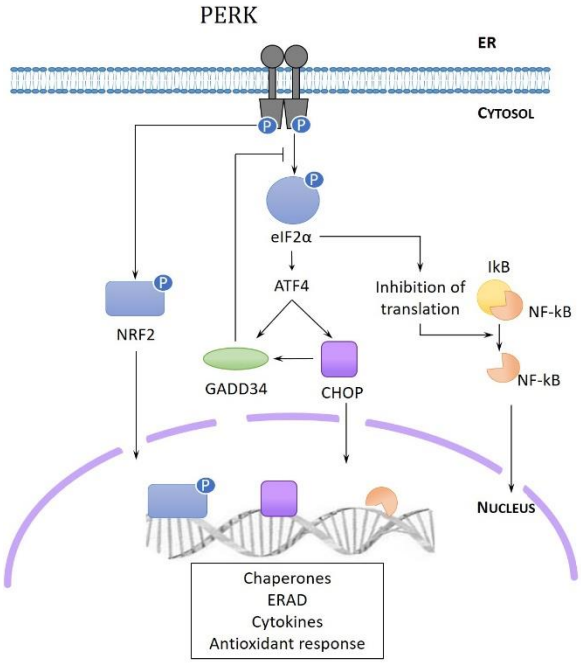

Fig. 11. PERK signaling in the UPR. PERK is a transmembrane kinase activated by dimerization and autophosphorylation. PERK phosphorylates eIF2α, leading to general inhibition of protein translation, with the exception of ATF4, which escapes inhibition of translation through an alternative translation initiation site. ATF4 induces the expression of CHOP and GADD34, a phosphatase acting as regulator of eIF2α phosphorylation. PERK can also phosphorylate and activate the transcription factor NRF2, which induces the expression of genes involved in antioxidant response. PERK-mediated eIF2α phosphorylation and consequent attenuation of translation can trigger the activation of NF-κB, since the half-life of its inhibitor (IκB) is much shorter (Galluzzi *et al.*, 2017 modified).

ATF6 is a transmembrane protein containing a bZIP in the N-terminal. Under ER stress conditions, ATF6 is translocated to the Golgi apparatus, where it undergoes proteolytic cleavage, releasing the transcriptionally active N-terminal portion. The activated ATF6 N-terminal elicits XBP1 transcription and contributes to the UPR by monitoring a number of genes associated with protein folding and lipid metabolism, some of which are controlled also by XBP1 (Figure 12) (Bettigole and Glimcher, 2015; Maiuolo *et al.*, 2011; Wu *et al.*, 2007). Two isoforms of ATF6, named ATF6α and ATF6β, are cleaved in response to ER stress. The ATF6α N-terminal is a strong transcriptional activator which is rapidly degraded, while ATF6β N-terminal is a weak and slowly degraded transcriptional activator. ATF6β acts as an endogenous inhibitor of ATF6α (Thuerauf *et al.*, 2007). ATF6α and XBP1 induce an increase in ER volume, through stimulation lipid synthesis and therefore reducing protein–protein aggregation (Bravo et al., 2013).

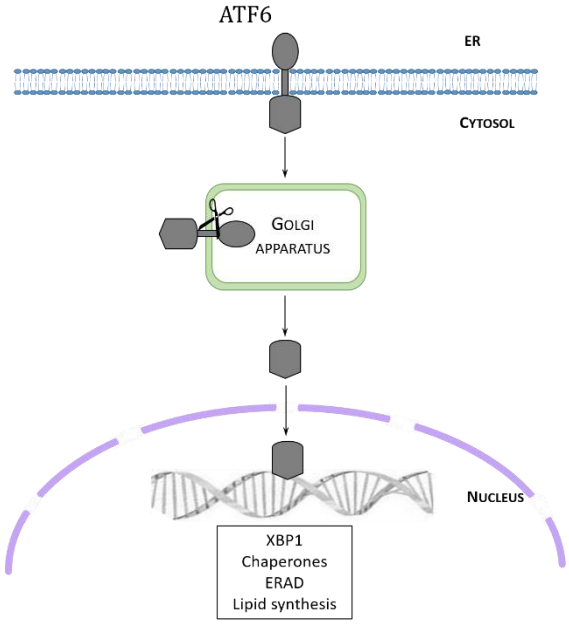

Fig. 12. ATF6 signaling in the UPR. Following ER stress, ATF6 is transported to the Golgi apparatus, where it undergoes proteolytisis and subsequent release of the transcriptionally active N-terminal portion. The active domain migrates to the nucleus, where it triggers the upregulation of XBP1 and genes related to protein folding, ERAD and lipid synthesis (Galluzzi *et al.*, 2017 modified).

These three signaling pathways have been widely investigated, but communication among them has been less investigated. It is known that ATF6 induces the transcription of XBP1, and that the increase in IRE1α expression is dependent on PERK-ATF4 pathway (Tsuru *et al.*, 2016).

These pathways are activated to restore the physiological status of the ER and to reduce the ER stress, promoting cell survival. However, if the ER stress is sustained and cannot be restored the physiological cellular status, the cell death occurs, generally by apoptosis and/or autophagy (Bhat *et al.*, 2017).

The UPR is an evolutionary mechanism conserved among eukaryotes. However, protozoans lack recognizable orthologs of Ire1, Xbp1 and ATF6, while there are evidences concerning Perk-like control of translation (Hollien, 2013).

1.6.1 The UPR in immunity and inflammation

The UPR and the innate immune response pathways are interconnected at different levels. In the innate immune response, pattern recognition receptors (PRRs), such as Toll-like receptors (TLRs), nucleotide-binding oligomerization domain (NOD)-like receptors or RIG-I (Lencer *et al.*,

2015) receptors recognize molecular patterns associated with pathogens (*e.g.* lipopolysaccharides or nucleic acids such as CpG DNA or dsRNA). PRRs are proteins expressed by innate immune system cells such as neutrophils, dendritic cells, monocytes, macrophages, but also other cells, activating the expression of several genes involved in immune cell regulation, inflammation, proliferation and survival. TLRs are Membrane-bound PRRs and represent the most characterized PRRs (Kawai and Akira, 2010). Interconnections between TLRs and UPR signaling pathways have been described: TLR2 and TLR4 specifically trigger the branch of the UPR regulated by IRE1-XBP1, promoting the production of mediators of inflammation (*i.e.*, IL-6). During this activation there is not a general ER stress response, indicating that a specific branch of the UPR can be triggered independently of the others (Martinon *et al.*, 2010). Recently, it has been shown that cytoplasmic PRRs NOD1 and NOD2, belonging to the NOD-like receptor family, have a major role in inducing inflammation during ER stress (Keestra-Gounder *et al.*, 2016). It has been shown that ER stress inducers thapsigargin and dithiothreitol (DTT), led to the production of the pro-inflammatory cytokine IL-6 via NOD1/2. Moreover, following the infection with *Brucella abortus*, which is known to activate ER stress (de Jong *et al.*, 2013), it was observed an induction of IL-6 production via TRAF2, NOD1/2 in a murine model. The activation of the key regulator for immune and inflammatory responses NF-κB, has being connected to UPR (Zhang, 2010; Zhang and Kaufman, 2008), since NF-κB could be activated through PERK-mediated eIF2α phosphorylation and consequent reduction of translation (Figure 11). When inactivated, NF-κB is bound to an inhibitor protein named IκB. The IκB half-life is much shorter than that of NF-κB, therefore the reduction of translation diminishes neo-synthesized IkB levels, leading to an increase in the amount of free NF-κB, independently from IκB phosphorylation (Deng *et al.*, 2004). Furthermore, the IkB degradation could be trigger by the IRE1α–TRAF2 complex leading to the nuclear translocation of NF-κB (Figure 10) (Hu *et al.*, 2006). The activation of NF-κB could also depend on the UPR intensity: pre-treating endothelial cells with low concentration of ER stress inducers was shown to reduce the activation of NF-κB (Li *et al.*, 2011). In addition, ER stress may have a positive or negative influence on NF-κB activity. It has been suggested that activation of NF-κB by ER stress occurs in the early stage, while its inhibition occurs at the later stage (Kitamura, 2011); NF-κB-mediated signaling inhibition has been shown to be dependent on the induction of C/EBP-β by UPR (Hayakawa *et al.*, 2010). UPR is also responsible for JNK activation and the production of reactive oxygen species (ROS). While the activation of JNK could be promote by recruitment of TRAF2 and ASK1

after phosphorylation of IRE1α (Urano *et al.*, 2000) and by the eIF2α-kinase PKR (Nakamura *et al.*, 2010), ROS can be produced during the protein folding process, by NADPH oxidase 4 (Nox4), NADPH-P450 reductase and glutathione (Zeeshan *et al.*, 2016).

1.6.2 The UPR in parasitized cells

A considerable amount of information have been provided about the role and modulation of UPR pathways in viruses and bacteria-infected cells. On the contrary, there are not a lot of studies on the UPR pathways in cells infected by intracellular protozoan parasites. The only studies present in literature are reviewed in Galluzzi *et al.* (2017) and include *Plasmodium berghei, Toxoplasma gondii*, *Cryptosporidium parvum* and *Leishmania amazonensis*.

1.6.2.1 *Plasmodium berghei*

Plasmodium spp, is a protozoan obligate intracellular parasite causing malaria. In mammals, the motile sporozoites infect hepatocytes, develop into merozoites and are released in the bloodstream where invade red blood cells, developing the disease. Malaria could lead to several complications due to the endothelial dysfunction and tissue inflammation (i.e., acute respiratory distress syndrome, cerebral or placental malaria) (Gazzinelli *et al.*, 2014). Recently, the role of UPR in hepatocytes infected with *P. berghei* has been investigated in *in vitro* and *in vivo* murine models (Inácio *et al.*, 2015). Mainly in the liver, the UPR is interconnected with metabolic pathways such as lipid and glucose metabolism (Fu *et al.*, 2012). Notably, it has been evidenced a further hepatocyte-specific UPR branch, mediated by the ER transcription factor CREBH, which does not regulate protein folding transcriptional programs but rather controls liver metabolic pathways (Lee *et al.*, 2011; Lee *et al.*, 2010). In hepatocytes, *P. berghei* induces UPR via both XBP1 and CREBH pathways. Moreover, also PERK and ATF6 arms appear to be involved. The elimination of XBP1 splicing or knockdown of CREBH is harmful to parasite development, suggesting a beneficial role for *Plasmodium* of the host UPR during hepatocytes infection (Inácio *et al.*, 2015). It is plausible that UPR supports parasite growth by regulating lipid metabolism, in particular that relating to phosphatidylcholine. In fact, the spliced XBP1 can trigger the production of phospholipids, such as phosphatidylcholine (Sriburi *et al.*, 2004), which is necessary for the correct localization of parasite proteins on the parasitophorous vacuole membrane (PVM). In this way *P. berghei* can survive inside the PV and avoid the elimination by the host during liver stage infection (Itoe *et al.*, 2014). The PVM constitutes the critical interface

between the parasite and a potentially hostile host cell environment, and the presence of *Plasmodium* proteins on the PVM was shown to be indispensable for the parasite to avoid elimination by the host cell. One of the most serious complications following *Plasmodium* infection is cerebral malaria. To examine the role of ER stress response in modulating neuronal cell death, it has been utilized an experimental murine model of cerebral malaria exploiting susceptible mice to *Plasmodium berghei* (Anand and Babu, 2013). The brains of infected and non-infected mice were examined by western blotting and immunohistochemistry, showing the activation of the three ER stress sensors such as ATF6, PERK and IRE1α. Additionally, phospho-eIF2α, sXBP1, CHOP, ATF4, GADD34 were also significantly upregulated, confirming a complete UPR activation in this infection model. The results obtained with the experimental cerebral malaria model described above, and in association with monitoring of apoptotic markers highlight a role of UPR in modulating neuronal cell death.

1.6.2.2 *Toxoplasma gondii*

Toxoplasma gondii is an obligate intracellular parasite belonging to the phylum Apicomplexa, responsible for the disease named toxoplasmosis. This parasite could invade any cell type, causing severe disease in infant, HIV/AIDS patients, or immunocompromised individuals in general. It also causes abortion, blindness or mental defects in newborns. During infection, *T. gondii* releases numerous proteins targeted to the host nucleus or to the surface of PV. ROP18 is a Ser/Thr protein kinase secreted by *T. gondii* into the host cell, where it associates to the PV membrane (Hunter and Sibley, 2012). Recently, ATF6β, which is located in the host ER and act as transcription factor in the UPR pathway, was identified as a target of ROP18. ROP18 induces the phosphorylation of ATF6β leading to its proteosomal degradation and decrease in ATF6β-mediated gene expression after induction of UPR. ATF6β-deficient mice reveal an increased susceptibility to infection, indicating that ATF6β has a crucial role in resistance against infection by *T. gondii* (Yamamoto *et al.*, 2011). The mechanism of neuropathogenesis following brain toxoplasmosis has been examined in C17.2 cells (Zhou *et al.*, 2015) and in murine neural stem cells isolated from mouse embryos (Wang *et al.*, 2014). The authors found that infection with *T. gondii* lead to apoptosis in murine neural stem cells through activation of DDIT3/CHOP, caspase-12 and JNK, all target related with UPR.

1.6.2.3 *Cryptosporidium parvum*

Cryptosporidium parvum belonging to phylum Apicomplexa, class Coccidia. This intracellular parasite can cause both anthroponotic and zoonotic disease through exposure to infected animals or exposure to water contaminated by feces of infected animals. *C. parvum* is dependent upon host derived polyamines (Cook *et al.*, 2007), as it is lacking in ornithine decarboxylase. Morada *et al*. showed that infection of human epithelial HCT-8 cells by *C. parvum* leads to an increased activity of host SAT1 (encoding for the Diamine acetyltransferase 1) in the infected cells and elevated levels of intracellular acetylspermine, which can be taken up by the parasite. Moreover, they showed in human epithelial HCT-8 cells infected with *C. parvum* an increase of the activity of host SAT1 (encoding for the Diamine acetyltransferase 1), resulting in an increase of intracellular acetylspermine, which can be taken up by the parasite. The authors also evidenced the upregulation of several UPR markers in infected HCT-8 cells, including phospho-eIF2α, CHOP, NRF2 and the chaperones GRP78 and calreticulin. These results together, suggest that infection of HCT-8 cells by *C. parvum* could trigger the UPR, leading to an increase of host SAT1 and N1-acetylpolyamines, which could be utilized by the pathogen, lacking in ornithine decarboxylase (Morada *et al.*, 2013).

1.6.2.4 *Leishmania amazonensis*

Leishmania has developed complex mechanisms to infect and survive within host cells, to evade macrophage defenses such as immune activation, oxidative damage, antigen presentation and apoptosis, and at the same time to increase nutrient availability (Podinovskaia and Descoteaux, 2015). Recently, it has been evidenced an inflammatory response, mediated by ROS and JNK signaling and triggered by *Leishmania major* in macrophages from resistant C57BL/6 mice (Filardy *et al*., 2014). Nevertheless, there are few evidence about the role of UPR following *Leishmania* infection. It has been explored the role of UPR in RAW 264.7 macrophages infected with *L. amazonensis* (Dias-Teixeira *et al.*, 2016). *L. amazonensis* infection triggers the IRE1-XBP1 branch of UPR in parasitized cells in a TLR2-dependent manner, leading to an increase of IFN-β, (Vivarini *et al.*, 2011). Moreover, sXBP1 was required to induce the expression of the gene HO-1, an antioxidant able to inhibit ROS production. Taken together these results suggest that the activation of IRE1-XBP1 branch has an important role in infection by increasing the expression IFN-β and protecting the parasites from oxidative stress, thereby promoting parasite survival and proliferation (Dias-Teixeira *et al.*, 2016).

1.6.3 The UPR pathway and miRNAs interactions

1.6.3.1 Biogenesis of miRNAs and their mechanism of action

The miRNAs are short (22-23 nucleotides) non-coding RNA molecules that regulate messenger RNAs post-transcriptionally and are synthesized within the nucleus as primary transcripts, defined pri-miRNA. These pri-miRNA have a hairpin loop structures are composed of about 70 nucleotides each and are cleaved by the Microprocessor complex formed by Drosha and DGCR8. Following this first modification a second precursor, called pre-miRNA, is produced. pre-miRNA are generate through cleaving intronic miRNAs by a microprocessor or, alternatively, evading the microprocessor, are directly recognized after splicing as pre-miRNA. The pre-miRNA is transferred in cytoplasm through Exportin 5-Ran GTP (XPO5) where mature miRNA are produced by the RNAse III Dicer. The mature miRNA is loaded within the RNA-induced silencing complex (RISC) comprising Argonaute protein (AGO) (Figure 13) (Kim *et al.*, 2009). Here, the miRNA is able to recognize target mRNA exploiting a small sequence situated at positions 2-7 at the 5' end of the miRNA, named seed region, (Lewis *et al.*, 2005). Even though the miRNA does not match perfectly with its mRNA target, the seed sequence has to be perfectly complementary.

To help the miRNA:mRNA pairing, RISC is directed to the target mRNA. miRNAs are mostly considered as negative posttranscriptional regulators of gene expression (Fabian *et al.*, 2010); in fact, molecules associated with RISC, such as AGO2, GW182, or eIF6, prevent translation initiation.

In mammals, the genome comprises several copies of miRNAs paralogs, belonging to conserved miRNA families with a lot of targets in common (each family is able to control around 300 mRNAs) (Friedman *et al.*, 2009). In fact, a single miRNA could identify numerous target mRNAs and at the same time, a single mRNA could be recognized by different miRNAs, providing a further regulation or control mechanism of gene expression (Peter, 2010). Thereby, miRNA could influence different cellular signaling pathways and functions, becoming fine-tuning controllers, which efficiently regulate the most important physiological and pathophysiological mechanisms including immunity, cell growth, metabolism, cell death. On the other hand, dysregulation of miRNAs system seems to have a central role in different human diseases (Maurel and Chevet, 2013).

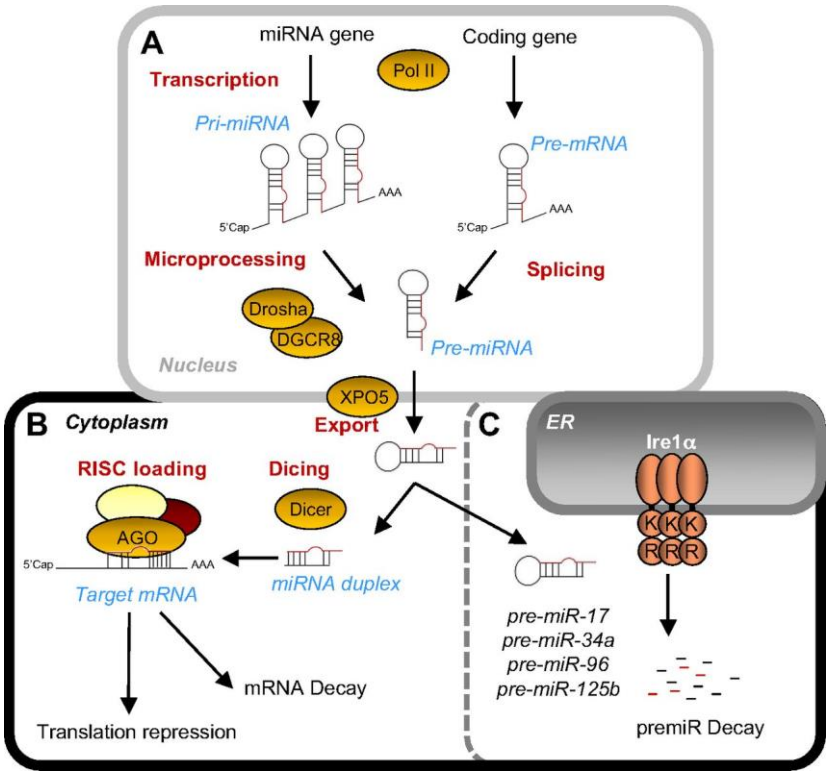

Fig. 13 miRNA biogenesis machinery. **(A)** nuclear biogenesis of pre-miRNA (miRNA) through the transcription of pri-miRNA or directly forms intronic miRNA. This mechanism is PolIII dependent and requires the presence of Drosha/DGCR8. **(B)** pre-miRNA is exported to the cytoplasm wehre is processed by Dicer into a miRNA duplex and loaded to the RNA-induced silencing complex (RISC) complex. **(C)** alternatively, it has been recently shown that pre-miRNAs were degraded by IRE1 endoribonuclease. (Maurel and Chevet, 2013).

1.6.3.2 UPR and miRNAs crosstalk

The UPR exploits multiple mechanisms in response to ER stress; among these, miRNAs induced by UPR could reveal more complexity in the regulation of protein homeostasis within the ER.

Many evidences have suggested a role of miRNAs in the UPR, such as the relocalization of AGO and the alteration of miRNAs expression pattern following ER stress. In physiological conditions, the majority of AGO proteins is diffusely distributed in the cytoplasm; on the contrary, during ER stress, AGO proteins are accumulated within structures, named stress granules (Leung *et al.*, 2006; Leung and Sharp, 2006). Stress granules are dynamic cytoplasmic macrostructures including translationally stalled mRNA/protein complexes formed in response to stress conditions (Anderson and Kedersha, 2008). During ER stress, PERK activation promotes the eIF2α phosphorylation, which induce translational arrest and inactivation of mRNA release from polysomes and stress granules formation (Kimball *et al.*, 2003). The complete organization/composition of stress granules is not clear; however, it is known that these granules

are enriched in small ribosomal subunits, inhibitors of mRNA stability/translation, miRNAs, and AGO proteins (Adeli, 2011; Anderson and Kedersha, 2008). Moreover, miRNAs are necessary for AGO localization within the stress granules, suggesting a repression role of miRNAs during ER stress (Leung *et al.*, 2006; Leung and Sharp, 2006).

Global approaches in different cellular contexts revealed that ER stress modifies the expression of many miRNAs. In fact, several miRNAs have been defined as positive or negative agent on the UPR, either through specific targets or through not well described mechanisms. For example, overexpression of miR-23a, miR-27a, and miR-24-2 (also known as miR-23a~27a~24-2 cluster) in HEK293T cells triggered the induction of CHOP, TRIB3, ATF3, and ATF4 and subsequent apoptotic cell death (Chhabra *et al.*, 2012). Moreover, it was also demonstrated that overexpression of miR-122 in liver cancers induced the decrease of UPR-signaling pathways via CDK4-PSMD10 and increased cisplatin-mediated apoptosis (Yang *et al.*, 2011). Other miRNAs have been described to directly influence the expression of specific ER constituents.

Among different miRNA found to be related to the UPR, three were well described to directly target UPR effectors: (i) miR-214 induces ATF4 downregulation, leading to inhibition of bone formation (Wang *et al.*, 2013); Duan and colleagues showed that miR-214 could modulate XBP1 expression through an unclear mechanism. They also demonstrated that following ER stress in hepatocellular cancer the expression of the miR-199a/miR-214 cluster is suppressed via NF-κB signaling pathway (Duan *et al.*, 2012). (ii) miR-140, targeting the transmembrane transcription factor OASIS (Vellanki *et al.*, 2012), lead to the expression modulation of extracellular matrix encoding genes in pancreatic β-cells under stress conditions. (iii) miR-1291 was revealed in hepatoma cells to directly target the 5'-UTR of IRE1α, inducing the overexpression of the pro-oncogenic protein glypican-3 (Maurel *et al.*, 2013).

Taken together, these data suggest a tight connection between miRNA activity and ER functions, adding new information regarding the UPR signaling pathways, which play a relevant role in physiology and pathophysiology status.

1.6.3.3 PERK-dependent miRNAs

miR-708 expression is controlled by CHOP in brain and eyes and inhibits i) neuronatin (NNAT), which regulates intracellular calcium level and leads to metastasis in brain cancer (Ryu *et al.*, 2013), and ii) rhodopsin (RHO), to prevent its excessive enter in the ER in mice (Behrman *et al.*, 2011). PERK-mediated signaling pathway was found to modulate the expression of miRNAs

involved in the modulation of the UPR. PERK activation was shown to induce the expression of miR-30-c-2*, a miRNA that in turn would inhibit XBP1 expression (Byrd *et al.*, 2010). This mechanism seems to combine the transcriptional induction of XBP1 by ATF6 in response to ER stress (Yoshida *et al.*, 2001), followed by splicing of XBP1 mRNA via IRE1α and, at last, repression of the expression of unspliced and spliced XBP1 mRNA by miR-30-c-2* to inactivate the XBP1 branch of the UPR (Byrd *et al.*, 2010). Recently, it has been shown that PERK signaling induces miR-211, which in turn reduces the proapoptotic transcription factor CHOP expression, through increase of the histone methylation of the proximal CHOP promoter (Chitnis *et al.*, 2012). Moreover, it has been demonstrated in mouse embryonic fibroblasts that miR-106b-25 cluster expression is downregulated by ATF4 and NRF2 following ER stress induced by hypericin, leading to an increase in BIM expression and a reduction in cell resistance to apoptosis (Gupta *et al.*, 2012). These findings suggest that miRNA-dependent signaling are finely regulated to control PERK and IRE1 signaling pathways.

1.6.3.4 ATF6-mediated repression of miR-455

During ischemia, ATF6 is activated to protect the heart from ischemic damage. Belmont *et al*. have shown that miR-455, normally targets the expression of calreticulin (CALR): ATF6-mediated repression of miR-455 induces an increase in CALR expression in the pathologic heart, reducing hypertrophic growth (Belmont *et al.*, 2012).

1.6.3.5 IRE1-mediated regulation of miRNA expression

Following ER stress induced by tunicamycin, it has been displayed that the increase of sXBP1 levels reflects in an increase of miR-346 expression (Figure 14). Genes target of miR-346 are involved in the immune response, including the major histocompatibility complex (MHC) class I gene products, interferon-induced genes, and the ER antigen peptide transporter 1 (TAP1). mir-346 inhibits TAP1 expression and, because TAP1 is essential for correct MHC class I-associated antigen presentation, TAP1 mRNA reduction during pathological conditions associated with UPR induction, lead to inhibition of peptide influx into the ER contributing to decreased MHC class I-associated antigen presentation (Bartoszewski *et al.*, 2012).

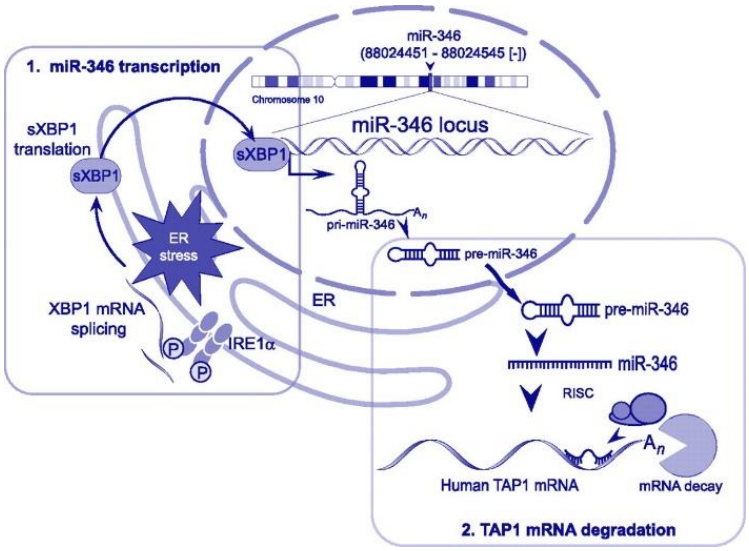

Fig. 14. ER stress-associated miR-346 induction. Step 1 miR-346 transcription. Activation of IRE1α, induces the XBP1 mRNA splicing, causing the sXBP1 protein translation. sXBP1 enters the nucleus and triggers the transcription of pri-miR-346. Step 2, target mRNA degradation. In the cytosol, is observed the maturation of pri-miR-346. Mir-346 mature recognizes the 3'-UTR of target TAP1 mRNA and recruits the RNA-induced silencing complex, inducing mRNA degradation (Bartoszewski et al., 2012).

Recently, has been shown a role of IRE1α in cleaving pre-miRNA [pre-miRNAs -17, -34a, -96, and -125b] in a different site from the canonical target of the DICER. These miRNAs normally suppress the translation caspase-2, and the IRE1α-induced cleavage triggers to the increase of protease levels and subsequently to initiation of the mitochondrial apoptotic pathway (Upton *et al.*, 2012). Moreover, destabilization of miR-17 mediated by IRE1α was demonstrate to intensify TXNIP mRNA stability. On the other hand, elevated levels of TXNIP protein activate the NLRP3 inflammasome, leading to procaspase-1 cleavage and interleukin 1β (IL-1β) secretion, therefore increasing the systemic or local inflammatory response (Lerner et al., 2012).

As showed above, there are different miRNAs associated with ER stress and the UPR signaling pathways, which were identified mostly in cancer models, but little is known about the role of miRNAs following *Leishmania* infection (Maurel and Chevet, 2013). Moreover only few information are available about the mechanisms underlying miRNAs activity in regulation of macrophage effector functions and their importance in the pathogenesis. It is likely that the identified miRNAs could also be utilized as markers to distinguish various pathological status such as cured, symptomatic and asymptomatic VL infections, and also can be used to design new drug targets and control strategies (Tiwari *et al.*, 2017).

2. AIMS

Intracellular pathogens hijack organelles such as Endoplasmic Reticulum to facilitate survival and replication, thus eliciting ER stress and activating/modulating the unfolded protein response (UPR) in the host cell. The UPR is aimed to mitigate ER stress, thereby promoting cell survival. However, prolonged ER stress will activate the apoptotic pathway. Several intracellular pathogens are known to modulate the ER stress response in host cells (i.e. viruses, bacteria). However, only few studies are available regarding the UPR pathways in cells infected by intracellular protozoan parasites (e.g. *Toxoplasma gondii*, *Cryptosporidium parvum*, *Plasmodium berghei*). Moreover only few information are available about the mechanisms underlying miRNAs activity in the context of ER stress/UPR regulation in infection models.

Concerning *Leishmania*, when this project started no studies regarding the UPR in parasitized cells were available. However, a recent study (Dias Teixeira et al 2016) evidenced the role of XBP1 in *L. amazonensis* infection model.

Because mammalian leishmaniasis has a worldwide distribution and appears with different clinical forms, depending on which specie is responsible for the disease, it is important to understand and characterize the molecular mechanisms underlying *Leishmania* infection and the pathogen survival in host cells. This could contribute to identify new targets for therapeutic approaches, since current drug treatments are characterized by high toxicity, high costs and possible development of resistance forms.

The main species of *Leishmania* in Italy is *L. infantum*, responsible for CanL and sporadic cases of human VL and CL. However, most of the information in literature does not include (or marginally include) this species. Therefore, the aim of this project was to analyze the ER stress response in macrophages infected with *L. infantum* to gain insights about the pathogenic mechanisms in parasitized cells. To this end, the project has been structured in the following points:

- Optimization of infection model using *L. infantum* reference strain or isolates and cell line-derived human macrophages and murine peritoneal macrophages;
- Analysis of host stress pathways elicited following *L. infantum* infection (or exosome treatment), with particular attention to genes/proteins involved in the ER stress response.
- Evaluation of ER stressors such as tunicamycin and DTT in infected cells.
- Identification of host miRNAs potentially elicited by infection.

3. MATERIALS AND METHODS

3.1 EVANS' MODIFIED TOBIE'S MEDIUM (EMTM) PREPARATION

Leishmania parasites were cultivated in in Evans' Modified Tobie's Medium (EMTM). EMTM is a biphasic medium consisting of a liquid and a solid component (Tab. 2), and it is known to be the gold-standard for the isolation and the growth of all *Leishmania* species (Castelli *et al.*,2014). Solid Tobie was completed by adding mechanical defibrinated rabbit blood (15 ml/100 ml) (Allevamento Blood, Italy) and placed under sterile conditions in 8 ml tubes (1.5 ml) or 50 ml flask (4 ml). A 25 ml volume of liquid Tobie was supplemented just before use with 0.1% of L-proline, 2.5 µl of a 1% phenol red solution, 10% heat inactivated fetal bovine serum, 250 µg/ml gentamicin, 500 µg/ml 5-fluorocytosine, 5% human female urine. After pH adjustment to 7.1-7.2 and sterile filtration, 0.5 ml or 2 ml were added to the solid medium contained in tubes or flask, respectively. In the attempt to substitute rabbit blood, defibrinated horse blood has also been tested to prepare complete solid medium. However, *Leishmania* promastigotes did not growth in this condition and the medium was discarded.

Tab. 2. Composition of solid and liquid phases of Tobie medium.

Solid phase	(g/L)
Beef extract (+4°)	3
Bacteriological peptone	5
NaCl	8
Agar	20
Liquid phase	(g/L)
KCl	0.4
Na_2HPO_4 x 2 H_2O	0.03
KH_2PO_4	0.06
$CaCl_2$	0.14
$MgSO_4$ x 7 H_2O	0.1
$MgCl_2$ x 6 H_2O	0.1
NaCl	8

3.2 PARASITE CULTURE AND ISOLATION

The WHO international reference strain *Leishmania infantum* MHOM/TN/80/IPT1 was provided by the OIE Reference Laboratory National Reference Center for Leishmaniasis (C.Re.Na.L.) located in Palermo (Italy).

Two *L. infantum* clinical isolates were obtained from lymph node aspirates of two infected dogs, furnished by the veterinary clinic Santa Teresa (Fano, Italy). *L. infantum* infection in dogs was assessed by qPCR assay from conjunctival swabs and lymph nodes (Ceccarelli *et al.*, 2014a). Furtehrmore, the dogs were diagnosed using an indirect fluorescent antibody test (IFAT), which utilized whole fixed *L. infantum* MHOM/TN/80/IPT1 promastigotes as antigen (Reale *et al.*,1999).

A further *Leishmania* spp clinical isolate was obtained from a pharyngo-laryngeal biopsy from human patient with suspect MCL. In this case, a preliminary genotyping test was performed with two previously described qPCR assays using primer pairs MLF/MLR (Ceccarelli *et al.*, 2014b) or LMi-amaF/MLR (Ceccarelli *et al.*, 2017) followed by melting curve analysis performed from 82°C to 90°C. Purified DNA from this isolate has also been sent to the OIE Reference Laboratory National Reference Center for Leishmaniasis (C.Re.Na.L.) (Palermo, Italy) for complete genotyping and species identification through NGS approaches.

Both dog and human clinical isolates were obtained as follows: the biopsied materials were collected in 5 ml of sterile liquid Tobie medium each. After centrifugation at 1300 g 10 min at 4°C, the supernatants were discarded and tissue pellets were resuspended in 1 ml sterile Tobie medium and disrupted by pipetting. A 0.5 ml volume was added to a flask containing EMTM for parasite isolation (Galluzzi *et al.*, 2016). After 5-7 days at 26 °C, the presence of parasites was assessed by phase-contrast microscope observation at 40X magnification.

L. infantum reference strain and *Leishmania* isolates were cultivated in EMTM at the optimal temperature of 26–28°C. Stationary promastigote were transferred to fresh medium (ratio 1:5) every 5 days.

3.3 CELL CULTURE, STIMULATION AND INFECTION

The human monocytic cell lines U937 (ATCC CRL-1593.2) and THP-1 (ATCC TIB-202) were cultured at 37 °C and 5% CO_2 in a humidified incubator in RPMI-1640 medium supplemented with 10% heat-inactivated Fetal Bovine Serum (FBS), 2 mM L-glutamine, 100 µg/ml streptomycin, 100 U/l penicillin. To induce differentiation into macrophages-like cells, 6 x 10^5 cells were seeded in 35

mm dishes and stimulated with 10 ng/ml phorbol myristic acid (PMA) for 24 h. Then, the medium was replaced with fresh complete medium and cells were further incubated for 48 h.

Murine primary macrophages were removed by peritoneal washing from seven ICR/CD-1 mice (Harlan Nossan, Milan, Italy) and cultured in RPMI-1640 complete medium overnight in a humidified incubator at 37 °C and 5% CO2. Warm PBS was used to remove non-adherent cells by gentle washing. Adherent cells were incubated for a further 24 h in RPMI-1640 complete medium before infection with *L. infantum*. All cell culture reagents were purchased from Sigma Aldrich.

Macrophages derived from U937 and THP-1 cells were infected with stationary promastigotes at a parasite-to-cell ratio of 10:1. To synchronize the infection, dishes were centrifuged at 450 x g for 3 min. The murine peritoneal macrophages were infected with $5x10^6$ stationary promastigotes per dish. In order to investigate the ER stress response modulation during infection, we treated cells with 0.5 µg/ml tunicamycin or vehicle (DMSO) or for 2±6 h. As alternative ER stress inducer, 1mM dithiothreitol (DTT) were added to cells. After 6 h, 18 h and/or 24 h cells were washed three times to remove non-internalized parasites and directly lysed for successive analyses, while one dish was stained with Hoechst dye to monitor infection with a fluorescence microscope.

3.4 INFECTION INDEX CALCULATION

Cells were fixed and stained with Hoechst 6-8 hours and 21-24 hours post-infection. The infection index was evaluated over 10 images for each condition and was obtained by multiplying the percentage of infected macrophages by the average number of parasites per macrophage. At least 300 total macrophages were counted for each time of infection. Alternatively, the amount of *L. infantum* parasites infecting macrophages were quantified using a previously developed qPCR assay with a standard curve established with serial dilutions of *L. infantum* MHOM/TN/80/IPT1 DNA (Ceccarelli *et al.*, 2014b).

3.5 TOTAL RNA EXTRACTION AND REVERSE TRANSCRIPTION

To perform RNA purification, cells infected with *L. infantum* MHOM/TN/80/IPT1 and two *L. infantum* canine clinical isolates were direct lysed with 700 µl of QIAzol® Lysis Reagent (Qiagen, Hilden, Germany). Total RNA was extracted using the miRNeasy Mini Kit (Qiagen, Hilden, Germany) following manufacturer's procedure. A DNase digestion step with RNase-free DNase

set (Qiagen) was included to eliminate small amount of genomic DNA. The RNA was quantified using a NanoVue PlusTM spectrophotometer (GE Healthcare Life Sciences, Piscataway, NJ, USA). The integrity/quality of RNA was evaluated by 1% agarose gel stained with GelRed (Biotium, Hayward, CA).

The mRNAs have been reverse transcribed from 500 ng total RNA using PrimeScriptTM RT Master Mix (Perfect Real Time) (Takara Bio Inc., Otsu, Shiga, Japan) through incubation at 37°C for 15 min followed by 85°C 10 sec.

3.6 PRIMER DESIGN

The primers for gene expression analysis were designed using Primer Express 2.0 software (Applied Biosystem) or primer-BLAST tool (https://www.ncbi.nlm.nih.gov/tools/primer-blast/). Primers for human and murine targets are listed in Table 3 and Table 4, respectively. All primers were drawn on two different exons or across two exons to avoid amplification of genomic DNA, with the exception of primers amplifying MAP1LC3B and CEBPB genes. Primer's specificity was confirmed using BLAST. As reference genes, four candidate genes were considered for human samples (B2M, GAPDH, HPRT1, GUSB) and two genes for murine samples (B2M, GAPDH). All primers were purchased from Sigma-Aldrich, were resuspended in TE at 100 μM and stored at -20°C.

Tab. 3. Human qPCR primers.

Target mRNA	Accession number	Forward primer (5'-3')	Reverse primer (5'-3')
DDIT3	NM_001195053	GGAGCATCAGTCCCCCACTT	TGTGGGATTGAGGGTCACATC
HSPA5	NM_005347	CCCCGAGAACACGGTCTTT	CAACCACCTTGAACGGCAA
ATF3	NM_001674	GCCATCCAGAACAAGCACCT	GGCTACCTCGGCTTTTGTGAT
ATF4	NM_001675	CCCTTCACCTTCTTACAACCTC	TGAAGGAGATAGGAAGCCAGAC
MAP1LC3B	NM_022818	AAACGGGCTGTGTGAGAAAAC	TGAGGACTTTGGGTGTGGTTC
CEBPB	NM_005194	CGAAGTTGATGCAATCGGTTT	TTAAGCGATTACTCAGGGCCC
CHAC1	NM_024111	TGGTGACGCTCCTTGAAGATC	GCACTGCCTCTCGCACATT
sXBP1	NM_001079539	CTGAGTCCGCAGCAGGT	TGTCCAGAATGCCCAACAGG
uXBP1	NM_005080	CCGCAGCACTCAGACTACG	TGTCCAGAATGCCCAACAGG
RFX1	NM_002918	CTCCCTGAACCCCCTGGA	CCAGCCGCCAGTGAGATG
TAP1	NM_000593	CCCAGAAGCCAACTATGGAGG	AGCCTCGTCTACCTCTGTGT
IL-18	NM_001562	TGACTGTAGAGATAATGCACCCC	AGTTACAGCCATACCTCTAGGC
BCAP31	NM_001139457	TGCTGTCCTTCCTGCTTAGA	CACTAGCACTCTCCGCCTG
B2M	NM_004048	ACTGAATTCACCCCCACTGA	CCTCCATGATGCTGCTTACA
GAPDH	NM_002046	CCATGTTCGTCATGGGTGTG	GGTGCTAAGCAGTTGGTGGTG
GUSB	NM_000181	GCTACTACTTGAAGATGGTGATCG	AGTTAGAGTTGCTCACAAAGGTC
HPRT1	NM_000194	TATGCTGAGGATTTGGAAAGGG	AGAGGGCTACAATGTGATGG

DDIT3, DNA-damage-inducible transcript 3; HSPA5, heat shock 70kDa protein 5 (glucose-regulated protein, 78kDa); ATF3, activating transcription factor 3; ATF4, Activating Transcription Factor 4; MAP1LC3B, microtubule-associated protein 1 light chain 3 beta; CEBPB, CCAAT/enhancer binding protein (C/EBP), beta; CHAC1, ChaC Glutathione-Specific Gamma-Glutamylcyclotransferase 1; sXBP1, X-Box Binding Protein 1, transcript variant 2 (spliced); uXBP1, X-Box Binding Protein 1, transcript variant 1 (unspliced); RFX1, regulatory factor X1; TAP1 transporter 1, ATP binding cassette subfamily B member; IL-18 interleukin 18; B-cell receptor associated protein 31; B2M, Beta-2-Microglobulin; GAPDH, glyceraldehyde-3-phosphate dehydrogenase; GUSB, Glucuronidase, Beta; HPRT1, Hypoxanthine Phosphoribosyltransferase 1.

Tab. 4. Mouse qPCR primers

Target mRNA	Accession number	Forward primer (5'-3')	Reverse primer (5'-3')
Ddit3	NM_007837	GAGTCCCTGCCTTTCACCTT	TTCCTCTTCGTTTCCTGGGG
Hspa5	NM_001163434	TCCGGCGTGAGGTAGAAAAG	GGCTTCATGGTAGAGCGGAA
Atf3	NM_007498	CTCTCACCTCCTGGGTCACT	TCTGGATGGCGAATCTCAGC
Atf4	NM_001287180	GCAGTGTTGCTGTAACGGAC	ATCTCGGTCATGTTGTGGGG
Cebpb	NM_009883	ACCGGGTTTCGGGACTTGA	TTGCGTCAGTCCCGTGTCCA
Chac1	NM_026929	TATAGTGACAGCCGTGTGGG	GCTCCCCTCGAACTTGGTAT
sXbp1	NM_001271730	CTGAGTCCGCAGCAGGT	TGTCCAGAATGCCCAAAAGG
uXbp1	NM_013842	CCGCAGCACTCAGACTATG	TGTCCAGAATGCCCAAAAGG
B2m	NM_009735	TGCTATCCAGAAAACCCCTCAA	GGATTTCAATGTGAGGCGGG
Gapdh	NM_001289726	TGCCCCCATGTTTGTGATG	TGTGGTCATGAGCCCTTCC

Ddit3, Mus musculus DNA-damage inducible transcript 3; Hspa5, Mus musculus heat shock protein 5; Atf3, Mus musculus activating transcription factor 3; Atf4, Mus musculus activating transcription factor 4; Cebpb, Mus musculus CCAAT/enhancer binding protein (C/EBP), beta; Chac1, Mus musculus ChaC, cation transport regulator 1; sXbp1, Mus musculus X-Box Binding Protein 1, transcript variant 2 (spliced); uXbp1, Mus musculus X-Box Binding Protein 1, transcript variant 1 (unspliced); B2m, Mus musculus Beta-2-Microglobulin; Gapdh, Mus musculus glyceraldehyde-3-phosphate dehydrogenase.

3.7 QUANTITATIVE REAL-TIME PCR (QPCR)

All amplification reactions for gene expression studies were performed in a final volume of 20 µl in duplicate, using SYBR Green PCR master mix (Diatheva, Italy) or RT² SYBR Green ROX FAST Mastermix (Qiagen), 200 nM primers, in a RotorGene 6000 instrument (Corbett life science, Sydney, Australia). The corresponding amount to 2 ng of total RNA used for cDNA synthesis was loaded per each PCR tube. The amplification conditions for all targets were the following: 95 °C for 10 min, 40 cycles at 95 °C for 15 s and 60 °C for 50 s. The only exception was for the human gene ATF3: in this case the annealing/extension step was 40 s, followed by a step at 84 °C for 10 s to allow fluorescence acquisition without interferences by primer dimers. As negative control, a duplicate non-template control was included for each primer pair reaction. To confirm the absence of non-specific products or primer dimers, a melting curve analysis from 65 °C to 95 °C was conducted at the end of each run. B2M (beta-2-microglobulin) and/or GUSB (Beta-D-Glucuronidase) were selected among four candidates (B2M, GAPDH, HPRT1, GUSB) as reference genes for human targets. For mouse target, B2m was chosen as reference gene after evaluation of B2m and Gapdh. Relative mRNA expression was calculated using then comparative quantification application of the RotorGene 6000 software, followed by analysis on excel spreadsheet.

To better characterize the human clinical isolated strain, a region of kinetoplast DNA (kDNA) was amplified by two qPCR assays previously described using primer pairs MLF/MLR (Ceccarelli *et al.*, 2014a; Ceccarelli *et al.*, 2014b) LMi-amaF/MLR (Ceccarelli *et al.*, 2017). Briefly, PCR reactions were carried out in 25 µl volume containing 1 µl template DNA and 24 µl SYBR green PCR master mix (Diatheva srl, Italy) with 1U Taq Polymerase and 200 nM of each primer, using a Rotor-Gene 6000 instrument (Corbett life science, Australia). At the end of each run, a melting curve analysis was performed from 82°C to 90°C. The PCR reactions were performed in duplicate. Chelex-purified DNA from *L. infantum* strains MHOM/TN/80/IPT1 and MHOM/IT/86/ISS218, *L. amazonensis* strain MHOM/BR/00/LTB0016, *L. braziliensis* strain MHOM/BR/75/M2904 were used as controls.

3.8 XBP1 mRNA SPLICING DETECTION

Detection of XBP1 mRNA splicing was performed by conventional PCR (GeneAmp PCR System 2700) using cDNA as template and primers designed upstream (Xbp1-F 5'-GGGAATGAAGTGAGGCCAGT-3') and downstream (Xbp1-R 5'-TGAAGAGTCAATACCGCCAGA-3') of the 26-nucleotides spliced sequence. The PCR mixture had a final volume of 50 µl containing 200 nM of each primer, 2 mM $MgCl_2$, 0.2 mM dNTPs, 1 unit of Hot Rescue DNA Polymerase (Diatheva srl). The thermal amplification profile was: 94 °C for 7 min followed by 40 cycles at 94 °C for 10 s, 57 °C for 5 s and 72 °C for 15 s. The unspliced and spliced XBP1 forms gave rise to 137 bp and 111 bp products, respectively. Murine Xbp1 was amplified with primer forward (5'-ACACGCTTGGGAATGGACAC-3') and reverse (5'-CCATGGGAAGATGTTCTGGG-3') with the following conditions: 94 °C for 7 min followed by 40 cycles at 94 °C for 10 s, 58 °C for 10 s and 72 °C for 20 s. In this case, the amplification products of the murine unspliced and spliced Xbp1 were 171 bp and 145 bp, respectively. The PCR products were analyzed on 3.5% agarose gel stained with GelRedTM (Biotium, Hayward, CA). As a size standard, the GeneRuler 100-bp Plus DNA Ladder (Thermo Scientific) was included on the gels.

The relative amount of uXBP1 and sXBP1 were also monitored by qPCR using primers specific for the spliced and unspliced XBP1 forms (Tab. 3 and 4). The PCR mixtures and amplification conditions were as described above.

3.9 WESTERN BLOTTING ANALYSIS

U937 and THP-1 derived macrophage-like cells were processed for Western blot analysis as previously described (De Santi, *et al*., 2015). Briefly, cells were harvested directly in a lysis buffer containing 20 mM Hepes pH 7.9, 25% glycerol, 0.42 M NaCl, 1.5 mM MgCl2, 0.2 mM EDTA, 1 mM DTT, 1 mM Naf, 1 mM Na3VO4, and 1X complete protease inhibitor cocktail (Roche Diagnostics Ltd.). The samples were incubated 20 min on ice, and then were frozen and thawed twice. Whole cell extracts were collected after centrifugation at 10,000 x g for 10 min. Cell lysates were separated by SDS-PAGE. The gels were transferred onto a 0.2 µm pore-size nitrocellulose membrane (Bio-Rad Laboratories) and the membranes were probed with the following primary antibodies: anti-phospho-Akt (9271), anti-Akt (9272), anti-Cleaved Caspase-3 (9661) and anti-CHOP (2895) (Cell Signaling Technology); anti-XBP1 (M-186:sc-7160), anti-GRP78/HSPA5 (sc-166490) and anti-phospho-eIF2α (sc-101670) (Santa Cruz Biotechnology); anti-actin (A2066)

(Sigma-Aldrich). Signals were detected using horseradish peroxidase-conjugated secondary antibodies (Bio-Rad Laboratories). Blots were treated with ECL Kit (Amersham Bioscience) and the chemiluminescent signals were detected with light-sensitive film (Amersham Hyperfilm ECL, GE Healthcare Life Sciences) and quantified using a Chemi-Doc System (Bio-Rad Laboratories) equipped with Quantity One software.

3.10 PCR PRODUCT SEQUENCING

For genotyping purposes of the *Leishmania* human clinical isolate (see paragraph 3.2), the PCR products obtained with primers MLF/MLR were purified using the MinElute PCR purification kit (Qiagen) and directly sequenced using both forward and reverse primers. DNA sequencing was performed using the BigDye Terminator v. 1.1 Cycle Sequencing Kit on ABI PRISM 310 Genetic Analyzer (Applied Biosystems). Sequences were manually edited and aligned with 16 available *Leishmania (Leishmania)* or *Leishmania (Viannia*) sequences using default options in MUSCLE (Edgar, 2004). Phylogenetic analysis was performed with PhyML and phylogenetic tree was drawn using TreeDyn (Dereeper *et al.*, 2008).

3.11 miRNA EXPRESSION ANALYSIS

Macrophages derived from U937 and THP-1 cells infected with *L. infantum* MHOM/TN/80/IPT1 or two *L. infantum* canine clinical isolates were directly lysed at different time points with 700 µl buffer QIAzol (Qiagen). Total RNA was extracted using the miRNeasy plus kit (Qiagen) as described above. The extracted RNA was quantified using a NanoVue PlusTM spectrophotometer (GE Healthcare Life Sciences).

The expression of three microRNAs (miR-126, miR-146a and miR-346) was monitored in cell-line-derived macrophages infected by *L. infantum*. 12.5 ng of total RNA were used for cDNA synthesis through the TaqMan™ MicroRNA Reverse Transcription Kit (Applied Biosystems). The qPCR analyses were performed on a ABIPRISM 7500 Real Time PCR System (Applied Biosystems) using specific Taqman small RNA assays (Applied Biosystems). The reactions were performed in a final volume of 20 µL with the following thermal protocol: 95 °C 10 min, 40 cycles at 95 °C 15 sec and 60 °C 1 min. The relative expression levels were calculated using the 2^{-DDCt} method (Pfaffl, 2001). The data were normalized against two small nucleolar RNAs (RNU44 and RNU48).

3.12 EXOSOME ISOLATION AND CHARACTERIZATION

Medium from 10.0×10^6 cells/ml of *L. infantum* amastigote or promastigote was used to isolate exosomes at the C.Re.Na.L in Palermo, Italy. Culture medium was centrifuged sequentially for 5 min at 300 × g, 15 min at 3,000 × g, 30 minutes at 10,000 × g and ultracentrifuged 90 min at 100,000 × g in a Type 70 Ti fixed angle rotor. Pellets were washed and resuspended in PBS. To further characterize vesicles as exosomes, isolation on a 30% sucrose/D2O cushions was conducted, as described by Lamparski and colleagues (Lamparski *et al.*, 2002). Vesicles contained in the cushion were recovered, washed several times, ultracentrifuged for 90 min in PBS and collected for use. Exosome protein content was determined with the Bradford assay. Moreover, exosomes obtained as described above were analyzed by measuring the rate of Brownian motion with the NanoSight LM10 (NanoSight Ltd, Amesbury, United Kingdom) system configured with a 405 nm laser and a high-sensitivity camera sCMOS (OrcaFlash2.8, Hamamatsu C11440, NanoSight Ltd). Videos were analyzed using NTA software (version 2.3, build 0025).

3.13 CELL TREATMENTS WITH EXOSOMES

Preliminary experiments were conducted using a murine macrophagic cell line (Raw 264.7). 10 µg/ml of purified exosome were added to dishes containing $6x10^5$ cells cultured in 2ml DMEM. As control, cells were infected with *L. infantum* at two different ratio (1:10 and 1:50). Dishes were centrifuged at 1300 g for 3 min and incubated at 37°C for 24 h. After 24h cells were directly lysed and the total RNA was purified as described above.

3.14 LIBRARIES PREPARATION FOR RNA SEQUENCING

Total RNA was extracted after 24h and 48h from macrophage-derived U937 infected with *L. infantum* promastigotes or amastigotes following the phenol/chloroform extraction and isopropanol/ethanol precipitation protocol. RNA amount was evaluated with the Qubit 2.0 Fluorometer and the RNA integrity was tested with the Bioanalyzer 2100 (Agilent) using the Agilent RNA 6000 Nano Kit (Agilent) (Figure 15). Two different types of RNA libraries were prepared in parallel for successive analyses with Illumina HiSeq system: library from total RNA of non-infected and infected U937 using the TruSeq Stranded mRNA Library Prep Kit (Illumina) and enriched library from *Leishmania* RNA using the SL-seq protocol. Both libraries were first

analyzed to ensure their quality with FlashGel™ DNA System (Lonza), and then quantified using the KAPA Library Quantification kit for Illumina platforms before sequencing (Cuypers *et al.*, 2017). The preparation of the libraries was carried out at the laboratory of prof. Peter Myler at the Center for Infectious Disease in Seattle. RNA sequencing on Illumina HiSeq system and data analysis are still ongoing in the same laboratory at the time of writing this thesis.

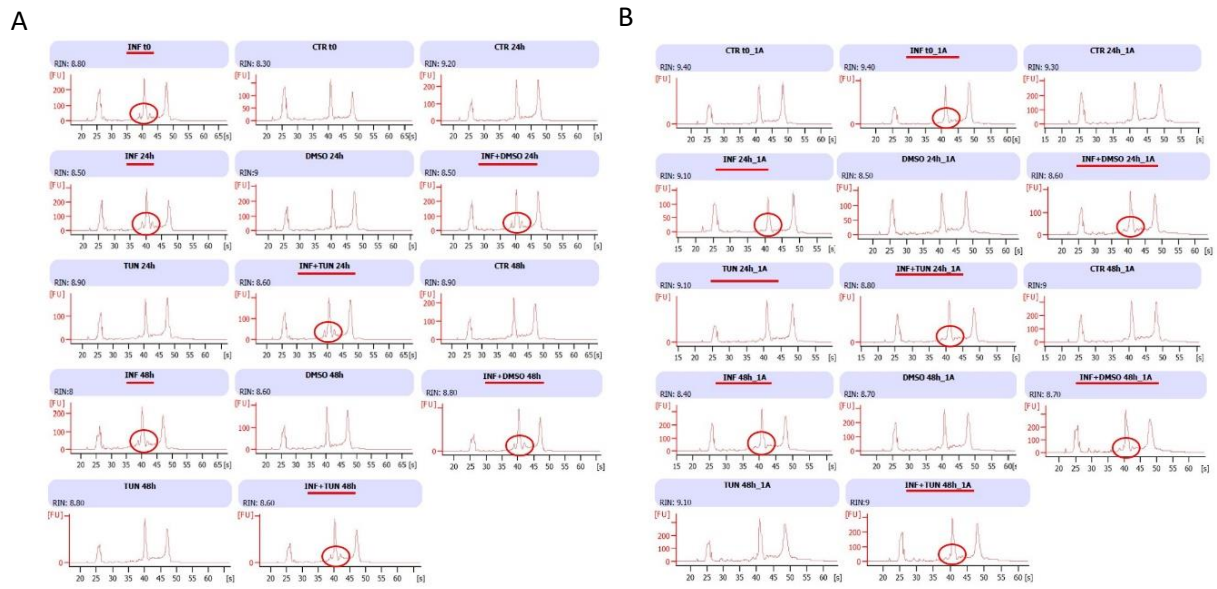

Fig. 15. RNA integrity evaluation with the Bioanalyzer 2100 (Agilent) **(A)** Extracted RNA from U937 infected *with L. infantum* promastigotes after 24h and 48h. The double peak relative to *Leishmania*-derived 16S and 23S rRNAs are evidenced **(B)** RNA extracted from U937 infected with *L. infantum* amastigotes after 24h and 48h. The double peak relative to *Leishmania*-derived 16S and 23S rRNAs is not visible, due to the semi-quiescent status of the amastigote, that lead to a decrease of genes related to translation and ribosome structure, low rates of transcription and protein turnover.

3.15 STATISTICAL ANALYSIS

Data were analyzed with Prism software (GraphPad, San Diego, CA, USA) by non-parametric test (Wilcoxon signed-rank test or Mann-Whitney test) or by two-way ANOVA followed by Bonferroni post hoc test respectively for gene expression and western blotting. All data are shown as the mean ± standard error of the mean (SEM).

3.16 ETHICS STATEMENT

Housing and treatment of mice were in compliance with the recommendations in the Guide for the Care and Use of Laboratory Animals by the Health Ministry, law 116, 1992. Mice were euthanized by carbon dioxide. Experiments were approved by the Committee on the Ethics of Animal Experiments of the University of Urbino Carlo Bo (Prot. CESA 2/2012).

4. RESULTS

4.1 PARASITE ISOLATION AND CHARACTERIZATION

Two *L. infantum* clinical strains were successfully isolated from two infected dogs as described in methods. *L. infantum* is the predominant species infecting dogs in Italy, however species identification was also assessed by a species-specific PCR (Reale *et al.*, 1999). The human isolated parasites were obtained from a biopsy from a patient with suspect MCL. In fact, after 5-7 days incubation at 26°C, the liquid phase of EMTM presented numerous motile promastigotes and several rosettes (Figure 16).

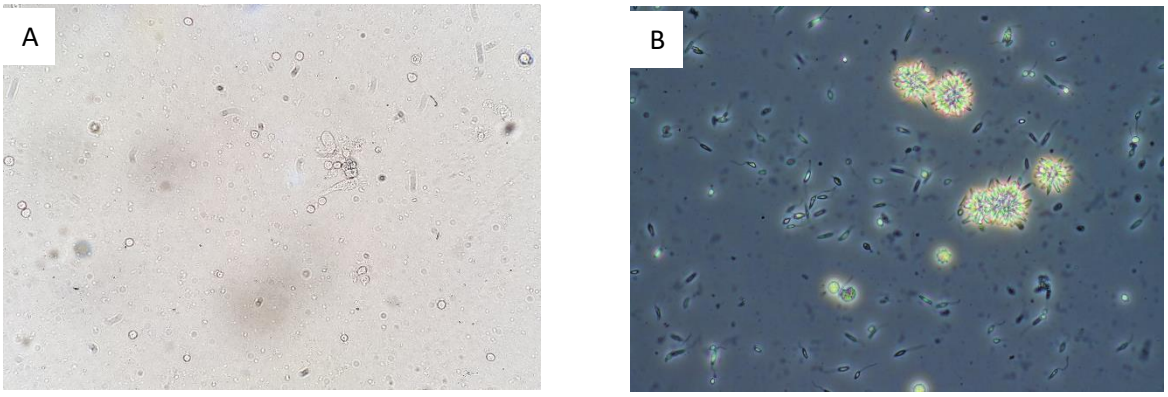

Fig. 16. Parasite isolation after cultivation in EMTM. **(A)** optical microscope examination at time 0 evidenced Only epitelial cells in the biopsied sample (20X magnification). **(B)** Phase contrast microscope examination of parasites isolated from a human pharyngo-laryngeal biopsy after 7 days incubation in EMTM (40X magnification).Individual promastigotes and promastigotes within rosettes are evident.

In this case, parasite characterization was performed by two qPCR assays followed by melting analysis as described in methods. The qPCR assay with primers MLF/MLR gave positive amplification results while no amplification was observed with primers LMi-amaF/MLR, therefore excluding the presence of *L. (L.) amazonensis* (Ceccarelli *et al.*, 2017). Moreover, Tm analysis of MLF/MLR amplicons, performed with the genotyping analysis tool of Rotor-Gene 6000 software, allowed assigning amplicons to *Viannia* subgenus (Ceccarelli *et al.*, 2014b) (Figure 17).

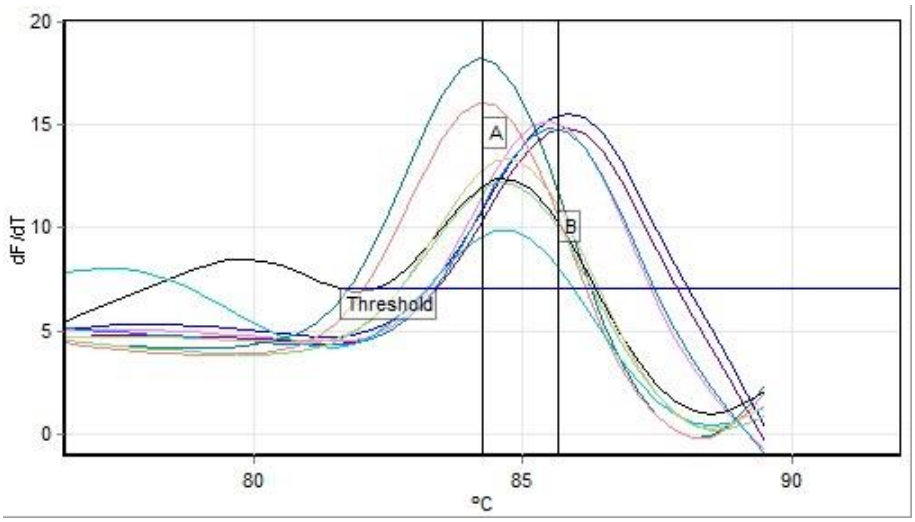

No.	Colour	Name	Type	Genotype	Peak 1
3		L. infantum MHOM/TN/80/IPT1	Unknown	Leishmania	85.8 (B)
4		L. infantum MHOM/TN/80/IPT1	Unknown	Leishmania	85.8 (B)
5		L. amazonensis MHOM/BR/00/LTB0016	Unknown	Leishmania	85.5 (B)
6		L. amazonensis MHOM/BR/00/LTB0016	Unknown	Leishmania	85.5 (B)
7		L. braziliensis MHOM/BR/75/M2904	Unknown	Viannia	84.2 (A)
8		L. braziliensis MHOM/BR/75/M2904	Unknown	Viannia	84.3 (A)
11		**Leishmania spp human isolate**	Unknown	**Viannia**	84.7 (A)
12		**Leishmania spp human isolate**	Unknown	**Viannia**	84.7 (A)
13		**Leishmania spp human isolate**	Unknown	**Viannia**	84.7 (A)
14		**Leishmania spp human isolate**	Unknown	**Viannia**	84.7 (A)

Fig. 17. Melt report generated by the genotyping analysis tool of Rotor-Gene 6000 software. The amplicons from *Leishmania* spp human isolate were assigned to *Viannia* subgenus (Ceccarelli *et al.*, 2014b).

This result was confirmed by PCR product sequence analysis, followed by alignment with *Leishmania (Leishmania*) or *Leishmania (Viannia*) sequences available in our laboratory and phylogenetic tree construction (Figure 18). This finding was consistent with the patient clinical history and presentation. The DNA from human isolate was purified and sent to the National Reference Center for Leishmaniasis (C.Re.Na.L.) (Palermo, Sicily) for further characterization through NGS techniques. Typing results are not available at the moment of writing this thesis. Due to lack of species determination, this human isolate was not used for further infection experiments.

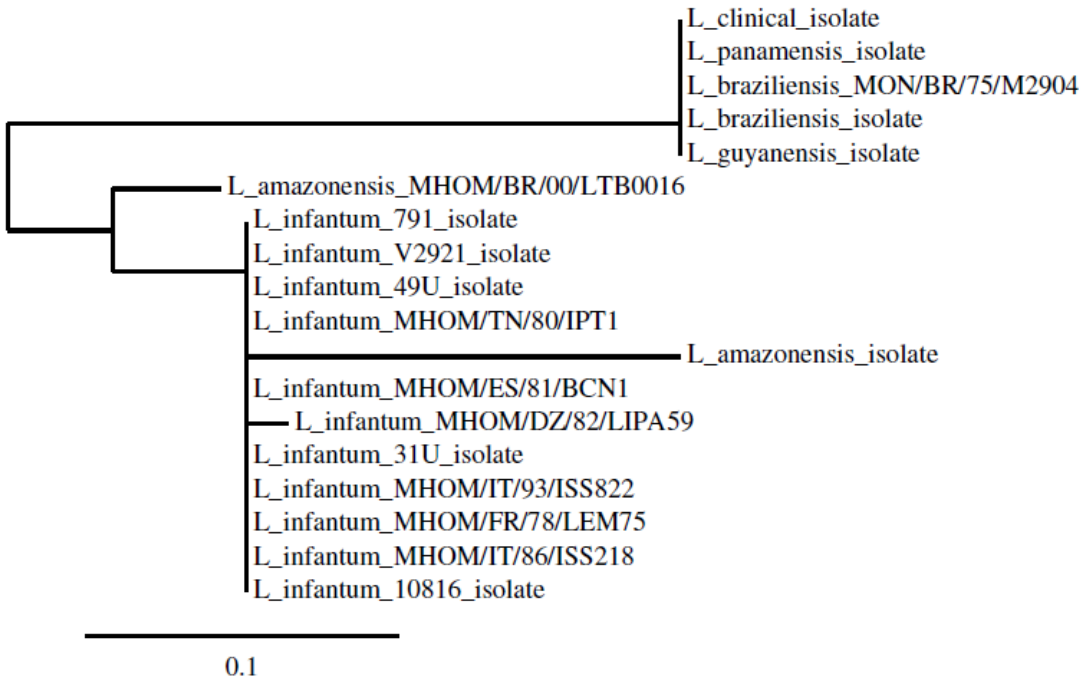

Fig. 18. Phylogenetic tree based on the kDNA region amplified with MLF/MLR primers. The phylogenetic analysis was performed with PhyML after alignment with MUSCLE. Phylogenetic tree was drawn using TreeDyn. The sequence of *Leishmania* spp clinical isolate clusterizes with species belonging to *Leishmania* (*Vianna*) subgenus.

4.2 OPTIMIZATION OF THE INFECTION MODEL AND MONITORING OF INFECTION

Leishmania (Leishmania) infantum MHOM/TN/80/IPT1 (WHO international reference strain) obtained from the OIE Reference Laboratory National Reference Center for Leishmaniasis in Palermo, Italy (Centro di Referenza Nazionale per la Leishmaniosi, C.Re.NaL.) was used to optimize the infection protocol. Macrophages differentiated following appropriate stimulation with phorbol myristic acid (PMA) from a human monocytic cell line (U937) were also used. Different cell to parasite ratio have been tested (*i.e.* 1:5, 1:10, 1:20). The optimal infection rate was found to be 1:10 (macrophages:parasites).

The infected cells were monitored by microscope observation after removal of not internalized parasites by washing with cold PBS. Initially, May-Grünwald Giemsa stain was used to observe infected macrophage, after 4% formaldehyde fixation. This method has been found to be problematic since it was difficult to identify the extra/intra cellular position of *Leishmania*. Subsequently, fluorescence stain with Hoechst dye (for nucleic acid staining) was used in cells fixed with formaldehyde 4% and permeabilized with pure cold methanol. Using this stain, it was possible, in a time-course experiment, from 15 minutes to 72h post infection, to analyse the parasite uptake of the cells. The results showed that the parasites started to infect cells after 15 minutes (Figure 19A); after 24 hours the percentage of infected cells was about 40% and after 48 hours of about 90% (Figure 19B). At 72h post infection, a few amount of infected cells were still viable, therefore the infection time was limited to 48 h in further experiments.

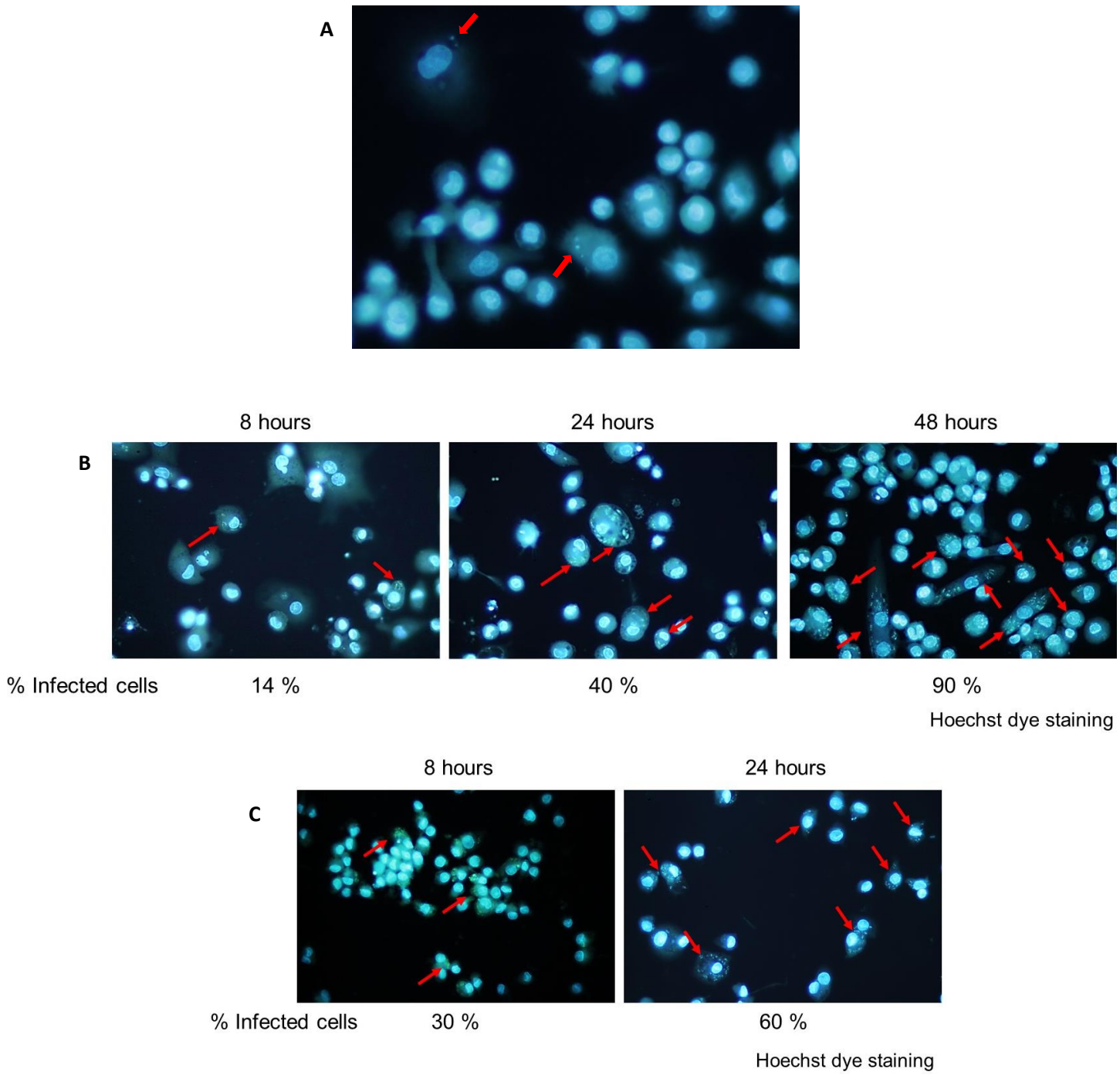

Fig.19. U937-derived macrophages infection with *Leishmania infantum*. The results showed a parasite uptake after 15 minutes of infection **(A).** After 24 hours of infection the percentage of infected cells was about 40% and after 48 hours of about 90% **(B).** After addition of a cytocentrifugation step after infection, it is observed an increase of the percentage on infected cells after 8 hours and 24 hours **(C)** (Galluzzi *et al.*, 2016).

This infection protocol was initially used in experiments for gene expression analyses; ER stress response was evaluated following the expression of several marker genes, as well as monitoring of XBP1 splicing. The first infection experiments performed on U937-derived macrophages did not show significant variations of the ER stress markers analyzed.

This may be due to the fact that mRNA variations are transient events, which may require simultaneous uptake of more *Leishmania* parasites by the cells.

To further optimize the infection protocol and therefore to synchronize the *Leishmania* entry in a shorter time, a cytocentrifugation step was added after addition of the parasites.

The monitoring of infection by microscope after Hoechst dye staining allowed to establish a sensible increase in the infection rate. In fact, the centrifugation step markedly increased macrophages infection, revealing about 30% and 60% of infected cells after 8 and 24 h, respectively (Figure 19C). Therefore, the infection protocol including a centrifugation step was utilized in the subsequent experiments.

As indicated in methods, U937-derived macrophages were infected with *L. infantum* promastigotes. After 6 h or 24 h to monitor internalized parasites, cells were washed, stained with Hoechst dye and observed with a fluorescence microscope. The infection index was 59 ± 15.7 after 6 h and 266.8 ± 89.8 after 24 h of infection (average ± SD values from 3 independent experiments). Active infection was established also by quantification of *Leishmania* parasites within cells using a qPCR assay previously developed (Ceccarelli, *et al.*, 2014b). This assay was designed on kDNA minicircles and quantification relied on a standard curve constructed with DNA extracted from a known number of *L. infantum* MHOM/TN/80/IPT1 promastigotes (Figure 20). Both methods allowed to establish that infection was time-dependent and significantly higher at 24h respect to 6 h (t-test $p < 0.01$unpaired t-test Welch corrected).

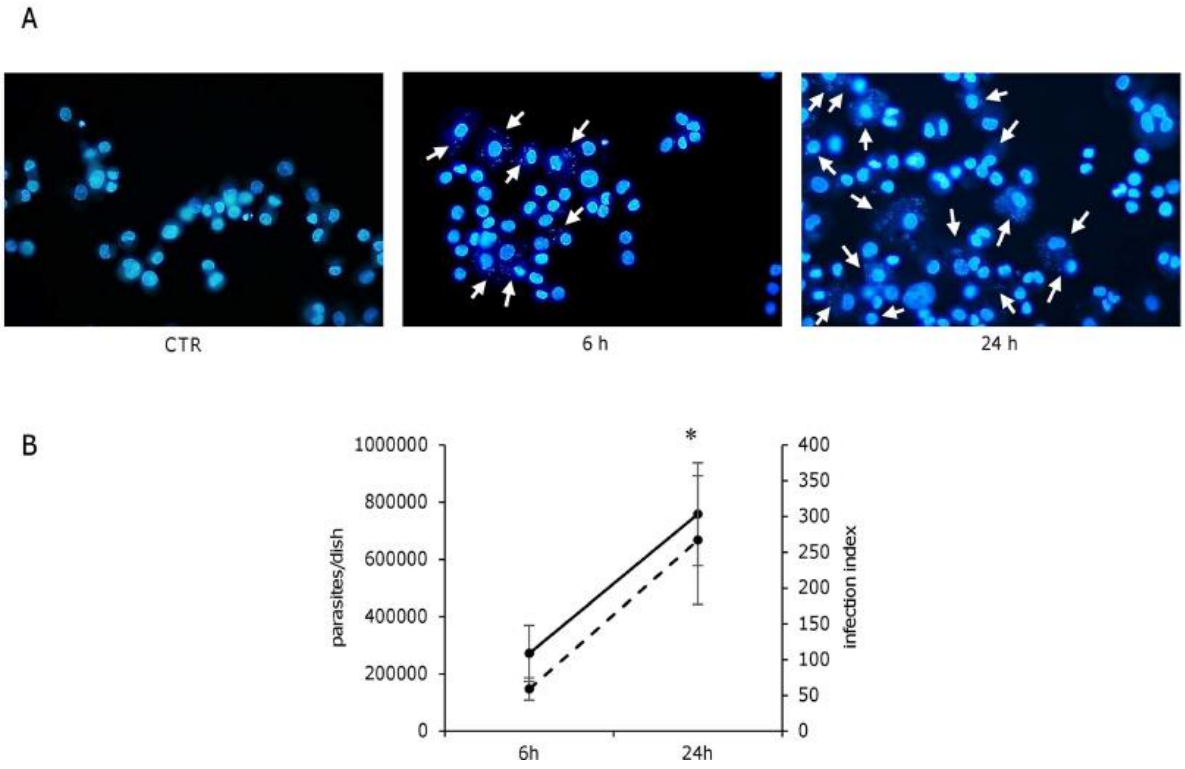

Fig. 20. *L. infantum* actively infects U937-derived macrophages. A) Hoechst dye staining of U937-derived macrophages infected with *L. infantum* promastigotes Arrows indicate parasitized cells. B) Active infection was monitored by calculating the infection index: at least 300 total macrophages per infection time (dotted line), and a qPCR assay targeting kDNA of *Leishmania* (solid line) were considered. The data are representative of three independent experiments. CTR, uninfected control. * $p < 0.05$ (unpaired t-test Welch corrected) (Galluzzi *et al.*, 2016).

4.3 *L. INFANTUM* INFECTION INDUCES AKT PHOSPHORYLATION AND INHIBITS THE TUNICAMYCIN-INDUCED CASPASE-3 ACTIVATION IN U937-DERIVED MACROPHAGES

Previously, Ruhland *et al.*, described the Akt phosphorylation at Ser473 and the inhibition of caspase-3 activation following treatment with camptothecin or actinomycin D in RAW 264.7 macrophages infected with *L. major*, *L. amazonensis* and *L. pifanoi* promastigotes (Ruhland *et al.*, 2007). Moreover, it was also shown that *L. infantum* affected the survival of U937 cells after treatment with actinomycin D via inhibition of caspase-3 activation (Lisi *et al.*, 2005). To better understand the mechanisms underlying the apoptosis resistance in parasitized cells, we first determined whether *L. infantum* infection was able to activate the Akt signaling pathway and inhibit caspase-3 cleavage in our infection model. As ER stressor and inducer of apoptosis it has been used tunicamycin (known an inhibitor of N-glycosylation). After 18 h infection, Akt phosphorylation and cleavage of caspase-3 were evaluated by western blotting, showing a significant increase in Akt phosphorylation in infected cells compared to non-infected controls. Tunicamycin treatment did not significantly influence Akt phosphorylation, neither in infected nor in non-infected cells (Figure 21). Moreover, the cleavage of caspase-3, evident in tunicamycin-treated cells, was completely prevented in cells infected with *L. infantum* (Figure 21). Taken together, these results confirmed the establishment of a productive infection, according to previous data obtained with the apoptosis inducers camptothecin and actinomycin D.

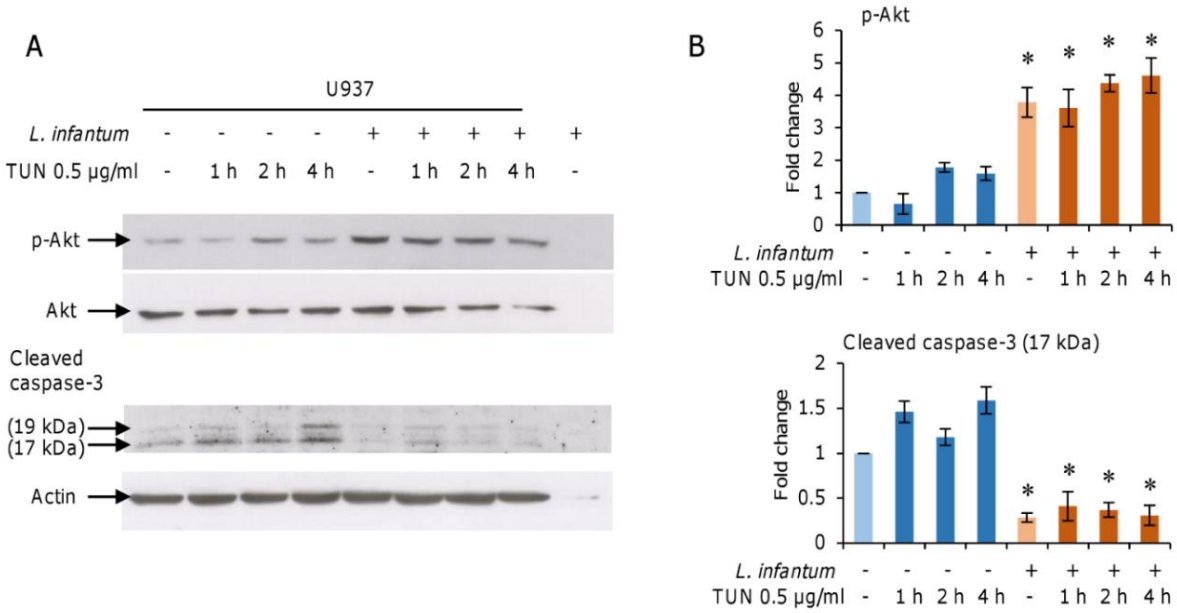

Fig. 21. *L. infantum* infection induces cell survival and inhibits apoptosis. U937 cell-derived macrophages infected with *L. infantum* promastigotes for 18 h. Non-infected and infected cells were treated with 0.5 µg/ml tunicamycin for 1 h, 2 h and 4 h. **(A)** Analysis in total cell lysates by western blotting of Akt phosphorylation and cleavage of caspase-3. **(B)** Band density quantification using a Chemi-Doc System. Results are representative of three experiments. * $p < 0.05$ (Galluzzi *et al.*, 2016).

4.4 *L. INFANTUM* INFECTION INDUCES MILD ER STRESS RESPONSE

To investigate the ER stress response in U937-derived macrophages infected with *L. infantum*, the expression of selected ER stress marker genes listed in Table 3 was monitored by qPCR at 6 h and 24 h post-infection. As reference genes, B2M and/or GUSB were selected since their expression did not change significantly after the infection (Figure 22A). The expression of the housekeeping genes decreased significantly starting from 48 h post-infection, and therefore later time points were not taken into consideration (Figure 22B). Furthermore, has been described a general downregulation of gene expression after 72 h post-infection (Buates *et al.*, 2001 and Ovalle-Bracho *et al.*, 2015).

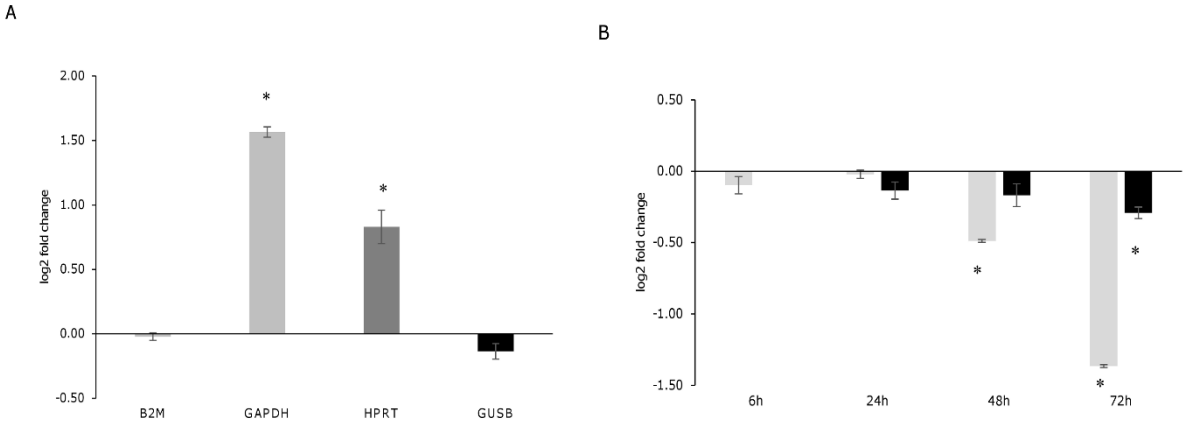

Fig .22. Evaluation of the housekeeping genes. **(A)** Log2 fold change of the four candidate housekeeping genes (B2M, GAPDH, HPRT, GUSB) in U937-derived macrophages after 24 h infection in comparison to the non-infected controls. **(B)** Analysis of B2M (grey bars) and GUSB (black bars) expression in U937-derived macrophages infected for 6 h, 24 h, 48 h, 72 h, in comparison to the non-infected controls. The quantity corresponding to 50 ng of total RNA used for cDNA synthesis was loaded per each PCR tube. * $p < 0.05$ (Galluzzi *et al.*, 2016).

The gene expression analysis showed a significant induction of the ER stress markers DDIT3/CHOP, ATF3, ATF4, CEBPB and the autophagy marker MAP1LC3B, both at 6 h and 24 h post-infection; HSPA5 was significantly induced only after 24 h, while CHAC1 did not show any significant variation (Figure 23A). A similar trend of gene expression was detected after infection with two *L. infantum* isolates (Figure 24). As positive control of UPR, cells were treated with 0.5 µg/ml of the ER stress inducer tunicamycin. All genes tested resulted significantly upregulated after treatment with tunicamycin (Figure 23B). In this case, the magnitude of induction was significantly higher as compared with infected cells ($p < 0.05$, Wilcoxon matched-pairs signed-rank test). DTT treatment also induced a significant

upregulation of ER stress markers, although to a lesser extent in comparison with tunicamycin treatment (Figure 25).

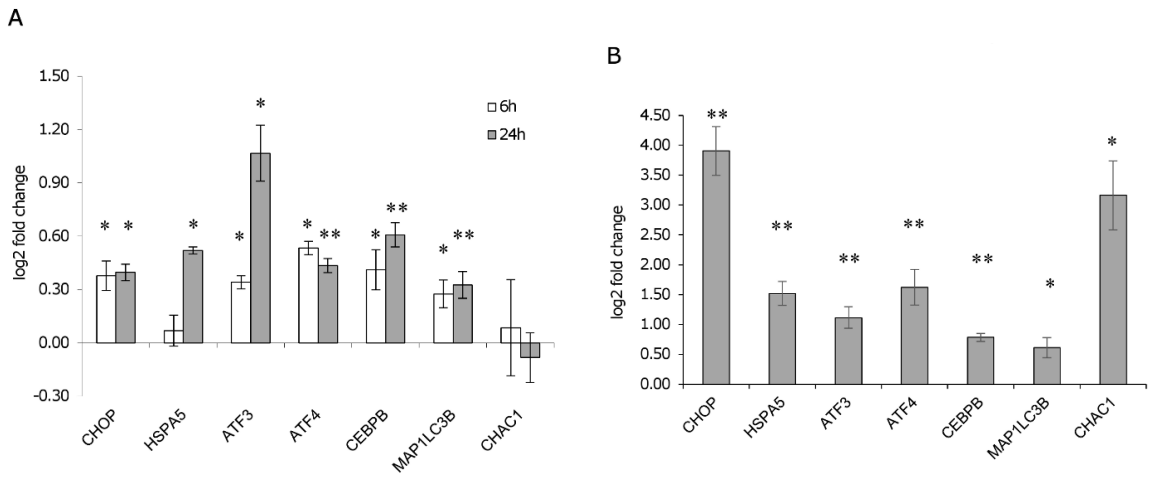

Fig. 23. ER stress expression markers in infected U937-derived macrophages. **(A)** Gene expression analysis in U937-derived macrophages infected for 6 h and 24 h with *L. infantum*. The graph shows the log2 fold changes in comparison to the non-infected control. **(B)** Gene expression in U937-derived macrophages following tunicamycin treatment (0.5 µg/ml, 6 h). The graph shows the log2 fold changes in comparison to the control (DMSO) values. Data are represented as the mean ± SEM of at least three experiments. * $p < 0.05$, ** $p < 0.01$ (Galluzzi *et al.*, 2016).

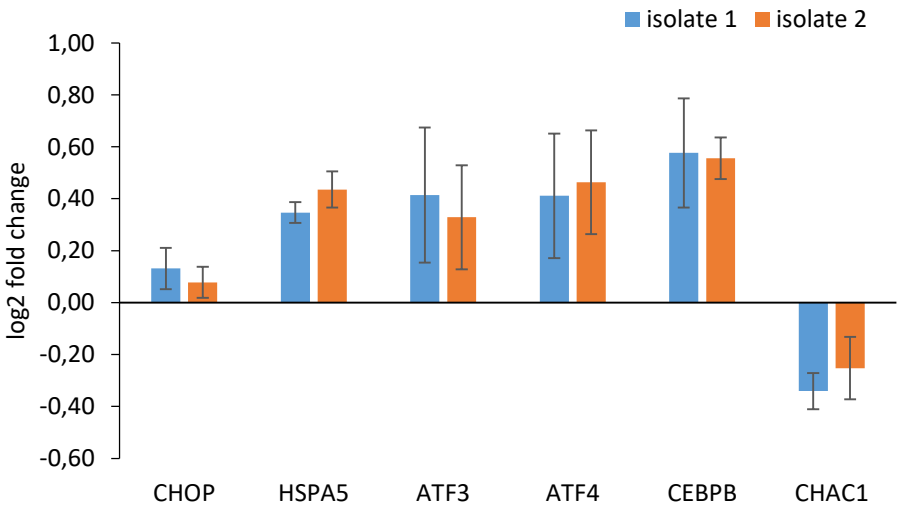

Fig. 24. ER stress expression markers in U937-derived macrophages infected with two *L. infantum* isolates. Gene expression profiling in U937-derived macrophages 24 h after infection with *L. infantum* isolate 1 (blue bars) and isolate 2 (orange bars). The graph shows the log2 fold changes in comparison to the control (non-infected). Data are represented as the mean ± SEM of two experiments. * $p < 0.05$ (Galluzzi *et al.*, 2016).

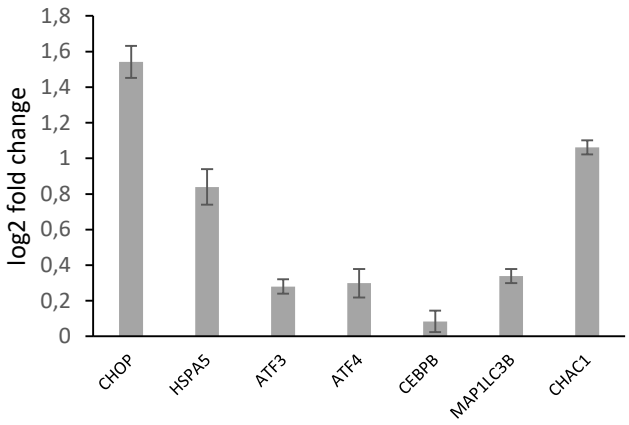

Fig. 25. ER stress expression markers in U937-derived macrophages treated with DTT. Gene expression in U937-derived macrophages following 2 h treatment with 1 mM DTT. The graph shows the log2 fold changes in comparison to the control (mean ± SEM) (Galluzzi *et al.*, 2016).

The splicing of XBP1 mRNA was never detected in cells infected with *L. infantum* using conventional PCR (Figure 26A). However, with a specific qPCR assay aimed to amplify the spliced and the unspliced sequence, was revealed a significant increase in the spliced form after 24 h of infection (Figure 26B). Interestingly, in contrast to the canonical UPR induced by tunicamycin, also uXBP1 expression increased significantly, although to a less extent compared to sXBP1.

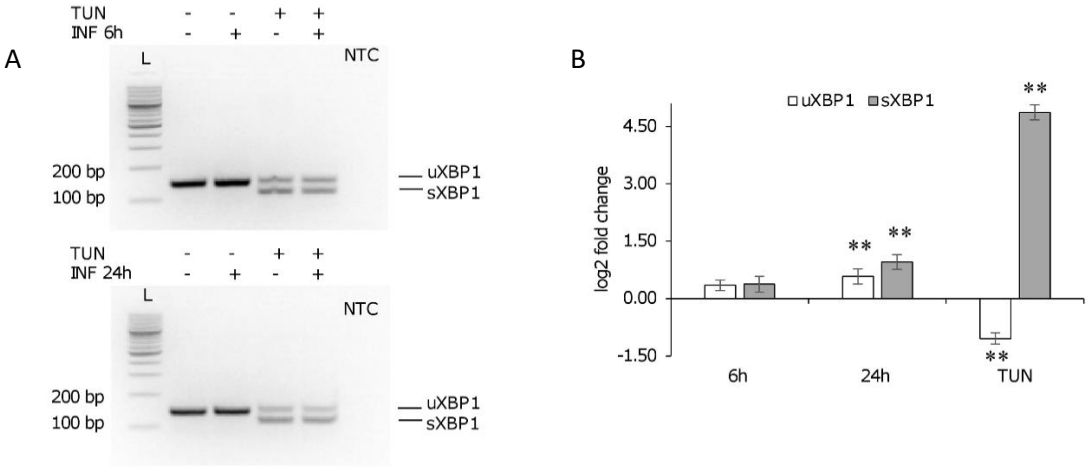

Fig. 26. *XBP1* splicing following *L*. *infantum* infection in U937-derived macrophages. U937-derived macrophages were infected with *L*. *infantum* promastigotes for 6 h or 24 h. *XBP1* splicing/induction in infected and non-infected cells treated with 0.5 µg/ml tunicamycin for 6 h was used as positive control. **(A)** *XBP1* splicing was not detected using conventional PCR in infected cells. **(B)** qPCR revealed a significant induction of both uXBP1 and sXBP1 after 24 h of infection, while tunicamycin treatment induced an increase in sXBP1 and a decrease in the uXBP1. ** $p < 0.01$. TUN, tunicamycin; L, 100 bp DNA ladder; NTC, no template control (Galluzzi *et al.*, 2016).

A similar tendency of gene expression was observed in murine macrophages at 24 h post-infection (Figures 27 and 28) with an infection index 83 ± 33, even though there were differences in the expression of Chac1 and Cebpb (Figure 27A). Moreover, the unspliced form of Xbp1 did not appear significantly affected neither by infection nor by tunicamycin treatment (Figure 28).

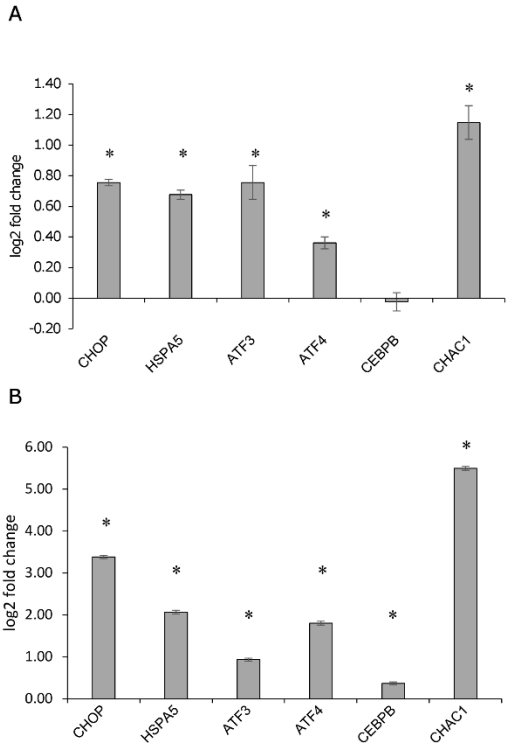

Fig. 27. ER stress expression markers in infected murine macrophages. **(A)** Gene expression analysis in murine macrophages infected for 24 h with *L*. *infantum*. The graph shows the log2 fold changes in comparison to the control (non-infected). **(B)** Gene expression analysis in murine macrophages treated with tunicamycin treatment (2 µg/ml) for 4 h. The graph shows the log2 fold changes in comparison to the control (DMSO) values. Data are represented as the mean ± SEM of two experiments, * $p < 0.05$ (Galluzzi *et al.*, 2016).

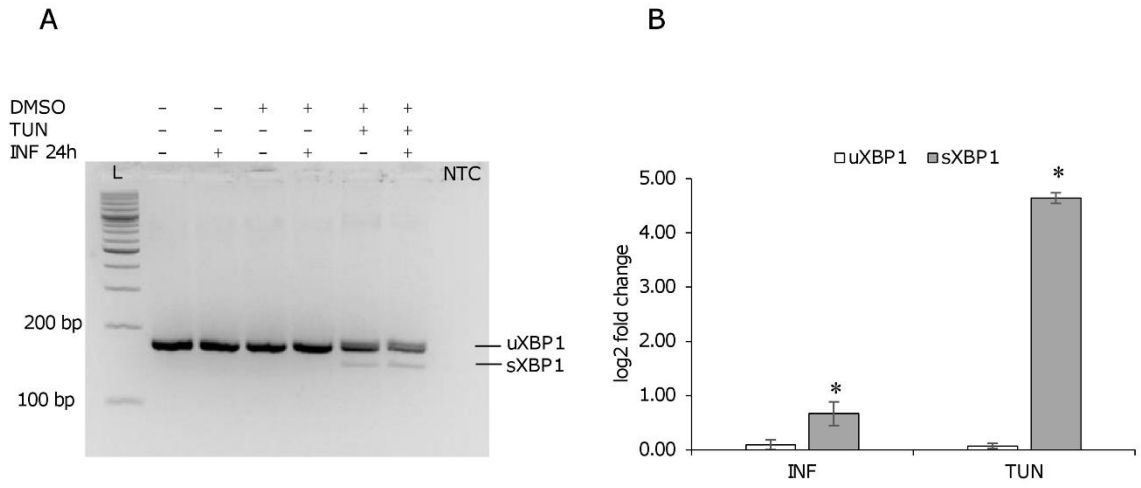

Fig. 28. *Xbp1* splicing following *L*. *infantum* infection in murine macrophages. Murine macrophages were infected with *L*. i*nfantum* promastigotes for 24 h. Infected and non-infected cells treated with 2 µg/ml tunicamycin for 4 h were used as positive control. **(A)** *Xbp1* splicing was not detected using conventional PCR in infected cells. **(B)** qPCR revealed a significant induction of sXbp1 after 24 h infection or tunicamycin treatment. ** p < 0.01. TUN, tunicamycin; L, 100 bp DNA ladder; NTC, no template control (Galluzzi *et al.*, 2016).

The western blot analyses of U937-derived macrophages after *L. infantum* infection showed the induction of sXBP1 and GRP78/HSPA5 proteins (Figure 29). However, *L. infantum* infection did not appear to induce the ER stress markers phospho-eIF2α and DDIT3/CHOP (Figure 30). Taken together, these results account for a mild induction of ER stress and UPR following *L. infantum* infection.

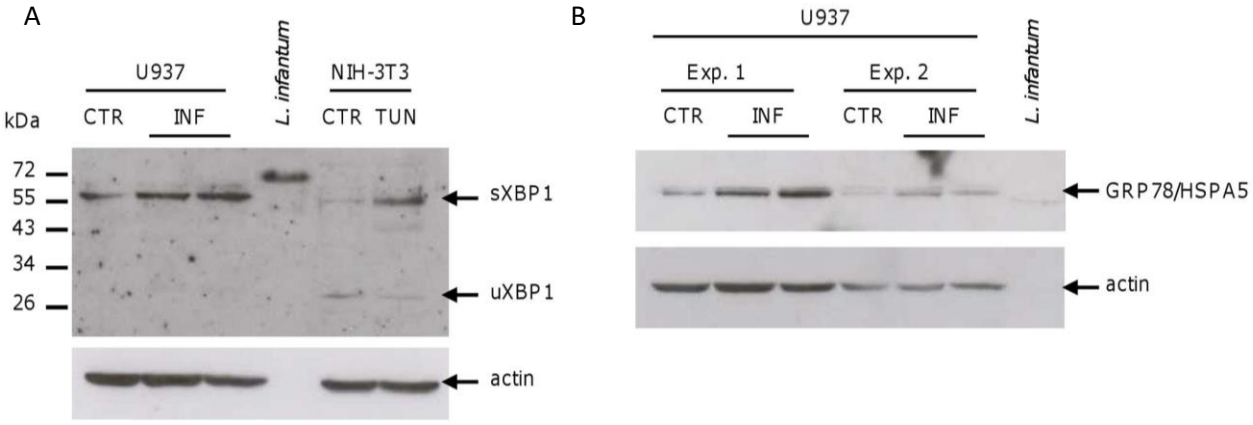

Fig. 29. *L*. *infantum* infection induces sXBP1 and GRP78/HSPA5 proteins. U937-derived macrophages were infected with *L*. *infantum* promastigotes for 18 h and protein changes were analyzed by western blotting. **(A)** The sXBP1 protein levels were analyzed in total cell lysates. Infected cells are shown in duplicate. NIH/3T3 cells treated with tunicamycin were used as positive control for antibody signal. **(B)** The HSPA5/GRP78 protein levels were analyzed in total cell lysates from two separate experiments. Infected cells are shown in duplicate (Galluzzi *et al.*, 2016).

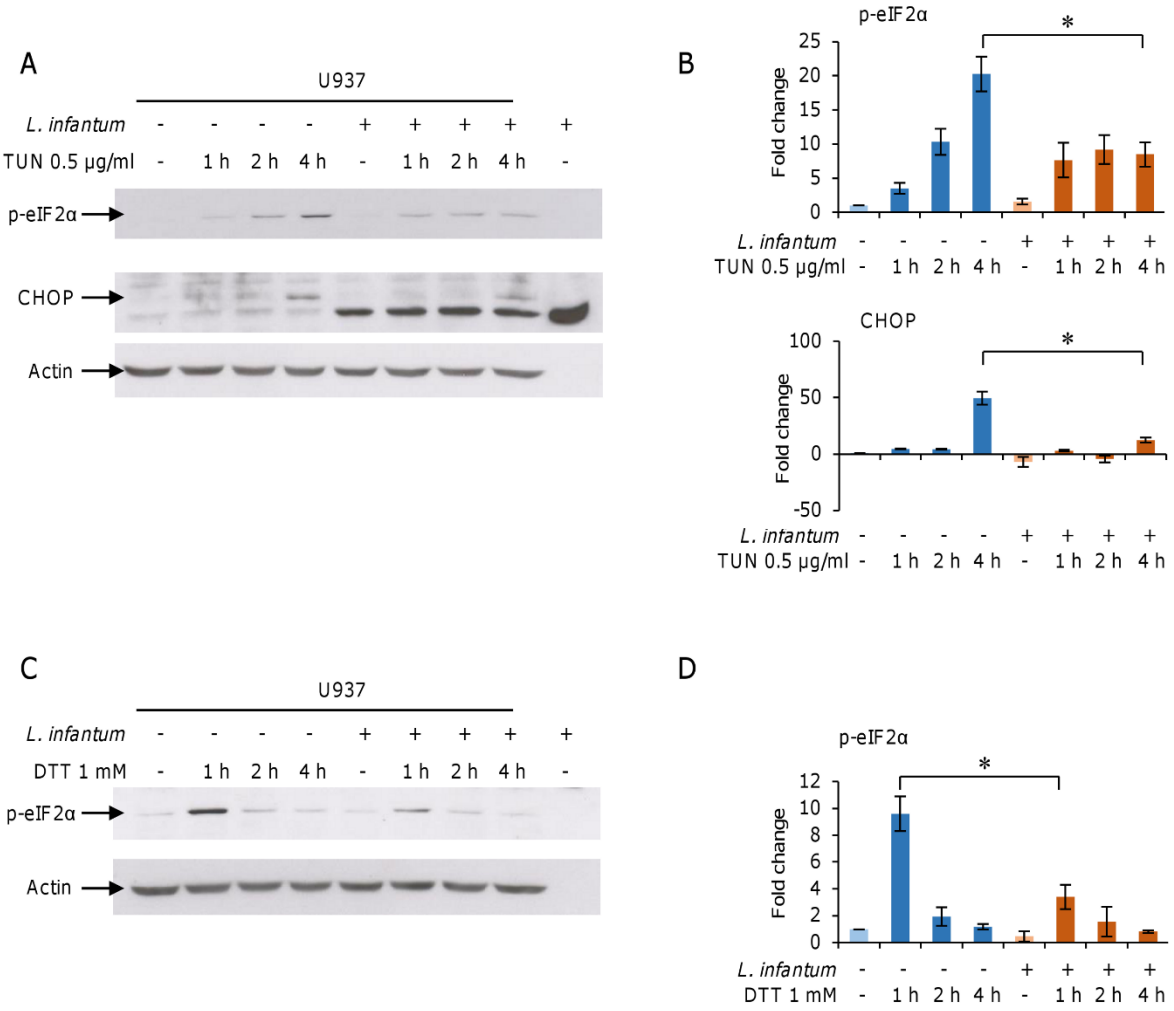

Fig 30. *L. infantum* inhibits tunicamycin- and DTT-induced ER stress. U937-derived macrophages were infected with *L. infantum* promastigotes for 18 h. Infected and non-infected cells were treated with 0.5 µg/ml tunicamycin **(A, B)** or 1 mM DTT **(C, D)** for 1 h, 2 h and 4 h. **(A, C)** The phosphorylation of eIF2α and DDIT3/CHOP protein levels were analyzed in total cell lysates by western blotting. **(B, D)** Densitometry was performed using a Chemi-Doc System. Results are representative of three experiments. * $p < 0.05$, two-way ANOVA followed by Bonferroni post hoc test. TUN, tunicamycin (Galluzzi *et al.*, 2016).

4.5 *L. INFANTUM* INFECTION DELAYS/ATTENUATES THE EFFECTS OF THE ER STRESSORS TUNYCAMYCIN AND DTT

Since mild ER stress has been shown to have a protective role in cell lines and disease models (Mollereau, 2013; Kennedy *et al.*, 2014; Mercado *et al.*, 2013), we investigated the ability of *L. infantum* to modulate the UPR in infected cells treated with ER stress inducers. For this purpose, U937 and THP1-derived macrophages were infected with promastigotes for 14 h, treated with 0.5 µg/ml tunicamycin or 1 mM DTT and harvested after 1 h, 2 h and 4 h. The phosphorylation of eIF2α and DDIT3/CHOP protein levels were performed by western blotting. In U937-derived macrophages, tunicamycin induced phosphorylation of eIF2α and the expression DDIT3/CHOP, in a time-dependent manner. Interestingly, after 4 h treatment with tunicamycin, was detected a significant reduction in both phospho-eIF2α and DDIT3/CHOP protein levels in infected cells compared to uninfected cells (Figure 30A and 30B), suggesting an attenuation of host UPR by *L. infantum* infection. The treatment with DTT also induced eIF2α phosphorylation as tunicamycin, although at earlier time. The reduction of eIF2α phosphorylation was evident following *L. infantum* infection (Figure 30C and 30D). These results were confirmed in THP1-derived macrophages. Also in this cell line *L. infantum* infection significantly reduced the induction of Eif2α phosphorylation and DDIT3/CHOP expression following tunicamycin treatment (Figure 31).

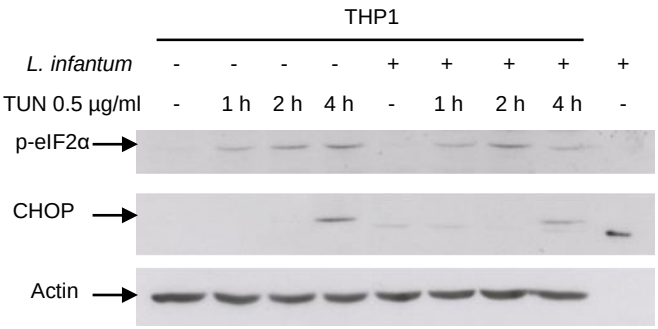

Fig. 31. *L. infantum* inhibits tunicamycin-induced ER stress in THP1-derived macrophages. THP1-derived macrophages were infected with *L. infantum* promastigotes for 18 h. Infected and non-infected cells were treated with 0.5 µg/ml tunicamycin for 1 h, 2 h and 4 h. The phosphorylation of eIF2α and DDIT3/CHOP protein levels were analyzed in total cell lysates by western blotting. TUN, tunicamycin (Galluzzi *et al.*, 2016).

The ER stress marker genes expression was also analyzed by qPCR in uninfected and infected U937-derived macrophages treated for two hours with tunicamycin or DTT. After treatment with tunicamycin, the induction of the ER stress marker genes, such as HSPA5, ATF3 and CHAC1 was significantly lower in infected cells, compared to uninfected cells (Figure 32). On the other hand, following DTT treatment was not evidenced significant changing in the expression of ER stress markers between infected and uninfected cells (not shown).

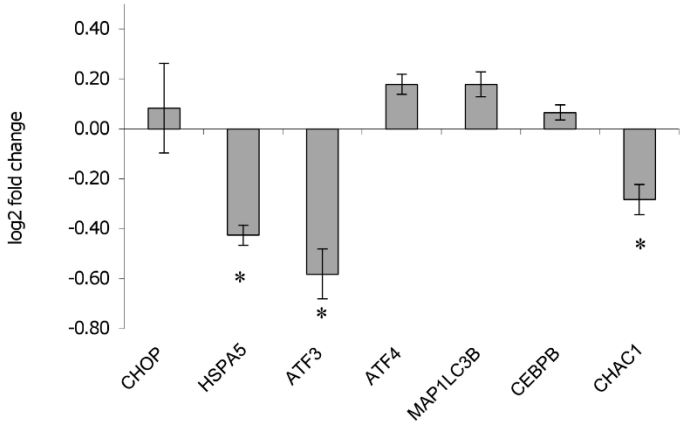

Fig. 32. *L. infantum* inhibits the expression of tunicamycin-induced ER stress marker genes. U937-derived macrophages were infected with *L. infantum* promastigotes for 18 h. Infected and non-infected U937-derived macrophages were treated with 0.5 µg/ml tunicamycin for 2 h. The graph shows the log2 fold changes of ER stress marker genes induced by tunicamycin in infected cells compared to the non-infected cells. * $p < 0.05$ (Galluzzi *et al.*, 2016).

4.6 INDUCTION OF miRNA-346 FOLLOWING *L. INFANTUM* INFECTION

The expression of three microRNAs (miR-126, miR-146a and miR-346) was monitored in cell-line-derived macrophages infected by *L. infantum* as described in methods. First, U937-derived macrophages have been analyzed after 18h infection with *L. infantum* MHOM/TN/80/IPT1. Infection was confirmed by microscopy and by induction of sXBP1 (Figue 33A). The results showed that miR-346 was the only miRNA significantly upregulated following infection (Figure 33B). Similar results were obtained with THP1-derived macrophages infected with *L. infantum* MHOM/TN/80/IPT1 and the two canine clinical isolates. In this case, however, the infection with *L. infantum* MHOM/TN/80/IPT1 was not effective (Figure 34).

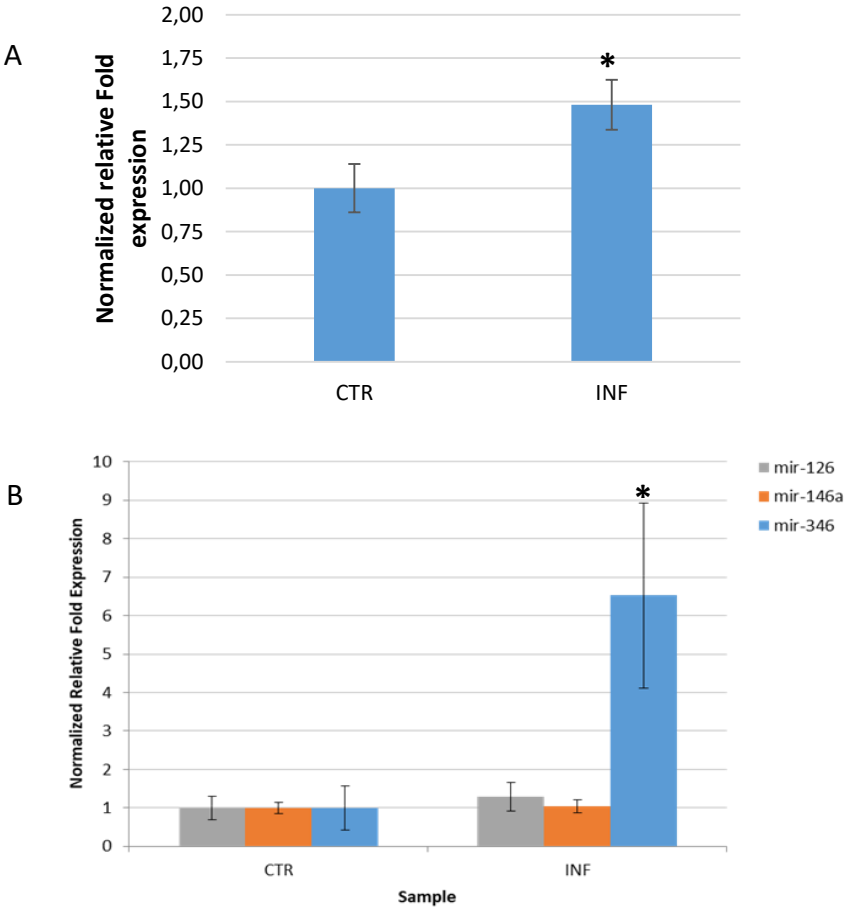

Fig 33. (A) Induction of XBP1 splicing in U937-derived macrophages after 24h infection. **(B)** Expression of mir-126, mir-146a e mir-346 in U937-derived macrophages after 24h infection. Results are average of two independent experiments. * $p < 0.05$. Expression of mir-126, mir-146a and mir-346 in macrophages derived from U937 cells after 24h infection. * $p < 0.05$.

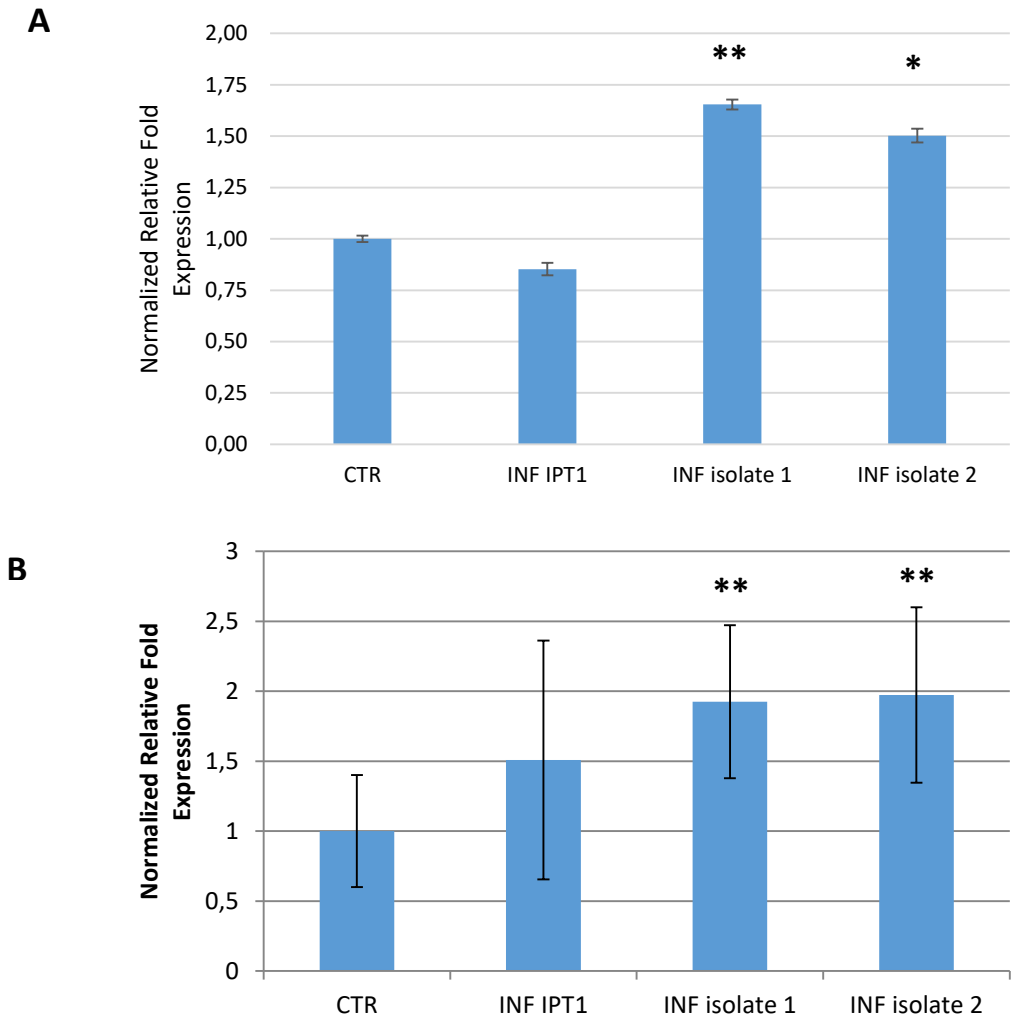

Fig. 34. (A) Induction of XBP1 splicing in THP1-derived macrophages after 18h infection. **(B)** Expression of mir-346 in THP1-derived macrophages after 18h infection. Results are average of two independent experiments. * $p < 0.05$. ** $p < 0.01$

In the attempt to monitor the effects of miR-346 upregulation, 92 validated miR-346 target genes were first identified using mirwalk 2.0 (Dweep *et al.*, 2015) (Table 5). Then, four of these genes (TAP1, IL18, BCAP31, RFX1) were selected and their expression was monitored in the same cells used to monitor miR-346 expression. The results did not show any significant changes in the TAP1, IL18, BCAP31 or RFX1 expression neither in U937-derived macrophages (Figure 33), nor in THP1-derived macrophages (not shown).

Tab. 5. Validated hsa-mir-346 target genes

Gene	EntrezID	PMID
INPP5J	27124	16822819
ZFP36	7538	21611196
DGCR14	8220	23622248
HRK	8739	24906430
PPP2R1B	5519	23824327
ENTPD1	953	16822819
MAPK8IP1	9479	16822819
TAP1	6890	22002058
PIK3R3	8503	23622248
ZNF417	147687	23446348
HRK	8739	23824327
FNTB	2342	16822819
MED16	10025	16822819
POU2F1	5451	22012620
APLP2	334	23622248
KMT2D	8085	23446348
FOXF2	2295	23824327
GGT5	2687	16822819
GJC2	57165	16822819
RFX1	5989	16822819
POLD3	10714	22012620
MLLT4	4301	23622248
CD164	8763	23446348
HSPE1-MOB4	100529241	23824327
SETD4	54093	16822819
LIF	3976	19011087
HNRNPA3	220988	23622248
TEAD2	8463	23622248
PDPK1	5170	23446348
MOB4	25843	23824327
TSTA3	7264	16822819
BTK	695	19342689
DCAF11	80344	23622248
RPL30	6156	23622248
MAP7D1	55700	23446348
ASGR2	433	23824327
CFLAR	8837	16822819
IL18	3606	19342689
RAD54B	25788	23622248
FAM46A	55603	23622248
PDPK1	5170	23313552
ETS1	2113	23824327
PPP2R1B	5519	22927820
SSH3	54961	16822819
FAM107A	11170	19536157
PSMD1	5707	23622248

Gene	EntrezID	PMID
CKB	1152	23622248
ETS1	2113	23313552
GSK3B	2932	24023731
CRELD1	78987	16822819
IFNGR2	3460	19536157
EZH1	2145	23622248
CCHCR1	54535	23622248
EMC8	10328	23313552
CNPY3	10695	16822819
PLEKHG4	25894	19536157
PRDM16	63976	23622248
PRMT5	10419	23622248
PVR	5817	23313552
NR2F6	2063	16822819
PTGS1	5742	19536157
GPI	2821	23622248
BCOR	54880	23622248
SLC39A1	27173	23313552
CD247	919	16822819
ENTHD1	150350	19536157
BCAP31	10134	23622248
LIMK1	3984	23622248
ZNF417	147687	21572407
TERF1	7013	16822819
C1orf95	375057	19536157
HDHD1	8226	23622248
PSMA3	5684	23622248
CD164	8763	21572407
RXRB	6257	16822819
ZNF417	147687	20371350
RAD51AP1	10635	23622248
USP22	23326	23622248
MAP7D1	55700	21572407
EFEMP2	30008	16822819
DGCR2	9993	16822819
CD164	8763	20371350
ZCCHC24	219654	23622248
CNN2	1265	23622248
NR6A1	2649	23592263
BDH2	56898	16822819
IL11RA	3590	16822819
EFEMP2	30008	21611196
SBF1	6305	23622248
PPP2R1B	5519	24906430
BSCL2	26580	23592263
GALT	2592	16822819

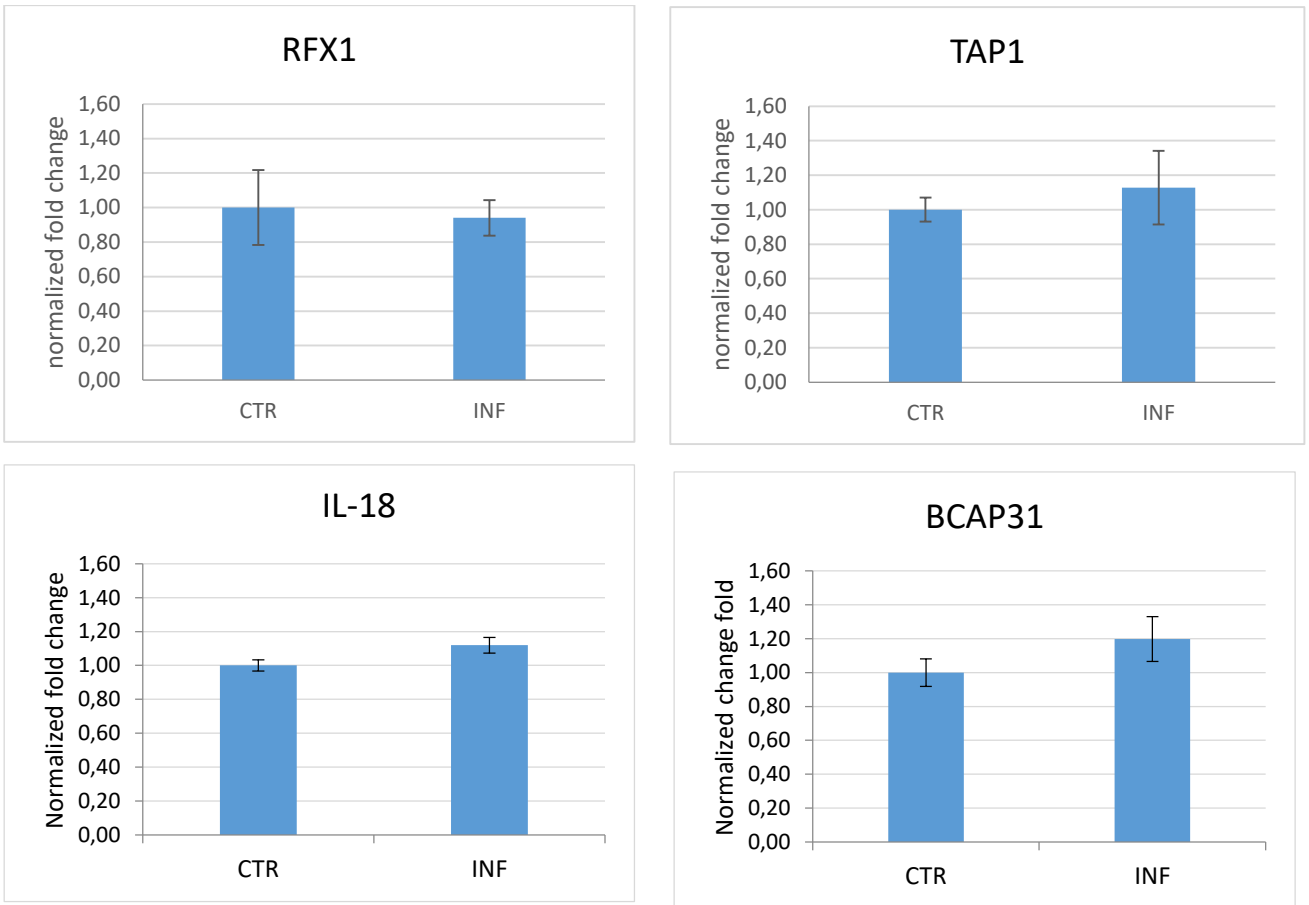

Fig. 35. Evaluation of TAP1, IL18, BCAP31 and RFX1 expression in U937-derived macrophages infected by *L. infantum* MHOM/TN/80/IPT1. The selected miR-346 target genes did not show any significant expression variation.

4.7 *L. INFANTUM* AMASTIGOTES AND PROMASTIGOTES RELEASE EXOSOMES

Extracellular vesicles released by *L. infantum* 31U promastigotes and amastigotes were purified on a sucrose gradient from the culture medium. They were isolated and characterized at National Reference Center for Leishmaniasis (C.Re.Na.L) through the analysis of well-established exosomal protein markers (i.e. HSP70, HSP83/90, acetylcholinesterase activity) (not shown). Additionally, a NanoSight nanoparticle tracking analysis were performed at University of Urbino in collaboration with Dr Michele Guescini to gain information about particle size, distribution and concentration. Results are resumed in Figure 34 and Table 6. All these data confirmed the capacity of *L. infantum* to release exosomes. To our knowledge, this is the first evidence of exosome production in this *Leishmania* species.

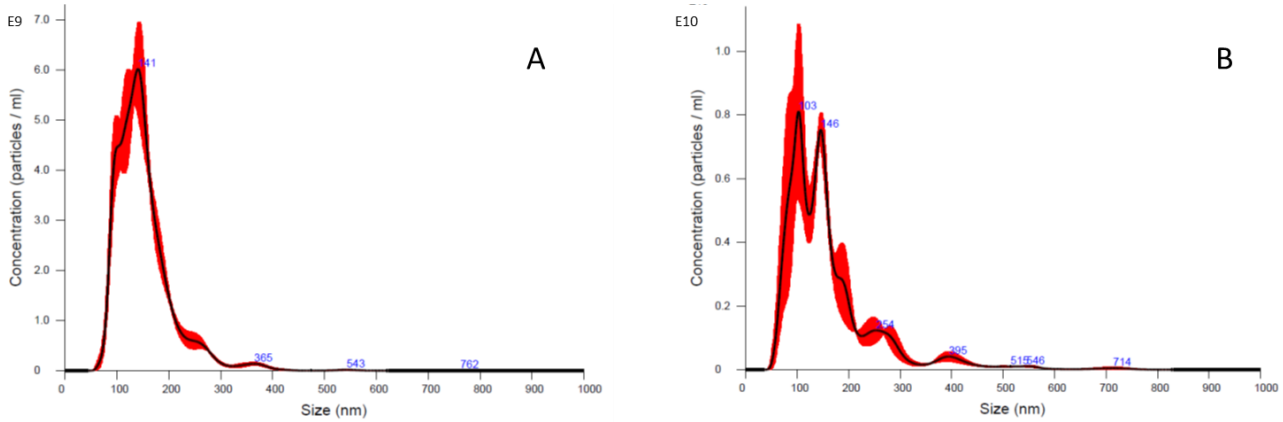

Fig. 36. Nanosight plots representing particle concentration vs particle size distribution of exosomes isolated from promastigotes cultures **(A)** and amastigote cultures **(B)**.

Tab. 6.

exosomes	µg/ml	mean particle diameter (± SE)	mode
Promastigotes	1.0	151.1 ± 2 nm	141 nm
Amastigotes	1.6	165.2 ± 13.5 nm	103 nm

4.8 *L. INFANTUM* EXOSOMES TREATMENT IS NOT SUFFICIENT TO ELICIT AN ER STRESS RESPONSE IN RAW 264.7 CELLS

Previous studies on different *Leishmania* species have shown that *Leishmania* exosomes possess immunomodulatory and signaling-inducing activities, corroborating the presence of parasite virulence factors in their content (Silverman *et al.*, 2011). In the attempt to investigate if exosome released by *L. infantum* parasites (either promastigotes or amastigotes) were able to elicit an ER stress response, we performed preliminary experiments using Raw 264.7 cells. These cells treated with 10 µg/ml of promastigote or amastigote exosomes for 24 h did not show any significant variation in the expression of ER stress marker genes analyzed (Figure 35).

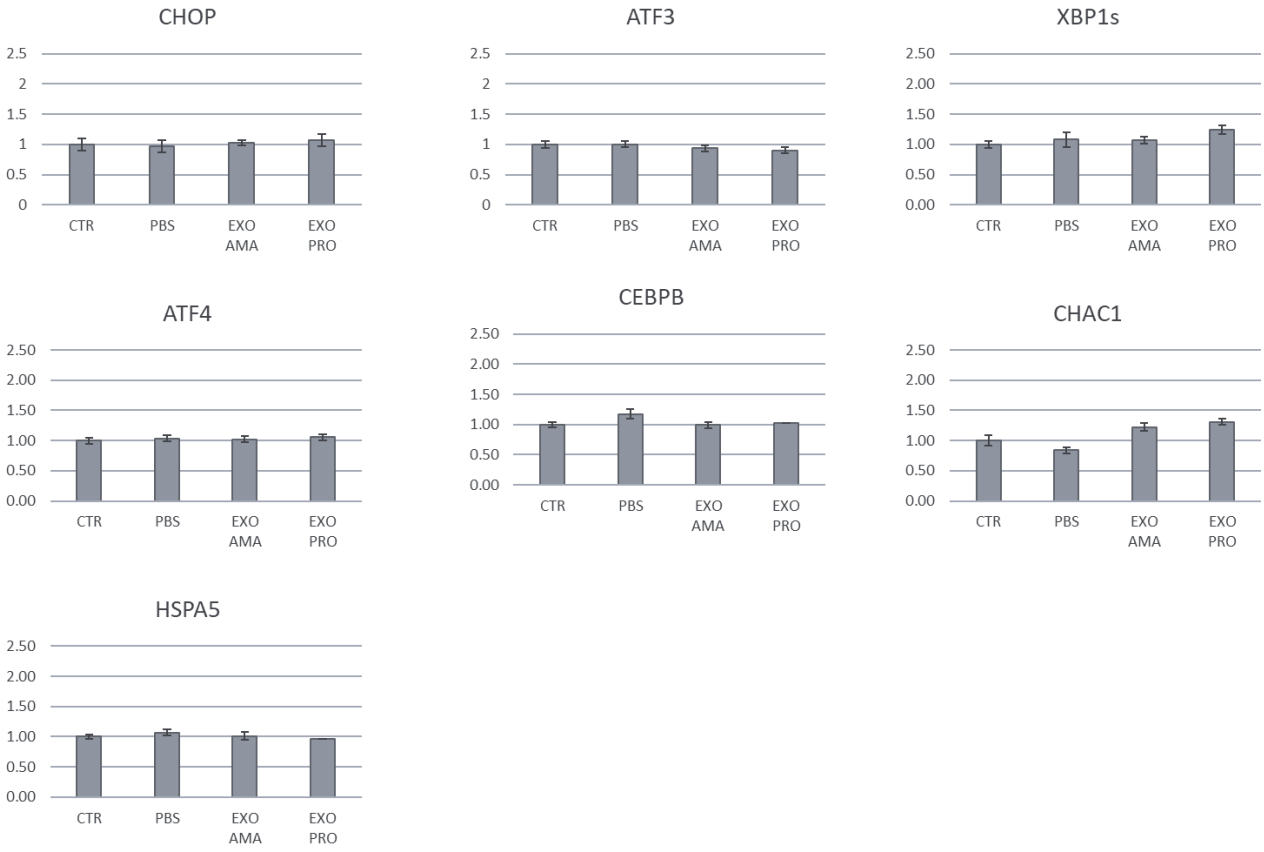

Fig. 37. The expression of ER stress marker genes did not show any significant variation after exosome treatment in RAW 264.7 cells. The data were normalized with GUSB as reference gene. CTR, untreated control cells; PBS, cells treated with exosome vehicle (phosphate buffered saline); EXO AMA, cells treated with exosome purified from *L. infantum* amastigote culture; EXO PRO cells treated with exosome purified from *L. infantum* promastigote culture.

5. DISCUSSION

Mammalian leishmaniasis shows a worldwide distribution. Leishmaniasis is endemic in tropics, subtropics and Mediterranean areas, in at least 98 countries and 3 territories, with the highest number of cases in developing nations (WHO, 2012).

Leishmania parasites replicate inside macrophages and has evolved strategies to elude host defense mechanisms such as ROS and NO production, antigen presentation, immune system activation and apoptosis (Podinovskaia and Descoteaux, 2015). Some of these strategies have been investigated using different *Leishmania* species and infection models. For example, *L. amazonensis* (belonging to *L. mexicana* complex responsible for cutaneous leishmaniasis) represses the iNOS expression through the NF-kB transcription factor, leading to the suppression of NO production (Calegari-Silva *et al.*, 2009) and induces SOD-1, reducing ROS accumulation (Vivarini *et al.*, 2011) in both human and mouse cells. Furthermore, it has been shown that *L. major* downregulates protein synthesis in murine macrophages by GP63-mediated cleavage of mTOR, (mammalian target of rapamycin), which is a serine/threonine kinase that regulates the translational repressor 4E-BP1 (Jaramillo *et al.*, 2011). ER stress is also responsible for the decrease in mTOR activity, which in turn leads to a reduction in 4E-BP1 phosphorylation and translation repression (Preston and Hendershot, 2013). 4E-BP1 is also regulated by the UPR-induced transcription factor ATF4 (Yamaguchi *et al.*, 2013). It is known that several intracellular pathogens are able to induce ER stress and trigger the UPR in the host cell. However, there are few information about ER stress and UPR in *Leishmania*- infected macrophages and its role in the pathogenesis. Moreover, most of the information in literature does not include (or marginally include) the species *L. infantum*, which is endemic in Italy, and it is responsible for CanL and sporadic cases of human VL and CL. Notably, concerning CL, the human cases could be underestimated due to lack or reports or recognition by physicians (Gradoni *et al.*, 2004).

In this thesis work, the ER stress response in macrophages infected by *L. infantum* parasites has been investigated in *in vitro* infection models using a reference strain (MHOM/TN/80/IPT1) and two canine clinical isolates. These isolates were recognized as *L. infantum* since i) dogs were diagnosed using an IFAT test having *L. infantum* promastigotes as immobilized antigens; ii) diagnosis was also corroborated by two qPCR assays designed on kDNA minicircles, one of which was species-specific for *L. infantum* (Manna *et al.*, 2008); iii) *L. infantum* is the only recognized species responsible for CanL in Italy. The case of human clinical isolate was different: it was recognized as *Viannia* subgenus by qPCR and melt analysis but its full characterization has not

been accomplished yet. Therefore, it has not been used in infection experiments reported in this thesis.

After optimization of the parasite cultivation and the infection model, the first experiments were perfomed to confirm previous findings regarding the resistance to apoptosis of parasitized cells, observed with different *Leishmania* species. The induction of Akt phosphorylation and inhibition of caspase-3 cleavage have been confirmed in our infection model using tunicamycin as apoptosis inducer. Tunicamycin induces apoptosis via ER stress activation, while other molecules used in previous studies, as camptothecin and actinomycin D are inhibitors of DNA topoisomerase I and DNA replication/transcription, respectively. Then, it has been shown that infection with *L. infantum* was associated with a mild UPR response in both human and murine macrophages. This response involved the upregulation of several ER stress marker genes, which was much lower respect to the one observed after treatment with the ER stressor tunicamycin, accounting for an averagely moderate ER stress response in the cell population. The induction of some ER stress marker proteins (*i.e.* GRP78/HSPA5 and sXBP1) and the lack of induction of others (*i.e.* phospho-eIF2α and DDIT3/CHOP), could be explained, in addition to the moderate activation of the UPR, by the fact that not all cells were simultaneously infected and/or by the different kinetic/activation of the three UPR arms. It is possible that *L. infantum* infection alters ER homeostasis in a moderate manner that it cannot be detected analyzing selected marker proteins in a heterogeneous pool of cells (infected and non-infected cells). Alternatively, specific UPR arms could be preferentially activated at the infection time analyzed.

Few differences resulted between infected cells and cells treated with tunicamycin. Chac1 expression did not vary significantly in U937-derived macrophages infected with *L. infantum* reference strain or isolates, while it was strongly upregulated after treatment with tunicamycin. However, in infected murine macrophages Chac1 resulted significantly upregulated while Cebpb expression did not vary. These differences may be due to some heterogeneity of the response in host cells population and/or in different infection rates.

Regarding XBP1 splicing analysis in infected cells, the sXBP1 form was never detected with conventional PCR neither in human nor in mouse macrophages following *L. infantum* infection (both reference strain and clinical isolates). On the contrary, a qPCR assay allowed to detect a significant induction of the sXBP1 form in both human and murine cells after 24 h infection. Interestingly, in U937 cells also the uXBP1 form resulted significantly upregulated, unlike in the canonical ER stress triggered by tunicamycin (Fig 26). It is known that the expression of HO-1 can

be induced by PERK (Cullinan and Diehl, 2004) and uXBP1 (Martin *et al.*, 2014) through NRF2 pathway; in particular, the induction of HO-1 has been evidenced after *L. chagasi* infection and this has been related with a decrease of TNF-α and ROS production and with an improvement in parasite survival (Luz *et al.*, 2012). Our findings could suggest that induction/modulation of ER stress may be a mechanism through which *Leishmania* triggers host antioxidant enzymes acting as scavengers of superoxide anion generated during host infection. Recently, XBP1 splicing activation has been described in a murine macrophagic cell line infected with *L. amazonensis* (Dias-Teixeira *et al.*, 2016). This finding were confirmed in our infection models, although with some differences, suggesting some common pathogenic mechanism among cutaneous and visceral species.

Although it is known that severe or prolonged ER stress can induce cell death, a slight ER stress levels may be useful to cells as it causes a mild (adaptive) UPR and increases its resistance to subsequent ER stress; this process, is called ER hormesis and it has been extensively reviewed by Mollereau *et al.* (Mollereau *et al.*,2014). In particular, both the PERK-ATF4 and IRE1-XBP1 branch contribute to the ER hormesis. In this view, the mild UPR induced by *L. infantum* infection can be seen as a pre-existing or adaptive stress response (*i.e.* hormesis). Indeed, the effects of ER stress inducers analyzed in both U937 and THP1-derived macrophages infected by *L. infantum* were mitigated. The differences observed in the gene expression after treatment using tunicamycin (a glycosilation inhibitor) and DTT (a disulfide bond-reducing agent) of infected cells could be caused by a differential activation kinetics of ER stress signaling (Li *et al.*, 2011). As a matter of fact, gene expression was observed after two hours treatment, though DTT effects were evident after 1h (see phosphorylation of eIF2α in Figure 30) therefore earlier compared to tunicamycin. The cellular signaling pathways and molecular mechanisms mediating hormetic responses typically include transcription factors such as NRF2 and NF-κB. As a result, there is an increase in the production of cytoprotective proteins including phase 2 and antioxidant enzymes, and protein chaperones by cells (Mattson, 2007). Therefore, the resistance to apoptosis of infected cells reported in literature could be due to ER hormesis triggered by *Leishmania* in the early phases (first 24 h) of infection. The enhanced resistance delays cell death, allowing parasite transformation into amastigotes and replication inside infected cells. Finally, *Leishmania* amastigotes exploits the apoptosis of host cell to spread to neighboring macrophages, reducing the exposure to immune recognition system in the extracellular environment (Real *et al.*, 2014). The activation of mild UPR in infected cells could also help to clarify many previous findings

regarding manipulation of host cellular mechanisms, such as induction of antioxidant enzymes, translation repression, induction of autophagy (Cyrino et al 2012) and Akt phosphorylation, which is triggered by ER stress via the PERK branch of the UPR (Hamanaka *et al.*, 2009). Moreover, it is known that the PERK/eIF2α/ATF4 arm plays a central role in autophagy regulation. In fact, the ER stress could lead to the transcription of MAP1LC3B, an essential autophagy gene, via ATF4 (B'chir *et al.*, 2013). Furthermore, through ATF4 (Whitney *et al.*, 2009), the ER stress can induce autophagy through activation of DDIT4/REDD1, an inhibitor of mTOR (Galluzzi *et al.*, 2012).
Leishmania could induce a mild UPR in parasitized cells through a slight perturbation of the ER homeostasis, inducing hormesis. Alternatively, the parasite could actively influence the host UPR at the transcriptional or post-transcriptional level, limiting it to a moderate response and thereby inducing protective mechanisms to prolong host cells survival. Further investigations will be needed to clarify these aspects.

Several studies have described host miRNA production after *Leishmania* infection. However, these studies were performed with different *Leishmania* species (*i.e. L. major* and *L. donovani*) and different cellular models/infection conditions, therefore making difficult to identify a common miRNA signature elicited by *Leishmania* infection (Tiwari *et al.*, 2017; Geraci *et al.*, 2015; Lemaire et al., 2013). Notably, two studies reported the deregulation of mir146a but in one case this miRNA was found upregulated (Lemaire *et al.*, 2013) while in the other it was found downregulated (Geraci *et al.*, 2015).
Several studies have also linked miRNAs to the UPR pathway. In fact, changes in miRNA levels following ER stress have been demonstrated by many research groups, with several miRNAs induced or repressed by the UPR sensors or by their downstream effectors. Moreover, several miRNAs have been shown to directly regulate key components of the UPR pathway, contributing to direct the cell towards death or survival (Harmeet, 2014). Examples of miRNAs induced by ER stress, promoting cell adaptation, are: miR-346, miR-885-3p (Bartoszewski *et al.*, 2011), miR-708 (Behrman *et al.*, 2011), miR-211 (Chitnis *et al.*, 2012), etc. In particular, the induction of the mir-346 during ER stress has been shown in different cell lines and it has been demonstrated that its expression is mediated by spliced XBP1 (Bartoszewski *et al.*, 2011). Twenty-one genes with functional roles in the immune response (MHC-associated genes and interferon-inducible genes) have been identified as mir-346 targets. Specifically, mir-346 was shown to induce post transcriptional downregulation of TAP1 (ATP-binding subfamily B transporter cassettes), which

lead to a reduction in the antigen presentation associated with the class I MHC (major histocompatibility complex) (Bartoszewski *et al.*, 2011). Therefore, the mir-346 was considered an interesting target to study in our infection model.

A significant up-regulation of the mir-346 expression has been detected along with the induction of sXBP1 in both U937 and THP1-derived macrophages infected with *L. infantum*. This could contribute to relate the observed induction of a moderate UPR response with the mechanisms of the cell-mediated immune response elusion by the parasite.

In order to evaluate the effects of miR 346 upregulation, four genes (TAP1, IL18, BCAP31, RFX1) were selected among the 92 mir346-target genes (Table 6) and their expression was evaluated by qPCR in the same cells used to monitor miR 346 expression.

TAP1 is one of the best characterized mir-346 target and it is involved in the pumping of degraded cytosolic peptides across the endoplasmic reticulum into the membrane-bound compartment where class I molecules assemble. IL18 is a proinflammatory cytokine, involved in Th1 immune response, that stimulates interferon gamma production in T-helper type I cells. BCAP31 encodes for a transmembrane protein of the endoplasmic reticulum that is involved in the anterograde transport of membrane proteins from the endoplasmic reticulum to the Golgi and in caspase 8-mediated apoptosis. RFX1 encodes for a transcription factor which may activate or repress target gene expression depending on cellular context. This transcription factor has been shown to regulate a wide variety of genes involved in immunity and cancer, including the MHC class II genes.

Results did not show any significant changes in the TAP1, IL18, BCAP31 or RFX1 expression neither in U937-derived macrophages (Fig. 35), nor in THP1-derived macrophages (not shown). However, this could be explained by the fact that, despite the upregulation in infected cells, the low levels of mir 346 are not sufficient to trigger changes in the mir-346 target mRNAs, which are much more represented in cells used as model of infection. In fact, a considerable difference in terms of Ct has been observed between assays directed to mir-346 (>32) and target mRNAs (17-26); this difference remained significant also taking into consideration the variability due to template amounts and qPCR assay types. However, the increase in mir-346 could be sufficient to prevent the upregulation of the monitored targets.

Before internalization, promastigotes injected during the blood meal by sandflies, can release microvesicles or exosomes, into the extracellular environment carrying molecules directly into

macrophages, modulating their activity (Schorey *et al.*, 2015). Indeed, *Leishmania* exosomes are able to suppress the immune response and the heat-shock protein 100 (HSP100) to have a crucial role in the storage of parasite's proteins whitin exosomes. The absence into exosomes of HSP100 resulted in different packaging and a different pro-inflammatory effect on immune cells. *Leishmania* exosomes modulate innate and adaptive immune responses through effects on monocytes and dendritic cells (Silverman *et al.*, 2010b). Exosome composition is also influenced by external factors; in fact, exosome release is upregulated at 37°C and low pH in the external environment. A temperature change from 26 ° C to 37 ° C within 4 hours, induces a rapid increase in proteins release through exosomes secreted from the surface of *L. mexicana* promastigotes (Hassani *et al.*, 2011). It has been shown that *Leishmania* exosomes interrupt intracellular macrophage signaling pathways, including alteration of NF-κB and AP-1 translocation and inhibition of nitric oxide production (Lambertz *et al.*, 2012; Hassani *et al.*, 2011). We tested if *Leishmania* exosomes were able to induce some ER stress response in host cells. To this end, extracellular vesicles were purified and characterized from *L. Infantum* promastigotes and amastigotes cultures, demonstrating for the first time that also *L. infantum* was able to secrete exosomes. Preliminary results indicated that both promastigotes and amastigote-derived exosomes did not induce any ER stress markers in RAW 264.7 cells. However, since it is known that the immune response is actively influenced by exosome treatment in L. major or L. donovani infection models (Silverman et al., 2010), also L. infantum exosomes may regulate the host immune system. Further experiments (e.g. monitoring of cytokine production) will be needed to address this point.

6. CONCLUSIONS

The ER stress/unfolded protein response is highly interconnected with inflammation and immunity. In fact, the UPR can be triggered and/or modulated not only by overload of misfolded proteins in the ER lumen, but also by infections and inflammation. The UPR has been extensively investigated in bacterial and viral infections; however, only few studies regarding induction and/or modulation of UPR pathways in cells infected by intracellular protozoan parasites have been carried out. The understanding of the host UPR may contribute to explain some of the complex strategies that the parasites have evolved to survive/replicate into host cell.

Leishmaniasis is a complex neglected disease showing a worldwide distribution, including Mediterranean basin. In Italy, *L. infantum* is the main species responsible for CanL and sporadic cases of human VL and CL. Therefore, this thesis work has been focused on the analysis of host ER stress response in *in vitro L. infantum* infection model.

The subtle but significant increase in ER stress expression markers and the delay/attenuation of the effects of ER stress inducers (i.e. Tunicamycin and DTT) in infected cells support the hypothesis that *L. infantum* could promote survival of host cells by inducing a mild ER stress response (Galluzzi *et al.*, 2016). The mild ER stress response elicited by *Leishmania* infection could represent an upstream pathogenic mechanism common among different *Leishmania (Leishmania)* species, considering also the role of XBP1 evidenced in *L. amazonensis* infection (Dias Teixeira *et al.*, 2016). This mechanism could explain many previous findings regarding the subversion of host cellular pathways and could be part of the strategies, together with known virulence factors (e.g. GP63), that *Leishmania* has evolved to survive/replicate into host cell.

Preliminary experiments showed that the mild UPR was not induced by treating cells with exosomes purified from *L. infantum* promastigotes and amastigotes, indicating that UPR activation require active infection.

Moreover, a significant up-regulation of the miR-346 has been detected, together with induction of sXBP1, in both U937 and THP1-derived macrophages infected with *L. infantum.* Since among the miR-346 targets 21 genes have functional roles in the immune response (MHC-associated genes and interferon-inducible genes), the observed induction of a mild UPR could be also related to the elusion mechanisms of cellular-mediated immune response operated by the parasite.

However, more research is needed to deeply understand the complex interactions between host UPR signaling pathways and the *Leishmania* parasites. Since the knowledge regarding interaction between parasites and cellular stress responses (in particular UPR) will grow, new targets for the development of drugs directing on specific branches of UPR or related pathways (e.g. miR-346)

could be revealed. This could lead to the development of more effective/new therapeutic approaches, particularly useful in the cases of pharmacological resistance or toxicity of existing therapies.

7. REFERENCES

Adeli K, 2011. Translational control mechanisms in metabolic regulation: critical role of RNA binding proteins, microRNAs, and cytoplasmic RNA granules. Am J Physiol Endocrinol Metab.; 301(6):E1051-64. doi: 10.1152/ajpendo.00399.2011

Adl SM, Simpson AG, Lane CE, Lukeš J, Bass D, Bowser SS, Brown MW, Burki F, Dunthorn M, Hampl V, Heiss A, Hoppenrath M, Lara E, Le Gall L, Lynn DH, McManus H, Mitchell EA, Mozley-Stanridge SE, Parfrey LW, Pawlowski J, Rueckert S, Shadwick L, Schoch CL, Smirnov A, Spiegel FW, 2012. The revised classification of eukaryotes. J Eukaryot Microbiol.; 59(5):429-93. doi: 10.1111/j.1550-7408.2012.00644.x.

Akhoundi M, Kuhls K, Cannet A, Votýpka J, Marty P, Delaunay P, Sereno D, 2016. A Historical Overview of the Classification, Evolution, and Dispersion of *Leishmania* Parasites and Sandflies. PLoS Negl Trop Dis.; 3;10(3):e0004349. doi: 10.1371/journal.pntd.0004349.

Almeida TF, Palma LC, Mendez LC, Noronha-Dutra AA, Veras PS, 2012. *Leishmania amazonensis* fails to induce the release of reactive oxygen intermediates by CBA macrophages. Parasite Immunol.; 34(10):492-8. doi: 10.1111/j.1365-3024.2012.01384.x.

Alvar J, Velez ID, Bern C, Herrero M, Desjeux P, Cano J, Jannin J, den Boer M, 2012. Leishmaniasis worldwide and global estimates of its incidence. PLoS One 7:e35671. doi:10.1371/journal.pone.0035671.

Anand SS, Babu PP, 2013. Endoplasmic reticulum stress and neurodegeneration in experimental cerebral malaria. Neurosignals.; 21(1-2):99-111. doi: 10.1159/000336970.

Anderson P, Kedersha N, 2008. Stress granules: the Tao of RNA triage. Trends Biochem Sci.; 33(3):141-50. doi: 10.1016/j.tibs.2007.12.003.

Ball WB, Mukherjee M, Srivastav S, Das PK, 2014. *Leishmania donovani* activates uncoupling protein 2 transcription to suppress mitochondrial oxidative burst through differential modulation of SREBP2, Sp1 and USF1 transcription factors. Int J Biochem Cell Biol.; 48:66-76. doi: 10.1016/j.biocel.2014.01.004.

Barak E, Amin-Spector S, Gerliak E, Goyard S, Holland N, Zilberstein D, 2005. Differentiation of *Leishmania donovani* in host-free system: analysis of signal perception and response. Mol Biochem Parasitol.; 141(1):99-108.

Barnes JC, Stanley O, Craig TM, 1993. Diffuse cutaneous leishmaniasis in a cat. J Am Vet Med Assoc.; 1; 202(3):416-8.

Bartoszewski R, Brewer JW, Rab A, Crossman DK, Bartoszewska S, Kapoor N, Fuller C, Collawn JF, Bebok Z, 2011. The unfolded protein response (UPR)-activated transcription factor X-box-binding protein 1 (XBP1) induces microRNA-346 expression that targets the human antigen peptide transporter 1 (TAP1) mRNA and governs immune regulatory genes. J Biol Chem.; 286(48):41862-70. doi: 10.1074/jbc.M111.304956.

Bates, PA, 2007. Transmission of *Leishmania* metacyclic promastigotes by phlebotomine sand flies. Int J Parasitol.; 37(10), p. 1097–1106. doi: 10.1016/j.ijpara.2007.04.003

B'chir W, Maurin AC, Carraro V, Averous J, Jousse C, Muranishi Y, Parry L, Stepien G, Fafournoux P, Bruhat A, 2013. The eIF2alpha/ATF4 pathway is essential for stress-induced autophagy gene expression. Nucleic Acids Res.; 41(16):7683-99. doi: 10.1093/nar/gkt563.

Behrman S, Acosta-Alvear D, Walter P, 2011. A CHOP-regulated microRNA controls rhodopsin expression. J Cell Biol.; 192(6):919-27. doi: 10.1083/jcb.201010055.

Belmont PJ, Chen WJ, Thuerauf DJ, Glembotski CC, 2012. Regulation of microRNA expression in the heart by the ATF6 branch of the ER stress response. J Mol Cell Cardiol.; 52(5):1176-82. doi: 10.1016/j.yjmcc.2012.01.017.

Ben-Othman R, Flannery AR, Miguel DC, Ward DM, Kaplan J, Andrews NW, 2014. *Leishmania*-mediated inhibition of iron export promotes parasite replication in macrophages. PLoS Pathog.; 10(1):e1003901. doi: 10.1371/journal.ppat.1003901.

Besteiro S, Williams RAM, Coombs GH, Mottram JC, 2007. Protein turnover and differentiation in Leishmania. Int J Parasitol.; 37(10): 1063–1075. doi: 10.1016/j.ijpara.2007.03.008.

Bettigole SE, Glimcher LH, 2015. Endoplasmic reticulum stress in immunity. Annu Rev Immunol.; 33:107-38. doi: 10.1146/annurev-immunol-032414-112116

Bhat TA, Chaudhary AK, Kumar S, O'Malley J, Inigo JR, Kumar R, Yadav N, Chandra D, 2017. Endoplasmic reticulum-mediated unfolded protein response and mitochondrial apoptosis in cancer. Biochim Biophys Acta.; 1867(1):58-66. doi: 10.1016/j.bbcan.2016.12.002.

Bhattacharya P, Gupta G, Majumder S, Adhikari A, Banerjee S, Halder K, Majumdar SB, Ghosh M, Chaudhuri S, Roy S, Majumdar S, 2011. Arabinosylated lipoarabinomannan skews Th2 phenotype towards Th1 during *Leishmania* infection by chromatin modification: Involvement of MAPK signaling. PLoS One.; 6(9):e24141. doi: 10.1371/journal.pone.0024141.

Blackwell JM, Fakiola M, Ibrahim ME, Jamieson SE, Jeronimo SB, Miller EN, Mishra A, Mohamed HS, Peacock CS, Raju M, Sundar S, Wilson ME, 2009. Genetics and visceral leishmaniasis: of mice and man. Parasite Immunol.; 31(5):254-66. doi: 10.1111/j.1365-3024.2009.01102.x.

Bonfante-Garrido R, Urdaneta I, Urdaneta R, Alvarado J, 1991. Natural infection of cats with *Leishmania* in Barquisimeto, Venezuela. Trans R Soc Trop Med Hyg. ;85(1):53.

Bravo R, Parra V, Gatica D, Rodriguez AE, Torrealba N, Paredes F, Wang ZV, Zorzano A, Hill JA, Jaimovich E, Quest AF, Lavandero S, 2013. Endoplasmic reticulum and the unfolded protein response: dynamics and metabolic integration. Int Rev Cell Mol Biol.; 301:215-90. doi: 10.1016/B978-0-12-407704-1.00005-1.

Buates S, Matlashewski G, 2001. General suppression of macrophage gene expression during *Leishmania donovani* infection. J Immunol.; 166(5):3416-22

Byrd AE, Aragon IV, Brewer JW, 2010. MicroRNA-30c-2* limits expression of proadaptive factor XBP1 in the unfolded protein response. J Cell Biol.; 196(6):689-98. doi: 10.1083/jcb.201201077.

Calegari-Silva TC, Pereira RM, De-Melo LD, Saraiva EM, Soares DC, Bellio M, Lopes UG, 2009. NF-kappaB-mediated repression of iNOS expression in *Leishmania amazonensis* macrophage infection. Immunol Lett.; 127(1):19-26. doi: 10.1016/j.imlet.2009.08.009

Canton J, Kima PE, 2012a. Interactions of pathogen-containing compartments with the secretory pathway. Cell Microbiol.; 14(11):1676-86. doi: 10.1111/cmi.12000.

Canton J, Kima PE, 2012b. Targeting host syntaxin-5 preferentially blocks Leishmania parasitophorous vacuole development in infected cells and limits experimental *Leishmania* infections. Am J Pathol.; 181(4):1348-55. doi: 10.1016/j.ajpath.2012.06.041.

Canton J, Ndjamen B, Hatsuzawa K, Kima PE, 2012. Disruption of the fusion of *Leishmania* parasitophorous vacuoles with ER vesicles results in the control of the infection. Cell Microbiol.; 14(6):937-48. doi: 10.1111/j.1462-5822.2012.01767.x

Castelli G, Galante A, Lo Verde V, Migliazzo A, Reale S, Lupo T, Piazza M, Vitale F, Bruno F, 2014. Evaluation of Two Modified Culture Media for *Leishmania Infantum* Cultivation *Versus* Different Culture Media. J Parasitol.; 100(2):228-30. doi: 10.1645/13-253.1.

Cavalier-Smith T, 1981. Eukaryote kingdoms: seven or nine?. Biosystems, 14(3-4), pp. 461-481.

Cebrian I, Visentin G, Blanchard N, Jouve M, Bobard A, Moita C, Enninga J, Moita LF, Amigorena S, Savina A, 2011. Sec22b regulates phagosomal maturation and antigen crosspresentation by dendritic cells. Cell.; 147(6):1355-68. doi: 10.1016/j.cell.2011.11.021.

Ceccarelli M, Galluzzi L, Diotallevi A, Andreoni F, Fowler H, Petersen C, Vitale F, Magnani M, 2017. The use of kDNA minicircle subclass relative abundance to differentiate between *Leishmania (L.) infantum* and *Leishmania (L.) amazonensis*. Parasit Vectors.; 10(1):239. doi: 10.1186/s13071-017-2181-x.

Ceccarelli M, Galluzzi L, Migliazzo A, Magnani M, 2014b. Detection and Characterization of *Leishmania (Leishmania)* and *Leishmania (Viannia)* by SYBR Green-Based Real-Time PCR and High Resolution Melt Analysis Targeting Kinetoplast Minicircle DNA. PLoS One.; 9(2):e88845. doi: 10.1371/journal.pone.0088845..

Ceccarelli M, Galluzzi L, Sisti D, Bianchi B, Magnani M, 2014a. Application of qPCR in conjunctival swab samples for the evaluation of canine leishmaniasis in borderline cases or disease relapse and correlation with clinical parameters. Parasit Vectors.; 7:460. doi: 10.1186/s13071-014-0460-3.

Chakraborty D, Banerjee S, Sen A, Banerjee KK, Das P, Roy S, 2005. *Leishmania donovani* affects antigen presentation of macrophage by disrupting lipid rafts. J Immunol.; 175(5):3214-24.

Chan MM, Adapala N, Chen C, 2012. Peroxisome Proliferator-Activated Receptor-γ- Mediated Polarization of Macrophages in *Leishmania* Infection. PPAR Res. 2012; 2012:796235. doi: 10.1155/2012/796235.

Chhabra R, Dubey R, Saini N, 2012. Gene expression profiling indicate role of ER stress in miR-23a~27a~24-2 cluster induced apoptosis in HEK293T cells. RNA Biol.; 8(4):648-64. doi: 10.4161/rna.8.4.15583.

Chitnis NS, Pytel D, Bobrovnikova-Marjon E, Pant D, Zheng H, Maas NL, Frederick B, Kushner JA, Chodosh LA, Koumenis C, Fuchs SY, Diehl JA, 2012. miR-211 is a prosurvival microRNA that regulates chop expression in a PERK-dependent manner. Mol Cell.; 48(3):353-64. doi: 10.1016/j.molcel.2012.08.025.

Contreras I, Gomez MA, Nguyen O, Shio MT, Mcmaster RW, Olivier M, 2010. *Leishmania*-induced inactivation of the macrophage transcription factor AP-1 is mediated by the parasite metalloprotease GP63. PLoS Pathog.; 6(10):e1001148. doi: 10.1371/journal.ppat.1001148.

Cook T, Roos D, Morada M, Zhu G, Keithly JS, Feagin JE, Wu G, Yarlett N, 2007. Divergent polyamine metabolism in the Apicomplexa. Microbiology.; 153(Pt 4):1123-30.

Coura-Vital W, Marques MJ, Veloso VM, Roatt BM, Aguiar-Soares RD, Reis LE, Braga SL, Morais MH, Reis AB, Carneiro M, 2011. Prevalence and factors associated with *Leishmania infantum* infection of dogs from an urban area of Brazil as identified by molecular methods. PLoS Negl Trop Dis.; 5(8):e1291. doi: 10.1371/journal.pntd.0001291.

Craig TM, Barton CL, Mercer SH, Droleskey BE, Jones LP, 1986. Dermal leishmaniasis in a Texas cat. Am J Trop Med Hyg.; 35(6):1100-2.

Cullinan SB, Diehl JA, 2004. PERK-dependent activation of Nrf2 contributes to redox homeostasis and cell survival following endoplasmic reticulum stress. J Biol Chem.; 279(19):20108-17.

Cupolillo E, Medina-Acosta E, Noyes H, Momen H, Grimaldi G Jr, 2000. A revised classification for *Leishmania* and Endotrypanum. Parasitol Today.; 16: 142–144.

Cuypers B, Domagalska MA, Meysman P, Muylder G, Vanaerschot M, Imamura H, Dumetz F, Verdonckt TW, Myler PJ, Ramasamy G, Laukens K, Dujardin JC, 2017. Multiplexed Spliced-Leader Sequencing: A high-throughput, selective method for RNA-seq in Trypanosomatids. Sci Rep.; 7(1):3725. doi: 10.1038/s41598-017-03987-0.

Cyrino LT, Araujo AP, Joazeiro PP, Vicente CP, Giorgio S, 2012. *In vivo* and *in vitro Leishmania amazonensis* infection induces autophagy in macrophages. Tissue Cell.; 44(6):401-8. doi: 10.1016/j.tice.2012.08.003.

de Almeida AS, Medronho RA, Werneck GL, 2011. Identification of risk areas for visceral leishmaniasis in Teresina, Piaui State, Brazil. Am J Trop Med Hyg.; 84(5):681-7. doi: 10.4269/ajtmh.2011.10-0325.

de Jong MF, Starr T, Winter MG, den Hartigh AB, Child R, Knodler LA, van Dijl JM, Celli J, Tsolis RM, 2013. Sensing of bacterial type IV secretion via the unfolded protein response. MBio.; 4(1):e00418-12. doi: 10.1128/mBio.00418-12.

De Santi M, Carloni E, Galluzzi L, Diotallevi A, Lucarini S, Magnani M, Brandi G, 2015. Inhibition of Testosterone Aromatization by the Indole-3-carbinol Derivative CTet in CYP19A1-overexpressing MCF-7 Breast Cancer Cells. Anticancer Agents Med Chem.; 15(7):896-904. doi: 10.2174/1871520615666150121123053

Deng J, Lu PD, Zhang Y, Scheuner D, Kaufman RJ, Sonenberg N, Harding HP, Ron D, 2004. Translational repression mediates activation of nuclear factor kappa B by phosphorylated translation initiation factor 2. Mol Cell Biol.; 24(23):10161-8.

Dereeper A, Guignon V, Blanc G, Audic S, Buffet S, Chevenet F, Dufayard J-F, Guindon S, Lefort V, Lescot, M., Claverie, J.-M., Gascuel, O., 2008. Phylogeny.fr: robust phylogenetic analysis for the non-specialist. Nucleic Acids Res.; 36(Web Server issue):W465-9. doi: 10.1093/nar/gkn180.

Dias-Teixeira KL, Calegari-Silva TC, dos Santos GR, Vitorino Dos Santos J, Lima C, Medina JM, Aktas BH, Lopes UG, 2016. The integrated endoplasmic reticulum stress response in *Leishmania amazonensis* macrophage infection: the role of X-box binding protein 1 transcription factor. FASEB J.; 30(4):1557-65. doi: 10.1096/fj.15-281550.

Duan Q, Wang X, Gong W, Ni L, Chen C, He X, Chen F, Yang L, Wang P, Wang DW, 2012. ER stress negatively modulates the expression of the miR-199a/214 cluster to regulate tumor survival and progression in human hepatocellular cancer. PLoS One.; 7(2):e31518. doi: 10.1371/journal.pone.0031518.

Dujardin JC, Campino L, Cañavate C, Dedet JP, Gradoni L, Soteriadou K, Mazeris A, Ozbel Y, Boelaert M, 2008. Spread of Vector-borne Diseases and Neglect of Leishmaniasis, Europe. Emerg Infect Dis.; 14(7):1013-8. doi: 10.3201/eid1407.071589.

Dweep H, Gretz N, 2015. miRWalk2.0: a comprehensive atlas of microRNA-target interactions. Nat Methods.; 12(8):697. doi: 10.1038/nmeth.3485.

Edgar RC, 2004. MUSCLE: multiple sequence alignment with high accuracy and high throughput. Nucleic Acids Res.; 32(5):1792-7.

Esch, KJ, Petersen, CA, 2013. Transmission and Epidemiology of Zoonotic Protozoal Diseases of Companion Animals. Clin Microbiol Rev.; 26(1):58-85. doi: 10.1128/CMR.00067-12.

Fabian MR, Sundermeier TR, Sonenberg N, 2010. Understanding how miRNAs post-transcriptionally regulate gene expression. Prog Mol Subcell Biol.; 50:1-20. doi: 10.1007/978-3-642-03103-8_1.

Faria MS, Calegari-Silva TC, De Carvalho Vivarini A, Mottram JC, Lopes UG, Lima AP, 2014. Role of protein kinase R in the killing of *Leishmania major* by macrophages in response to neutrophil elastase and TLR4 via TNFalpha and IFNbeta. FASEB J.; 28(7):3050-63. doi: 10.1096/fj.13-245126.

Filardy AA, Costa-da-Silva AC, Koeller CM, Guimarães-Pinto K, Ribeiro-Gomes FL, Lopes MF, Heise N, Freire-de-Lima CG, Nunes MP, DosReis GA, 2014. Infection with *Leishmania major* induces a cellular stress response in macrophages. PLoS One.; 9(1):e85715. doi: 10.1371/journal.pone.0085715.

Flannery AR, Renberg RL, Andrews NW, 2013. Pathways of iron acquisition and utilization in *Leishmania*. Curr Opin Microbiol.; 16(6):716-21. doi: 10.1016/j.mib.2013.07.018.

Forestier CL, Machu C, Loussert C, Pescher P, Spath GF, 2011. Imaging host cell- *Leishmania* interaction dynamics implicates parasite motility, lysosome recruitment, and host cell wounding in the infection process. Cell Host Microbe. 2011 Apr 21; 9(4):319-30. doi:10.1016/j.chom.2011.03.011.

Franco AO, Davies CR, Mylne A, Dedet JP, Gállego M, Ballart C, Gramiccia M, Gradoni L, Molina R, Gálvez R, Morillas-Márquez F, Barón-López S, Pires CA, Afonso MO, Ready PD, Cox J, 2011. Predicting the distribution of canine leishmaniasis in western Europe based on environmental variables. Parasitology.; 138(14):1878-91. doi: 10.1017/S003118201100148X.

Friedman RC, Farh KK, Burge CB, Bartel DP, 2009. Most mammalian mRNAs are conserved targets of microRNAs. Genome Res.; 19(1):92-105. doi: 10.1101/gr.082701.108.

Fu S, Watkins SM, Hotamisligil GS, 2012. The role of endoplasmic reticulum in hepatic lipid homeostasis and stress signaling. Cell Metab.; 15(5):623-34. doi: 10.1016/j.cmet.2012.03.007.

Galluzzi L, De Santi M, Crinelli R, De Marco C, Zaffaroni N, Duranti A, Brandi G, Magnani M, 2012. Induction of endoplasmic reticulum stress response by the indole-3-carbinol cyclic tetrameric derivative CTet in human breast cancer cell lines. PLoS One.; 7(8):e43249. doi: 10.1371/journal.pone.0043249.

Galluzzi L, Diotallevi A, De Santi M, Ceccarelli M, Vitale F, Brandi G, Magnani M, 2016. *Leishmania infantum* Induces Mild Unfolded Protein Response in Infected Macrophages. PLoS One.; 11(12): e0168339.

Galluzzi L, Diotallevi A, Magnani M, 2017. Endoplasmic reticulum stress and unfolded protein response in infection by intracellular parasites. Future Sci OA.; 3(3):FSO198. doi: 10.4155/fsoa-2017-0020.

Gazzinelli RT, Kalantari P, Fitzgerald KA, Golenbock DT, 2014. Innate sensing of malaria parasites. Nat Rev Immunol.; 14(11):744-57. doi: 10.1038/nri3742.

Gebre-Michael T, Balkew M, Ali A, Ludovisi A, Gramiccia M, 2004. The isolation of *Leishmania* tropica and L. aethiopica from Phlebotomus (Paraphlebotomus) species (Diptera: Psychodidae) in the Awash Valley, northeastern Ethiopia. Trans. R. Soc. Trop. Med. Hyg.; 98(1):64 –70.

Geraci NS, Tan JC, McDowell MA, 2015. Characterization of microRNA Expression Profiles in *Leishmania* Infected Human Phagocytes. Parasite Immunol.; 37(1):43-51. doi: 10.1111/pim.12156.

Ghosh J, Bose M, Roy S, Bhattacharyya SN, 2013b. *Leishmania donovani* targets Dicer1 to downregulate miR-122, lower serum cholesterol, and facilitate murine liver infection. Cell Host Microbe.; 13(3):277-88. doi: 10.1016/j.chom.2013.02.005.

Ghosh J, Guha R, Das S, Roy S, 2013a. Liposomal cholesterol delivery activates the macrophage innate immune arm to facilitate intracellular *Leishmania donovani* killing. Infect Immun.; 82(2):607-17. doi: 10.1128/IAI.00583-13.

Gomez CP, Tiemi Shio M, Duplay P, Olivier M, Descoteaux A, 2012. The protein tyrosine phosphatase SHP-1 regulates phagolysosome biogenesis. J Immunol.; 189(5):2203-10. doi: 10.4049/jimmunol.1103021.

Gomez MA, Olivier M, 2010. Proteases and phosphatases during *Leishmania*-macrophage interaction: paving the road for pathogenesis. Virulence.;1(4):314-8. doi: 10.4161/viru.1.4.12194.

González C, Wang O, Strutz SE, González-Salazar C, Sánchez-Cordero V, Sarkar S, 2010. Climate Change and Risk of Leishmaniasis in North America: Predictions from Ecological Niche Models of Vector and Reservoir Species. PLoS Negl Trop Dis.; 19;4(1):e585. doi:10.1371/journal.pntd.0000585.

Gradoni L, Gramiccia M, Koury C Maroli M, 2004. Linee guida per il controllo del serbatoio canino della Leishmaniosi viscerale zoonotica in Italia. Rapporti ISTISAN 04/12 Istituto Superiore di Sanita, Roma, Italia.

Gramiccia M, Gradoni L, 2005. The current status of zoonotic leishmaniases and approaches to disease control. Int J Parasitol.;35(11-12):1169-80.

Gramiccia M, Scalone A, Di Muccio T, Orsini S, Fiorentino E, Gradoni L, 2013. The burden of visceral leishmaniasis in Italy from 1982 to 2012: a retrospective analysis of the multi-annual epidemic that occurred from 1989 to 2009. Euro Surveill.; 18(29): 20535.

Gupta P, Giri J, Srivastav S, Chande AG, Mukhopadhyaya R, Das PK, Ukil A, 2014. *Leishmania donovani* targets tumor necrosis factor receptor-associated factor (TRAF) 3 for impairing TLR4-mediated host response. FASEB J.; 28(4):1756-68. doi: 10.1096/fj.13-238428.

Gupta S, Read DE, Deepti A, Cawley K, Gupta A, Oommen D, Verfaillie T, Matus S, Smith MA, Mott JL, Agostinis P, Hetz C, Samali A, 2012. Perk-dependent repression of miR-106b-25 cluster is required for ER stress-induced apoptosis. Cell Death Dis.; 3:e333. doi: 10.1038/cddis.2012.74.

Hallé M, Gomez MA, Stuible M, Shimizu H, McMaster WR, Olivier M, Tremblay ML, 2009. The *Leishmania* surface protease GP63 cleaves multiple intracellular proteins and actively participates in p38 mitogen-activated protein kinase inactivation. J Biol Chem.; 284(11):6893-908. doi: 10.1074/jbc.M805861200.

Hamanaka RB, Bobrovnikova-Marjon E, Ji X, Liebhaber SA, Diehl JA, 2009. PERK-dependent regulation of IAP translation during ER stress. Oncogene.; 28(6):910-20. doi: 10.1038/onc.2008.428

Hardy PO, Diallo TO, Matte C, Descoteaux A, 2009. Roles of phosphatidylinositol 3-kinase and p38 mitogen-activated protein kinase in the regulation of protein kinase C-alpha activation in interferon-gamma-stimulated macrophages. Immunology.; 128(1 Suppl):e652-60. doi: 10.1111/j.1365-2567.2009.03055.x.

Harhay MO, Olliaro PL, Vaillant M, Chappuis F, Lima MA, Ritmeijer K, Costa CH, Costa DL, Rijal S, Sundar S, Balasegaram M, 2011. Who is a typical patient with visceral leishmaniasis? Characterizing the demographic and nutritional profile of patients in Brazil, East Africa, and South Am J Trop Med Hyg.; 84(4):543-50. doi: 10.4269/ajtmh.2011.10-0321.

Harmeet M, 2014. MicroRNAs in er stress: divergent roles in cell fate decisions. Curr Pathobiol Rep. Sep;2(3):117-122.

Hassani K, Antoniak E, Jardim A, Olivier M, 2011. Temperature-induced protein secretion by *Leishmania mexicana* modulates macrophage signalling and function. PLoS One.; 6(5):e18724. doi: 10.1371/journal.pone.0018724.

Hayakawa K, Nakajima S, Hiramatsu N, Okamura M, Huang T, Saito Y, Tagawa Y, Tamai M, Takahashi S, Yao J, Kitamura M, 2010. ER stress depresses NF-kB activation in mesangial cells through preferential induction of C/EBP. J Am Soc Nephrol.; 21(1):73-81. doi: 10.1681/ASN.2009040432.

Hollien J, 2013. Evolution of the unfolded protein response. Biochim Biophys Acta.; 1833(11):2458-63. doi: 10.1016/j.bbamcr.2013.01.016.

Hu P, Han Z, Couvillon AD, Kaufman RJ, Exton JH, 2006. Autocrine tumor necrosis factor alpha links endoplasmic reticulum stress to the membrane death receptor pathway through IRE1-mediated NF-kB activation and downregulation of TRAF2 expression. Mol Cell Biol.; 26(8):3071-84.

Hunter CA, Sibley LD, 2012. Modulation of innate immunity by Toxoplasma gondii virulence effectors. Nat Rev Microbiol.; 10(11):766-78. doi: 10.1038/nrmicro2858.

Ibraim IC, de Assis RR, Pessoa NL, Campos MA, Melo MN, Turco SJ, Soares RP, 2013. Two biochemically distinct lipophosphoglycans from *Leishmania braziliensis* and *Leishmania infantum* trigger different innate immune responses in murine macrophages. Parasit Vectors.; 6:54. doi: 10.1186/1756-3305-6-54.

Inácio P, Zuzarte-Luís V, Ruivo MT, Falkard B, Nagaraj N, Rooijers K, Mann M, Mair G, Fidock DA, Mota MM, 2015. Parasite-induced ER stress response in hepatocytes facilitates Plasmodium liver stage infection. EMBO Rep.; 16(8):955-64. doi: 10.15252/embr.201439979.

Isnard A, Shio MT, Olivier M, 2012. Impact of *Leishmania* metalloprotease GP63 on macrophage signaling. Front Cell Infect Microbiol.; 2:72. doi: 10.3389/fcimb.2012.00072.

Itoe MA, Sampaio JL, Cabal GG, Real E, Zuzarte-Luis V, March S, Bhatia SN, Frischknecht F, Thiele C, Shevchenko A, Mota MM, 2014. Host cell phosphatidylcholine is a key mediator of malaria parasite survival during liver stage infection. Cell Host Microbe.; 16(6):778-86. doi: 10.1016/j.chom.2014.11.006.

Jaramillo M, Gomez MA, Larsson O, Shio MT, Topisirovic I, Contreras I, Luxenburg R, Rosenfeld A, Colina R, McMaster RW, Olivier M, Costa-Mattioli M, Sonenberg N, 2011. *Leishmania* repression of host translation through mTOR cleavage is required for parasite survival and infection. Cell Host Microbe.; 9(4):331-41. doi: 10.1016/j.chom.2011.03.008.

Kawai T, Akira S, 2010. The role of pattern-recognition receptors in innate immunity: update on Toll-like receptors. Nat Immunol.; 11(5):373-84. doi: 10.1038/ni.1863

Keestra-Gounder AM, Byndloss MX, Seyffert N, Young BM, Chávez-Arroyo A, Tsai AY, Cevallos SA, Winter MG, Pham OH, Tiffany CR, de Jong MF, Kerrinnes T, Ravindran R, Luciw PA, McSorley SJ, Bäumler AJ, Tsolis RM, 2016. NOD1 and NOD2 signalling links ER stress with inflammation. Nature.; 532(7599):394-7. doi: 10.1038/nature17631.

Kennedy D, Mnich K, Samali A, 2014. Heat shock preconditioning protects against ER stress-induced apoptosis through the regulation of the BH3-only protein BIM. FEBS Open Bio.; 4:813-21. doi: 10.1016/j.fob.2014.09.004

Kim VN, Han J, Siomi MC, 2009. Biogenesis of small RNAs in animals. Nat Rev Mol Cell Biol.; 10(2):126-39. doi: 10.1038/nrm2632

Kimball SR, Horetsky RL, Ron D, Jefferson LS, Harding HP, 2003. Mammalian stress granules represent sites of accumulation of stalled translation initiation complexes. Am J Physiol Cell Physiol.; 284(2):C273-84.

Kimmig P, Diaz M, Zheng J, Williams CC, Lang A, Aragón T, Li H, Walter P, 2012. The unfolded protein response in fission yeast modulates stability of select mRNAs to maintain protein homeostasis. Elife.; 1:e00048. doi: 10.7554/eLife.00048.

Kitamura M, 2011. Control of NF-κB and inflammation by the unfolded protein response. Int Rev Immunol.; 30(1):4-15. doi: 10.3109/08830185.2010.522281..

Lainson R, Shaw JJ, 1987. Evolution, classification and geographical distribution. The leishmaniases in biology and medicine. Peters W, Killick-Kendrick R, p. 1–120.

Lambertz U, Silverman JM, Nandan D, McMaster WR, Clos J, Foster LJ, Reiner NE, 2012. Secreted virulence factors and immune evasion in visceral leishmaniasis. J Leukoc Biol. Jun;91(6):887-99. doi: 10.1189/jlb.0611326

Lamparski HG, Metha-Damani A, Yao JY, Patel S, Hsu DH, Ruegg C, Le Pecq JB, 2002. Production and characterization of clinical grade exosomes derived from dendritic cells. J Immunol Methods.; 270(2):211-26.

Lapara NJ, Kelly BL, 2013. Suppression of LPS-induced inflammatory responses in macrophages infected with *Leishmania*. J Inflamm (Lond).; 7(1):8. doi: 10.1186/1476-9255-7-8.

Lecoeur H, Giraud E, Prevost MC, Milon G, Lang T, 2013. Reprogramming neutral lipid metabolism in mouse dendritic leucocytes hosting live *Leishmania amazonensis* amastigotes. PLoS Negl Trop Dis.; 7(6):e2276. doi: 10.1371/journal.pntd.0002276.

Lee AH, Scapa EF, Cohen DE, Glimcher LH, 2008. Regulation of hepatic lipogenesis by the transcription factor XBP1. Science.; 320(5882):1492-6. doi: 10.1126/science.1158042.

Lee JH, Giannikopoulos P, Duncan SA, Wang J, Johansen CT, Brown JD, Plutzky J, Hegele RA, Glimcher LH, Lee AH, 2011. The transcription factor cyclic AMP–responsive element–binding protein H regulates triglyceride metabolism. Nat Med. 2011 Jun 12;17(7):812-5. doi: 10.1038/nm.2347.

Lee MW, Chanda D, Yang J, Oh H, Kim SS, Yoon YS, Hong S, Park KG, Lee IK, Choi CS, Hanson RW, Choi HS, Koo SH, 2010. Regulation of hepatic gluconeogenesis by an ER-bound transcription factor, CREBH. Cell Metab.; 11(4):331-9. doi: 10.1016/j.cmet.2010.02.016.

Lemaire J, Mkannez G, Guerfali FZ, Gustin C, Attia H, Sghaier RM, Sysco-Consortium, Dellagi K, Laouini D, Renard P, 2013. MicroRNA expression profile in human macrophages in response to *Leishmania major* infection. PLoS Negl Trop Dis.; 7(10):e2478. doi: 10.1371/journal.pntd.0002478.

Lencer WI, DeLuca H, Grey MJ, Cho JA, 2015. Innate immunity at mucosal surfaces: the IRE1-RIDD-RIG-I pathway. Trends Immunol.; 36(7):401-9. doi: 10.1016/j.it.2015.05.006.

Lerner AG, Upton JP, Praveen PV, Ghosh R, Nakagawa Y, Igbaria A, Shen S, Nguyen V, Backes BJ, Heiman M, Heintz N, Greengard P, Hui S, Tang Q, Trusina A, Oakes SA, Papa FR, 2012. IRE1alpha induces thioredoxin-interacting protein to activate the NLRP3 inflammasome and promote programmed cell death under irremediable ER stress. Cell Metab.; 16(2):250-64. doi: 10.1016/j.cmet.2012.07.007.

Leung AK, Calabrese JM, Sharp PA, 2006. Quantitative analysis of Argonaute protein reveals microRNA-dependent localization to stress granules. Proc Natl Acad Sci U S A.; 103(48):18125-30.

Leung AK, Sharp PA, 2006. Function and localization of microRNAs in mammalian cells. Cold Spring Harb Symp Quant Biol.; 71:29-38.

Lewis BP, Burge CB, Bartel DP, 2005. Conserved seed pairing, often flanked by adenosines, indicates that thousands of human genes are microRNA targets. Cell.; 120(1):15-20.

Li B, Yi P, Zhang B, Xu C, Liu Q, Pi Z, Xu X, Chevet E, Liu J, 2011. Differences in endoplasmic reticulum stress signalling kinetics determine cell survival outcome through activation of MKP-1. Cell Signal. 2011; 23: 35±45. doi: 10.1016/j.cellsig.2010.07.019 PMID: 20727407

Li J, Wang JJ, Zhang SX, 2011. Preconditioning with endoplasmic reticulum stress mitigates retinal endothelial inflammation via activation of X-box binding protein 1. J Biol Chem.; 286(6):4912-21. doi: 10.1074/jbc.M110.199729.

Lima ID, Queiroz JW, Lacerda HG, Queiroz PV, Pontes NN, Barbosa JD, Martins DR, Weirather JL, Pearson RD, Wilson ME, Jeronimo SM, 2012. *Leishmania infantum chagasi* in northeastern Brazil: asymptomatic infection at the urban perimeter. Am J Trop Med Hyg.; 86(1):99-107. doi: 10.4269/ajtmh.2012.10-0492.

Lisi S, Sisto M, Acquafredda A, Spinelli R, Schiavone M, Mitolo V, Brandonisio O, Panaro M, 2005. Infection with *Leishmania infantum* Inhibits actinomycin D-induced apoptosis of human monocytic cell line U-937. J Eukaryot Microbiol.; 52(3):211-7.

Liu D, Uzonna JE, 2012. The early interaction of *Leishmania* with macrophages and dendritic cells and its influence on the host immune response. Front Cell Infect Microbiol.; 2:83. doi: 10.3389/fcimb.2012.00083.

Llanos-Cuentas EA, Roncal N, Villaseca P, Paz L, Ogusuku E, Perez JE, Caceres A, Davies CR, 1999. Natural infections of *Leishmania peruviana* in animals in the Peruvian Andes. Vector Borne Zoonotic Dis.; 11(5):515-21. doi: 10.1089/vbz.2010.0138.

Lodge R, Diallo TO, Descoteaux A, 2006. *Leishmania donovani* lipophosphoglycan blocks NADPH oxidase assembly at the phagosome membrane. Cell Microbiol.;8(12):1922-31.

Lukes J, Skalický T, Týč J, Votýpka J, Yurchenko V, 2014. Evolution of parasitism in kinetoplastid flagellates. Mol Biochem Parasitol.; 195(2):115-22. doi: 10.1016/j.molbiopara.2014.05.007.

Luz NF, Andrade BB, Feijó DF, Araújo-Santos T, Carvalho GQ, Andrade D, Abánades DR, Melo EV, Silva AM, Brodskyn CI, Barral-Netto M, Barral A, Soares RP, Almeida RP, Bozza MT, Borges VM, 2012. Heme oxygenase-1 promotes the persistence of *Leishmania chagasi* infection. J Immunol.; 188(9):4460-7. doi: 10.4049/jimmunol.1103072.

Maiuolo J, Bulotta S, Verderio C, Benfante R, Borgese N, 2011. Selective activation of the transcription factor ATF6 mediates endoplasmic reticulum proliferation triggered by a membrane protein. Proc Natl Acad Sci U S A.; 108(19):7832-7. doi: 10.1073/pnas.1101379108

Manna L, Reale S, Vitale F, Picillo E, Pavone LM, Gravino AE, 2008. Real-time PCR assay in Leishmania-infected dogs treated with meglumine antimoniate and allopurinol. Vet J.; 177(2):279-82

Margariti A, Li H, Chen T, Martin D, Vizcay-Barrena G, Alam S, Karamariti E, Xiao Q, Zampetaki A, Zhang Z, Wang W, Jiang Z, Gao C, Ma B, Chen YG, Cockerill G, Hu Y, Xu Q, Zeng L, 2013. XBP1 mRNA splicing triggers an autophagic response in endothelial cells through BECLIN-1 transcriptional activation. J Biol Chem.; 288(2):859-72. doi: 10.1074/jbc.M112.412783.

Maroli M, Feliciangeli MD, Bichaud L, Charrel RN, Gradoni L, 2012. Phlebotomine sandflies and the spreading of leishmaniases and other diseases of public health concern. Med Vet Entomol.;27(2):123-47. doi: 10.1111/j.1365-2915.2012.01034.x.

Martin D, Li Y, Yang J, WangG, Margariti A, Jiang Z, Yu H, Zampetaki A, Hu Y, Xu Q, Zeng L, 2014. Unspliced X-box-binding protein 1 (XBP1) protects endothelial cells from oxidative stress through interaction with histone deacetylase 3. J Biol Chem.; 289(44): 30625–30634. doi: 10.1074/jbc.M114.571984

Martinon F, Chen X, Lee A-H, Glimcher LH, 2010. Toll-like receptor activation of XBP1 regulates innate immune responses in macrophages. Nat Immunol.; 11(5):411-8. doi: 10.1038/ni.1857.

Matheoud D, Moradin N, Bellemare-Pelletier A, Shio MT, Hong WJ, Olivier M, Gagnon E, Desjardins M, Descoteaux A, 2013. *Leishmania* evades host immunity by inhibiting antigen cross-presentation through direct cleavage of the SNARE VAMP8. Cell Host Microbe.; 14(1):15-25. doi: 10.1016/j.chom.2013.06.003.

Matte C, Descoteaux A, 2010. *Leishmania donovani* amastigotes impair gamma interferon-induced STAT1alpha nuclear translocation by blocking the interaction between STAT1alpha and importin-alpha5. Infect Immun.; 78(9):3736-43. doi: 10.1128/IAI.00046-10.

Mattson MP, 2008. Hormesis defined. Ageing Res Rev.; 7(1):1-7 doi: 10.1016/j.arr.2007.08.007

Maurel M, Chevet E, 2013. Endoplasmic reticulum stress signaling: the microRNA connection. Am J Physiol Cell Physiol.; 304(12):C1117-26. doi: 10.1152/ajpcell.00061.2013.

Maurel M, Chevet E, Tavernier J, Gerlo S, 2014. Getting RIDD of RNA: IRE1 in cell fate regulation. Trends Biochem Sci.; 39(5):245-54. doi: 10.1016/j.tibs.2014.02.008.

Maurel M, Dejeans N, Taouji S, Chevet E, Grosset CF, 2013. MicroRNA-1291-mediated silencing of IRE1 enhances Glypican-3 expression. RNA.; 19(6):778-88. doi: 10.1261/rna.036483.112.

Meier CL, Svensson M, Kaye PM, 2003. *Leishmania*-induced inhibition of macrophage antigen presentation analyzed at the single-cell level. J Immunol.; 171(12):6706-13.

Melo RC, Dvorak AM, 2012. Lipid body-phagosome interaction in macrophages during infectious diseases: host defense or pathogen survival strategy? PLoS Pathog 8(7): e1002729. doi.org/10.1371/journal.ppat.1002729

Mercado G, Valdes P, Hetz C, 2013. An ERcentric view of Parkinson's disease. Trends Mol Med.; 19(3):165-75. doi: 10.1016/j.molmed.2012.12.005.

Michel G, Pomares C, Ferrua B, Marty P, 2011. Importance of worldwide asymptomatic carriers of *Leishmania infantum (L. chagasi)* in human. Acta Trop.; 119(2-3):69-75. doi: 10.1016/j.actatropica.2011.05.012.

Mittra B, Andrews NW, 2013. IRONy OF FATE: role of iron-mediated ROS in *Leishmania* differentiation. Trends Parasitol.; 29(10):489-96. doi: 10.1016/j.pt.2013.07.007.

Mittra B, Cortez M, Haydock A, Ramasamy G, Myler PJ, Andrews NW, 2013. Iron uptake controls the generation of *Leishmania* infective forms through regulation of ROS levels. J Exp Med.; 210(2):401-16. doi: 10.1084/jem.20121368.

Mollereau B, 2013. Establishing links between endoplasmic reticulum-mediated hormesis and cancer. Mol Cell Biol.; 33(12):2372-4. doi: 10.1128/MCB.00315-13.

Mollereau B, Manie S, Napoletano F, 2014. Getting the better of ER stress. J Cell Commun Signal.; 8(4):311-21. doi: 10.1007/s12079-014-0251-9.

Morada M, Pendyala L, Wu G, Merali S, Yarlett N, 2013. Cryptosporidium parvum induces an endoplasmic stress response in the intestinal adenocarcinoma HCT-8 cell line. J Biol Chem.; 288(42):30356-64. doi: 10.1074/jbc.M113.459735.

Moradin N, Descoteaux A, 2012. *Leishmania* promastigotes: building a safe niche within macrophages. Front Cell Infect Microbiol.; 2:121. doi: 10.3389/fcimb.2012.00121.

Moreira D, López-García P, Vickerman K, 2004. An updated view of kinetoplastid phylogeny using environmental sequences and a closer outgroup: proposal for a new classification of the class Kinetoplastea. Int J Syst Evol Microbiol.; 54(Pt 5):1861-75.International Journal of Systematic and Evolutionary Microbiology, Volume 54, pp. 1861-1875.

Naderer T, Mcconville MJ, 2008. The *Leishmania* macrophage interaction: a metabolic perspective. Cell Microbiol.; 10(2):301-8. doi: 10.1111/j.1462-5822.2007.01096.x.

Nakamura T, Furuhashi M, Li P, Cao H, Tuncman G, Sonenberg N, Gorgun CZ, Hotamisligil GS, 2010. Double-stranded RNA-dependent protein kinase links pathogen sensing with stress and metabolic homeostasis. Cell.; 140(3):338-48. doi: 10.1016/j.cell.2010.01.001.

Nascimento ET, Moura ML, Queiroz JW, Barroso AW, Araujo AF, Rego EF, Wilson ME, Pearson RD, Jeronimo SM, 2011. The emergence of concurrent HIV-1/AIDS and visceral leishmaniasis in Northeast Brazil. Trans R Soc Trop Med Hyg. 2011 May;105(5):298-300. doi: 10.1016/j.trstmh.2011.01.006.

Ndjamen B, Kang BH, Hatsuzawa K, Kima PE, 2010. *Leishmania* parasitophorous vacuoles interact continuously with the host cell's endoplasmic reticulum; parasitophorous vacuoles are hybrid compartments. Cell Microbiol.; 12(10):1480-94. doi: 10.1111/j.1462-5822.2010.01483.x.

Novoa I, Zhang Y, Zeng H, Jungreis R, Harding HP, Ron D, 2003. Stress-induced gene expression requires programmed recovery from translational repression. EMBO J.; 22(5):1180-7.

Olivier M, Atayde VD, Isnard A, Hassani K, Shio MT, 2012. *Leishmania* virulence factors: focus on the metalloprotease GP63. Microbes Infect.; 14(15):1377-89. doi: 10.1016/j.micinf.2012.05.014.

Ovalle-Bracho C, Franco-Munoz C, Londono-Barbosa D, Restrepo-Montoya D, Clavijo-Ramirez C, 2015. Changes in Macrophage Gene Expression Associated with *Leishmania (Viannia) braziliensis* Infection. PLoS One.; 10(6):e0128934. doi: 10.1371/journal.pone.0128934

Paradies P, Capelli G, Cafarchia C, de Caprariis D, Sasanelli M, Otranto D, 2006. Incidences of canine leishmaniasis in an endemic area of southern Italy. J Vet Med B Infect Dis Vet Public Health.; 53(6):295-8.

Peter ME, 2010. Targeting of mRNAs by multiple miRNAs: the next step. Oncogene.; 29(15):2161-4. doi: 10.1038/onc.2010.59.

Petersen CA, 2009. Leishmaniasis, an Emerging Disease Found in Companion Animals in the United States. Top Companion Anim Med. ;24(4):182-8. doi: 10.1053/j.tcam.2009.06.006.

Pfaffl MW, 2001. A new mathematical model for relative quantification in real-time RT-PCR. Nucleic Acids Res.; 29(9):e45

Pinheiro RO, Nunes MP, Pinheiro CS, D'Avila H, Bozza PT, Takiya CM, Côrte-Real S, Freire-de-Lima CG, DosReis GA, 2009. Induction of autophagy correlates with increased parasite load of *Leishmania amazonensis* in BALB/c but not C57BL/6 macrophages. Microbes Infect.; 11(2):181-90. doi: 10.1016/j.micinf.2008.11.006.

Podinovskaia M, Descoteaux A, 2015. *Leishmania* and the macrophage: a multifaceted interaction. Future Microbiol.; 10(1):111-29. doi: 10.2217/fmb.14.103.

Polando R, Dixit UG, Carter CR, Jones B, Whitcomb JP, Ballhorn W, Harintho M, Jerde CL, Wilson ME, McDowell MA, 2013. The roles of complement receptor 3 and Fcγ receptors during *Leishmania* phagosome maturation. J Leukoc Biol.; 93(6):921-32. doi: 10.1189/jlb.0212086.

Preston AM, Hendershot LM, 2013. Examination of a second node of translational control in the unfolded protein response. J Cell Sci.; 126(18): 4253–4261. doi: 10.1242/jcs.130336

Real F, Florentino PT, Reis LC, Ramos-Sanchez EM, Veras PS, Goto H, Mortara RA, 2014. Cell-to-cell transfer of *Leishmania amazonensis* amastigotes is mediated by immunomodulatory LAMP-rich parasitophorous extrusions. Cell Microbiol.; 16(10):1549-64. doi: 10.1111/cmi.12311

Reale S, Maxia L, Vitale F, Glorioso NS, Caracappa S, Vesco G, 1999. Detection of *Leishmania infantum* in dogs by PCR with lymph node aspirates and blood. J Clin Microbiol.; 37(9): 2931–2935.

Reis LC, Ramos-Sanchez EM, Goto H, 2013. The interactions and essential effects of intrinsic insulin-like growth factor-I on *Leishmania (Leishmania) major* growth within macrophages. Parasite Immunol.; 35(7-8):239-44. doi: 10.1111/pim.12041.

Rodriguez NE, Gaur Dixit U, Allen LA, Wilson ME, 2011. Stage-specific pathways of *Leishmania infantum chagasi* entry and phagosome maturation in macrophages. PLoS One.; 6(4):e19000. doi: 10.1371/journal.pone.0019000.

Rogers M, Kropf P, Choi BS, Dillon R, Podinovskaia M, Bates P, Müller I, 2009. Proteophosophoglycans regurgitated by Leishmania-infected sand flies target the L-arginine metabolism of host macrophages to promote parasite survival. PLoS Pathog.; 5(8):e1000555. doi: 10.1371/journal.ppat.1000555.

Rogers ME, Corware K, Muller I, Bates PA, 2010. *Leishmania infantum* proteophosphoglycans regurgitated by the bite of its natural sand fly vector, Lutzomyia longipalpis, promote parasite establishment in mouse skin and skin-distant tissues. Microbes Infect.; 12(11):875-9. doi: 10.1016/j.micinf.2010.05.014.

Rogers, MB, Rogers MB, Hilley JD, Dickens NJ, Wilkes J, Bates PA, Depledge DP, Harris D, Her Y, Herzyk P, Imamura H, Otto TD, Sanders M, Seeger K, Dujardin JC, Berriman M, Smith DF, Hertz-Fowler C, Mottram JC. , 2011. Chromosome and gene copy number variation allow major structural change between species and strains of *Leishmania*. Genome Res.; 21(12):2129-42. doi: 10.1101/gr.122945.111.

Rojas-Bernabé A, Garcia-Hernández O, Maldonado-Bernal C, Delegado-Dominguez J, Ortega E, Gutiérrez-Kobeh L, Becker I, Aguirre-Garcia M, 2014. *Leishmania mexicana* lipophosphoglycan activates ERK and p38 MAP kinase and induces production of proinflammatory cytokines in human macrophages through TLR2 and TLR4. Parasitology.; 141(6):788-800. doi: 10.1017/S0031182013002187.

Rotureau B, Morales MA, Bastin P, Spath GF, 2009. The flagellum-mitogen-activated protein kinase connection in trypanosomatids: a key sensory role in parasite signalling and development? Cell Microbiol.; 11(5):710-8. doi: 10.1111/j.1462-5822.2009.01295.x.

Roy S, Kumar GA, Jafurulla M, Mandal C, Chattopadhyay A, 2014. Integrity of the Actin Cytoskeleton of Host Macrophages is Essential for *Leishmania donovani* Infection. Biochim Biophys Acta.; 1838(8):2011-8. doi: 10.1016/j.bbamem.2014.04.017.

Ruhland A, Leal N, Kima PE, 2007. *Leishmania* promastigotes activate PI3K/Akt signalling to confer host cell resistance to apoptosis. Cell Microbiol.; 9(1):84-96.

Rybicka JM, Balce DR, Chaudhuri S, Allan ER, Yates RM, 2012. Phagosomal proteolysis in dendritic cells is modulated by NADPH oxidase in a pH-independent manner. EMBO J.; 31(4):932-44. doi: 10.1038/emboj.2011.440.

Ryu S, McDonnell K, Choi H, Gao D, Hahn M, Joshi N, Park SM, Catena R, Do Y, Brazin J, Vahdat LT, Silver RB, Mittal V, 2013. Suppression of miRNA-708 by polycomb group promotes metastases by calciuminduced cell migration. Cancer Cell.; 23(1):63-76. doi: 10.1016/j.ccr.2012.11.019.

Saunders EC, Ng WW, Kloehn J, Chambers JM, Ng M, Mcconville MJ, 2014. Induction of a stringent metabolic response in intracellular stages of *Leishmania mexicana* leads to increased dependence on mitochondrial metabolism. PLoS Pathog.; 10(1):e1003888. doi: 10.1371/journal.ppat.1003888.

Savina A, Jancic C, Hugues S, Guermonprez P, Vargas P, Moura IC, Lennon-Duménil AM, Seabra MC, Raposo G, Amigorena S, 2006. NOX2 controls phagosomal pH to regulate antigen processing during crosspresentation by dendritic cells. Cell. 2006 Jul 14;126(1):205-18.

Schorey JS, Cheng Y, Singh PP, Smith VL, 2015. Exosomes and other extracellular vesicles in host–pathogen interactions. EMBO Rep.; 16(1):24-43. doi: 10.15252/embr.201439363

Sellon RK, Menard MM, Meuten DJ, Lengerich EJ, Steurer FJ, Breitschwerdt EB, 1993. Endemic visceral leishmaniasis in a dog from Texas. J Vet Intern Med.; 7(1):16-9.

Shio MT, Hassani K, Isnard A, Ralph B, Contreras I, Gomez MA, Abu-Dayyeh I, Olivier M, 2012. Host cell signalling and *Leishmania* mechanisms of evasion. J Trop Med.; 2012:819512. doi: 10.1155/2012/819512.

Silverman JM, Clos J, de'Oliveira CC, Shirvani O, Fang Y, Wang C, Foster LJ, Reiner NE, 2010a. An exosome-based secretion pathway is responsible for protein export from *Leishmania* and communication with macrophages. J Cell Sci.; 123(Pt 6):842-52. doi: 10.1242/jcs.056465.

Silverman JM, Clos J, Horakova E, Wang AY, Wiesgigl M, Kelly I, Lynn MA, McMaster WR, Foster LJ, Levings MK, Reiner NE, 2010b. *Leishmania* exosomes modulate innate and adaptive immune responses through effects on monocytes and dendritic cells. J Immunol.; 185(9):5011-22. doi: 10.4049/jimmunol.1000541

Silverman JM, Reiner NE, 2011. Exosomes and other microvesicles in infection biology: organelles with unanticipated phenotypes. Cell Microbiol.; 13(1):1-9. doi: 10.1111/j.1462-5822.2010.01537.x.

Sriburi R, Jackowski S, Mori K, Brewer JW, 2004. XBP1: a link between the unfolded protein response, lipid biosynthesis, and biogenesis of the endoplasmic reticulum. J Cell Biol.; 167(1):35-41.

Srivastav S, Basu Ball W, Gupta P, Giri J, Ukil A, Das PK, 2014. *Leishmania donovani* prevents oxidative burst-mediated apoptosis of host macrophages through selective induction of suppressors of cytokine signaling (SOCS) proteins. J Biol Chem.; 289(2):1092-105. doi: 10.1074/jbc.M113.496323.

Srivastava S, Pandey SP, Jha MK, Chandel HS, Saha B, 2013. *Leishmania* expressed lipophosphoglycan interacts with Toll-like receptor (TLR)-2 to decrease TLR-9 expression and reduce anti-leishmanial responses. Clin Exp Immunol.; 172(3):403-9. doi: 10.1111/cei.12074

Thuerauf DJ, Marcinko M, Belmont PJ, Glembotski CC, 2007. Effects of the isoform-specific characteristics of ATF6 alpha and ATF6 beta on endoplasmic reticulum stress response gene expression and cell viability. J Biol Chem.; 282(31):22865-78.

Tiwari N, Kumar V, Gedda MR, Singh AK, Singh VK, Singh SP, Singh RK, 2017. Identification and Characterization of miRNAs in Response to *Leishmania donovani* Infection: Delineation of Their Roles in Macrophage Dysfunction. Front Microbiol.; 8:314. doi: 10.3389/fmicb.2017.00314

Trainor KE, Porter BF, Logan KS, Hoffman RJ, Snowden KF, 2010. Eight cases of feline cutaneous leishmaniasis in Texas. Vet Pathol.; 47(6):1076-81. doi: 10.1177/0300985810382094.

Tsuru A, Imai Y, Saito M, Kohno K, 2016. Novel mechanism of enhancing IRE1α-XBP1 signalling via the PERK-ATF4 pathway. Sci Rep.; 6:24217. doi: 10.1038/srep24217.

Ueno N, Wilson ME, 2012. Receptor-mediated phagocytosis of Leishmania: implications for intracellular survival. Trends Parasitol.; 28(8):335-44. doi: 10.1016/j.pt.2012.05.002..

Upton JP, Wang L, Han D, Wang ES, Huskey NE, Lim L, Truitt M, McManus MT, Ruggero D, Goga A, Papa FR, Oakes SA 2012. IRE1alpha cleaves select microRNAs during ER stress to derepress translation of proapoptotic caspase-2. Science.; 338(6108):818-22. doi: 10.1126/science.1226191.

Urano F, Wang X, Bertolotti A, Zhang Y, Chung P, Harding HP, Ron D, 2000. Coupling of stress in the ER to activation of JNK protein kinases by transmembrane protein kinase IRE1. Science.; 287(5453):664-6.

Vellanki RN, Zhang L, Guney MA, Rocheleau JV, Gannon M, Volchuk A, 2012. OASIS/CREB3L1 induces expression of genes involved in extracellular matrix production but not classical endoplasmic reticulum stress response genes in pancreatic beta-cells. Endocrinology.; 151(9):4146-57. doi: 10.1210/en.2010-0137.

Vickerman, K, 1976. The diversity of the kinetoplastid flagellates. . Biology of the Kinetoplastida. Academic Press, p. 1–34.

Vivarini Ade C, Pereira Rde M, Teixeira KL, Calegari-Silva TC, Bellio M, Laurenti MD, Corbett CE, Gomes CM, Soares RP, Silva AM, Silveira FT, Lopes UG, 2011. Human cutaneous leishmaniasis: interferon-dependent expression of double-stranded RNA-dependent protein kinase (PKR) via TLR2. FASEB J.; 25(12):4162-73. doi: 10.1096/fj.11-185165

Wang T, Zhou J, Gan X, Wang H, Ding X, Chen L, Wang Y, DU J, Shen J, Yu L, 2014. Toxoplasma gondii induce apoptosis of neural stem cells via endoplasmic reticulum stress pathway. Parasitology.; 141(7):988-95. doi: 10.1017/S0031182014000183..

Wang X, Guo B, Li Q, Peng J, Yang Z, Wang A, Li D, Hou Z, Lv K, Kan G, Cao H, Wu H, Song J, Pan X, Sun Q, Ling S, Li Y, Zhu M, Zhang P, Peng S, Xie X, Tang T, Hong A, Bian Z, Bai Y, Lu A, He F, Zhang G, 2013. miR-214 targets ATF4 to inhibit bone formation. Nat Med.; 19(1):93-100. doi: 10.1038/nm.3026.

Weinkopff T, Mariotto A, Simon G, Hauyon-La Torre Y, Auderset F, Schuster S, Zangger H, Fasel N, Barral A, Tacchini-Cottier F, 2013. Role of toll-like receptor 9 signaling in experimental *Leishmania braziliensis* infection. Infect Immun.; 81(5):1575-84. doi: 10.1128/IAI.01401-12

Whitney ML, Jefferson LS, Kimball SR, 2009. ATF4 is necessary and sufficient for ER stress-induced upregulation of REDD1 expression. Biochem Biophys Res Commun.; 379(2):451-5. doi: 10.1016/j.bbrc.2008.12.079.

WHO, 2012 Leishmaniasis: epidemiology and access to medicines − an update based on the outcomes of WHO regional meetings, literature review and experts' opinion. Geneva, Switzerland

Wu J, Rutkowski DT, Dubois M, Swathirajan J, Saunders T, Wang J, Song B, Yau GD, Kaufman RJ, 2007. ATF6α optimizes long-term endoplasmic reticulum function to protect cells from chronic stress. Dev Cell.; 13(3):351-64.

Yaeger, RG, 1996. Protozoa: Structure, Classification, Growth, and Development. Medical Microbiology. 4th edition.

Yamaguchi S, Ishihara H, Yamada T, Tamura A, Usui M, Tominaga R, Munakata Y, Satake C, Katagiri H, Tashiro F, Aburatani H, Tsukiyama-Kohara K, Miyazaki J, Sonenberg N, Oka Y, 2008. ATF4-mediated induction of 4E-BP1 contributes to pancreatic beta cell survival under endoplasmic reticulum stress. Cell Metab.; 7(3):269-76. doi: 10.1016/j.cmet.2008.01.008.

Yamamoto M, Ma JS, Mueller C, Kamiyama N, Saiga H, Kubo E, Kimura T, Okamoto T, Okuyama M, Kayama H, Nagamune K, Takashima S, Matsuura Y, Soldati-Favre D, Takeda K, 2011. ATF6beta is a host cellular target of the Toxoplasma gondii virulence factor ROP18. J Exp Med.; 208(7):1533-46. doi: 10.1084/jem.20101660.

Yang F, Zhang L, Wang F, Wang Y, Huo XS, Yin YX, Wang YQ, Sun SH, 2011. Modulation of the unfolded protein response is the core of microRNA-122-involved sensitivity to chemotherapy in hepatocellular carcinoma. Neoplasia.; 13(7):590-600.

Yates RM, Hermetter A, Taylor GA, Russell DG, 2007. Macrophage activation downregulates the degradative capacity of the phagosome. *Traffic* 8(3), 241–250.

Yoshida H, Matsui T, Yamamoto A, Okada T, Mori K 2001. XBP1 mRNA is induced by ATF6 and spliced by IRE1 in response to ER stress to produce a highly active transcription factor. Cell. ; 107(7):881-91.

Zeeshan HMA, Lee GH, Kim H-R, Chae H-J, 2016. Endoplasmic reticulum stress and associated ROS. Int J Mol Sci.; 17(3):327. doi: 10.3390/ijms17030327.

Zhang K, 2010. Integration of ER stress, oxidative stress and the inflammatory response in health and disease. Int J Clin Exp Med.; 3(1):33-40.

Zhang K, Kaufman RJ, 2008. From endoplasmic-reticulum stress to the inflammatory response. Nature.; 454(7203): 455–462. doi: 10.1038/nature07203.

Zhou J, Gan X, Wang Y, Zhang X, Ding X, Chen L, Du J, Luo Q, Wang T, Shen J, Yu L, 2015. Toxoplasma gondii prevalent in China induce weaker apoptosis of neural stem cells C17.2 via endoplasmic reticulum stress (ERS) signaling pathways. Parasit Vectors.; 8:73. doi: 10.1186/s13071-015-0670-3.

CDC https://www.cdc.gov/parasites/leishmaniasis/biology.html

WHO http://www.who.int/leishmaniasis/burden/en/

Primer-BLAST – NCBI NIH https://www.ncbi.nlm.nih.gov/tools/primer-blast/